DESIGN OF ROBUST CONTROLLERS FOR A ROTARY WING HELICOPTER

by

Rabiya Ahmed

A Thesis Presented to the Faculty of the
American University of Sharjah
College of Engineering
in Partial Fulfillment
of the Requirements
for the Degree of

Master of Science in
Mechatronics Engineering

Sharjah, United Arab Emirates
June 2013

Approval Signatures

We, the undersigned, approve the Master's Thesis of Rabiya Ahmed.

Thesis Title: Design of Robust Controllers for a Rotary wing helicopter:

Signature **Date of Signature**

_____ _____
Dr. Ali A. Jhemi
Assistant Professor, Department of Mechanical Engineering
Thesis Advisor

_____ _____
Dr. Mohammad Abdel Kareem Rasheed Jaradat
Visiting Associate Professor, Department of Mechanical Engineering
Thesis Committee Member

_____ _____
Dr. Aydin Yesildirek
Associate Professor, Department of Electrical Engineering
Thesis Committee Member

_____ _____
Dr. Taha Landolsi
Associate Professor
Department of Computer Science and Engineering
Thesis Committee Member

_____ _____
Dr. Aydin Yesildirek
Director, Mechatronics Graduate Program

_____ _____
Dr. Hany A El-Kadi
Associate Dean, College of Engineering

_____ _____
Dr. Leland Blank
Interim Dean, College of Engineering

_____ _____
Dr. Khaled Assaleh
Director of Graduate Studies

Acknowledgements

First of all, I would like to express my gratitude to my advisor Dr. Ali Jhemi, Assistant professor Mechanical Engineering, from American University of Sharjah, for being highly patient and sharing with me his knowledge and enthusiasm throughout the development of my research. His suggestions and feedback were extremely important for the success of this research. I am grateful to my examiners Dr. Aydin Yesildirek, Dr. Taha Landolsi and Dr. Mohammad Abdel Kareem Rasheed Jaradat for accepting to join my examination committee and providing me with their wise suggestions and comments.

I wish to thank the Director of Mechatronics Graduate program Dr. Aydin Yesildirek and the program coordinator Ms. Salwa Mohammad for their constant support and guidance during the course of my studies without which I wouldn't have been able to complete my research on time. I want to thank my friends and fellow students Muhannad A.R Al-Omari, Amina Ammour, Milad Roigari, Alexander Avdeev, Bara Emran, Shilpa Baburajan and Syed Ali for helping me during my time here at AUS and for all the fruitful technical discussion we have had. My word of thanks also goes to Kent Bernales Roferos and John Mempin for their useful suggestions for my thesis and for providing a resourceful environment at the Mechatronics center. Finally I am most grateful to my parents without their loving support and guidance conducting this research wouldn't have been possible. My gratitude goes to Farrukh my loving fiancé for his patience and support while I conducted my research miles away from him.

Abstract

Due to inherent instability, parametric variations, changing properties during flight, and uncertainties in predicting aerodynamic coefficients, helicopter flight control requires strategies with enough robustness to cope with these uncertainties. The control laws developed in the last few decades are mostly of the PID type that does not take advantage of the helicopter full potential. In this thesis four different controller techniques have been explored for a small scaled single rotor joker 3 Helicopter. Uncertainties of system parameters have been injected in the Helicopter model and performance of each the controller has been evaluated. All controllers are tested in simulation. Hovering mode and robustness properties are verified within the range of inaccuracies expected to be encountered in real flight. The suggested controllers show excellent performance compared to classical controllers and can be good candidates for real flight test.

Table of Contents

List of Figures

List of Tables

Chapter 1

Introduction

1.1 Background

Unmanned Aerial Vehicles (UAV) are used in many military and civilian applications. Some applications require high agility and maneuverability, single rotor helicopters are considered to be best in these aspects. They are mainly used in civilian, military, rescue and search, transportation and construction purposes [1, 2]. When related to the fixed-wing aircraft, helicopters present a unique advantage in terms of maneuverability as they are able to fly forwards, backwards, sideways and can do vertical landing and take-off. The unmanned small helicopters are more attractive than the full size helicopters and can be used for applications like surveillance, monitoring of high voltage lines etc [3]. Moreover they are quite promising in environmental issues and in infrastructure maintainence since these helicopters are unmanned they provide a cost efftective and safe way to protect the pilots from dangerous situations. For high performance the unmanned aerial vehicles will see a cumulative need to perform flight missions where the dynamics of the UAV are not known. This together with the need of performance near stability for different maneuvers especially hovering gives the concept of modeling uncertainties a quite important role in flight control [3, 4]. Basically a mathematical model represents the dynamics of a real aircraft; however model uncertainties have profound effects on the performance and the stability of the UAV especially for an aircraft that has a low stability margin such as the joker 3 single rotor helicopter [4]. Robust controllers are developed for rotorcrafts to deal with the uncertainties, these controllers are first tested in simulation, if the response of these controllers is accurate then they are tested on the real rotorcraft for different flight missions.

1.2 Literature Review

Where the small scaled helicopters have advantages to a fixed wing aircraft they also have certain disadvantages. They are noisier and considerably more tedious to fly and have extremely vibrating systems, probably because of these aspects the aeronautical community all over the world is more dedicated in research of fixed-wing aircrafts rather than their rotary wing counterparts. In fact the commercial fixed wing aircraft has been flying fly-by-wire (FBW) technology for years now and the first fly-by-wire rotary wing aircraft flight took place in 2008 which is considered quite recent [3, 4]. In order to achieve enhanced performances for rugged applications a single rotor helicopter from the small scaled UAV's was considered because of its small size, unique flight capabilities, outstanding maneuverability and low cost [4]. An unmanned single rotor helicopter requires optimal flight control laws that shouldn't just provide the tracking of the reference inputted by the pilot but also stabilization of the helicopter in harsh weather conditions and in the presence of uncertainties. Many control laws have been developed for a UAV flight control system. In the last few years control techniques have been developed that include the classical control design techniques proportional integral derivative (PID) [5, 6], model following design technique Dynamic Inversion (DI) and methodologies that guarantee robustness like H∞ control. Flight control systems are mainly classified as linear or nonlinear where the classification mainly depends on the model of the rotorcraft that is used by the particular controller. Linear control is more application oriented and is usually implemented on the majority of the rotorcraft applications. Linear controllers are well known because of their simplicity which reduces the computational efforts. Nonlinear controllers are important because they provide more theoretical learning but are not used for actual flight missions [1]. In this thesis linearized model of the Joker 3 helicopter is used to implement different control laws mainly for the inner loop controlling i.e. the angular rates of a Joker 3 helicopter. The parameters used for the model of the helicopter are deduced from [7]. The parameters are obtained from complete system identification of real time flight test data. Four different control laws have been designed for the Joker 3 helicopter starting with the DI technique, H∞ design, loop shape designing procedure (LSDP) and the μ-synthesis design. H∞ mixed sensitivity problem has been optimized using the H∞ control theory. It uses frequency dependent

weights for tuning the controller and to minimize the ∞ norm of the closed loop sensitivity function. H∞ loop-shaping uses the H∞ control theory [8]. It was developed by McFarlane and Glover [9]. It uses the classical loop-shaping techniques. The designer can beforehand specify the performance specifications such as disturbance rejection by shaping the open loop gains. The LSDP has been used in many different real time aerospace missions like the westland Lynx [10], Bell 205 helicopters [11] and the DERA VAAC research Harrier [12]. The flight test for VAAC research Harrier was performed first in December 1993; it was the first H∞ controller to be flight tested on a real helicopter. μ-Synthesis is an extension of H∞ control theory. It uses the singular structured value μ for analysis. It is a technique that attempts to structure an uncertainty in the system model and design a controller that is robust for a special class of perturbations. It requires iterative cycles to find the best optimal solution but produces a high order controller as comapred to H∞ control design and thus requires reducing of the order. However this technique has been used in various aerospace application [13, 14]. A step by step procedure of how to develop the control laws has been provided in the chapters, as the thesis progresses one can see how the techniques differ from each other and how the next one overcomes the flaws of the one that precedes it.

1.3 Thesis Organization

The thesis has been organized in the following manner. Chapter 2 gives a description of the DI control technique development for the Joker 3 helicopter, it describes how the overall technique is integrated by using different blocks, also it shows the perfect responses achieved and concludes with the fact that DI lacks robustness. Chapter 3 covers a step by step procedure of how H∞ controller is developed for both the pitch and the roll rate of the Joker 3 helicopter, it even contains the robust control toolbox commands used for the purpose of developing the controller, responses for nominal performance, robust performance and robust stability are checked. Chapter 4 envelopes the LSDP, it gives a thorough explanation of how the uncertainties are modeled and added to the system, the new controller is developed and its performance is measured by checking its response for nominal performance and robustness analysis is implemented.

Chapter 5 evolves the μ-synthesis technique, it first gives a theoretical background to the singular structured value μ, the small gain theorem and how the μ bounds are computed. As the chapter progresses the μ controller has been developed and its performance has been analyzed for different perturbed systems. Chapter 6 provides a comparison between the robust controllers H∞, LSDP and μ-synthesis and chapter 7 provides a summary of the thesis.

Chapter 2

Design of Dynamic Inversion Controller

2.1 Introduction

Dynamic Inversion (DI) synthesis mainly cancels out the undesirable or deficient dynamics of the system and replaces them with desired dynamics. The replacement of the undesired dynamics is done through careful selection of feedback function which is why this technique is also known as feedback linearization [15, 16]. In this research DI controls the inner loop which means it controls the rates of the Joker 3 helicopter. DI applies to both single input single output systems (SISO) and multi input and multi output systems (MIMO). The DI control law exists for both non-linear and linear systems as mentioned in the literature review the linearized model of the joker 3 helicopter is used in this thesis therefore the linear DI technique would be studied in detail.
DI provides superior performance as compared to that of PID type controllers but the fundamental assumption in this methodology is that the plant dynamics are accurately modeled i.e. it requires perfect knowledge of the plant [15]. Dynamic inversion is similar to model-following control, in that both methodologies invert dynamical equations of the plant [15, 16]. Section 2.2 gives a brief description of how the control law works would be given followed by a detailed description of how each component of the controller works. Section 2.3 describes the implementation of DI process on the Joker 3 rotary wing helicopter.

2.2 Dynamic Inversion Concept

In general aircraft dynamics can be expressed as follows [19]:

$$\dot{x} = F(x,u) \tag{2.2-1}$$

$$y = H(x) \tag{2.2-2}$$

Where x is the state vector, u is the control vector and y is the measurement vector.
The aircraft dynamic equation can also be rewritten as:

$$\dot{x} = f(x) + g(x)u \tag{2.2-3}$$

The dynamic inversion control law can be obtained by subtracting $f(x)$ and multiplying both sides with $g(x)^{-1}$. If we assume that $g(x)$ to be invertible then the control input u is given as:

$$u = g^{-1}(x)[\dot{x} - f(x)] \tag{2.2-4}$$

Next, it is required to command the aircraft to desired states. Instead of commanding the desired states the rates of the desired states is commanded as it is the favored form of inputs for DI. Replacing $\dot{x}$ with $\dot{x}_{des}$ equation 2.2-4 can be rewritten as the final form of Dynamic Inversion control law [15].

$$u = g^{-1}(x)[\dot{x}_{des} - f(x)] \tag{2.2-5}$$

The dynamic inversion process can be represented in the below figure:

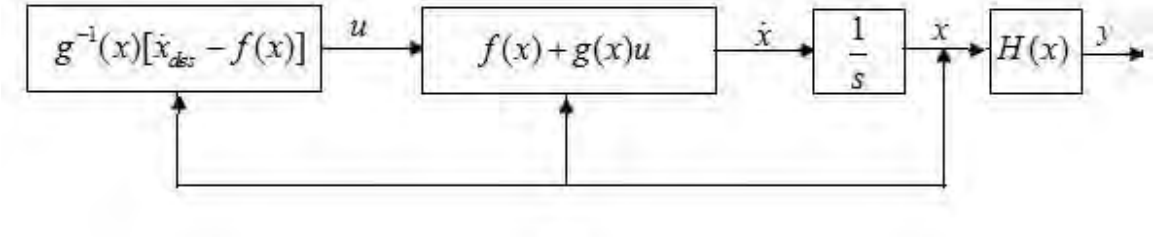

Figure 1: Dynamic Inversion concept flow diagram [15]

Figure 1 represents the DI process which seems to be simple but a few points need to be kept in consideration while designing a DI controller. First of all *g(x)* is assumed to be invertible for all values of *x*, this may not be the case if there are more states than controls. Also even if the *g(x)* is invertible the control effort *u* become large and result in actuator saturation.

2.3 Applying the Dynamic Inversion control to Joker 3 helicopter

The DI control laws will be developed in the further sections and would be integrated into an overall control structure. Figure 2 shows DI being used as an inner loop controller accompanied by θ and φ feedback outer loops. Although any type of feedback control technique can be used for the outer loop a simple feedback has been used for this research. The overall DI controller requires the commanded values of the pitch φ_{cmd} and the roll θ_{cmd} as inputs. Then the measured values φ_{meas} and θ_{meas} are subtracted from the commanded values to result in φ_{error} and θ_{error} this forms the outer loop. These error values are then fed into the command inverter block to be changed into the respective rate commands given as p_{cmd} and q_{cmd}. The next block is the desired dynamics block that uses the outputs from the command inverter block which are the rate commands and the rate measurements to create the desired acceleration terms, which are basically the favored forms of commands for the DI controller [15, 17]. The main block is the DI block which implements the control laws to produce the control efforts that are the control deflection angle commands. These deflection angles are then fed to the Joker3 longitudinal and lateral model to produce the rates.

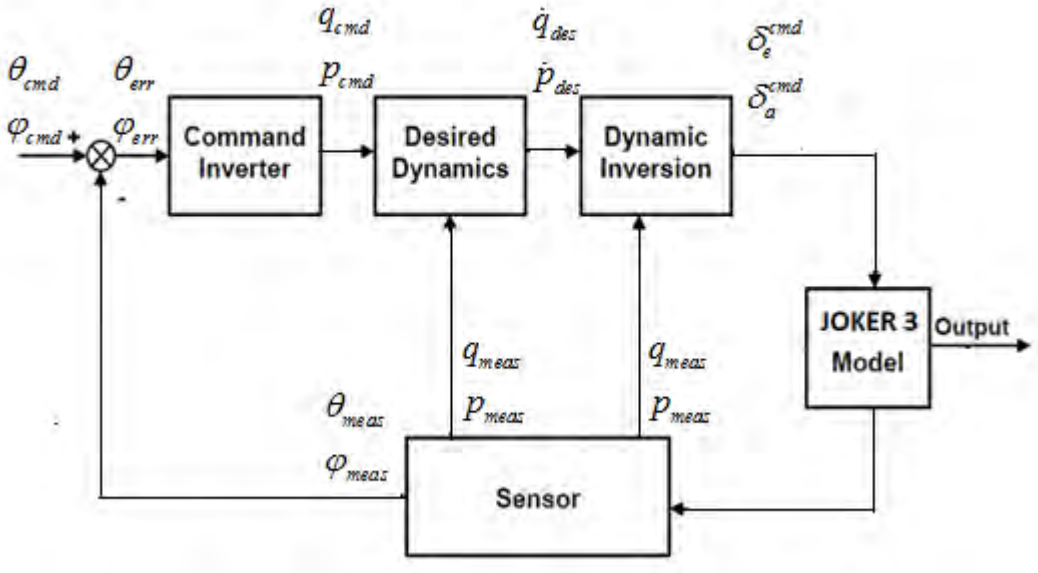

Figure 2: Overall Dynamic Inversion block [15]

2.3.1 Command Inverter

In most aircraft applications it's more appropriate to command the displacements φ and θ rather than the body axis rates p and q [15, 16]. However the next block which is the desired dynamics block requires the body axis rates as it's input therefore the command inverter block is used to produce the rates. The command inverter block converts the angular displacement commands into angular rate commands so that the displacement could be directly implemented into the DI controller. This section deals with how the displacement commands are transformed into the rate commands.

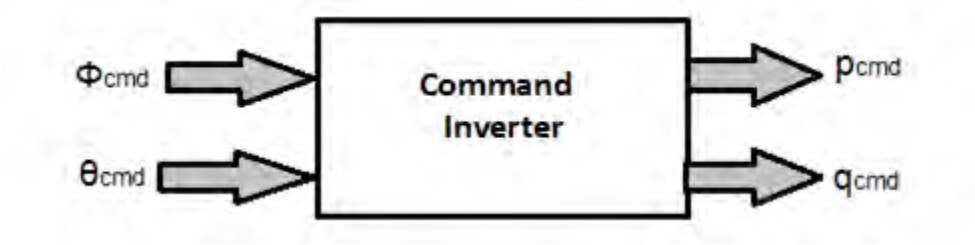

Figure 3: Command inverter block

As shown in Figure 3 the commanded roll rate can be obtained by simply differentiating the roll angle whereas the commanded pitch rate can be obtained by differentiating the pitch angle as given in the equations 2.3-1 and 2.3-2.

$$p_{cmd} = \frac{d}{dt}\phi_{cmd} \tag{2.3-1}$$

$$q_{cmd} = \frac{d}{dt}\theta_{cmd} \tag{2.3-2}$$

2.3.2 Desired Dynamics

The desired dynamics block which was introduced in section 2.3 is revisited here to come up with a detail explanation of how it works. The main purpose of a desired dynamics block is to achieve the desired rates and its derivatives. The desired dynamics block acts as a mapping function between the rate commands and the desired acceleration terms which are required form for the DI equations. There are no limitations to the desired dynamics block, it can take any form, usually the different forms of desired dynamics consist of proportional dynamics, proportional integral dynamics etc. [15, 17].

The desired dynamics block used to develop the DI control for longitudinal input and for lateral input for the Joker 3 helicopter is considered to be a 2nd order system that follows equation 2.3-3 and 2.3-4 respectively.

$$\ddot{q}_{des} + 2\zeta w\dot{q}_{des} + w^2 q_{des} = w^2 q_{in} \tag{2.3-3}$$

$$\ddot{p}_{des} + 2\zeta w\dot{p}_{des} + w^2 p_{des} = w^2 p_{in} \tag{2.3-4}$$

Where q_{in} is the pitch rate output and p_{in} is the roll rate output from the command inverter block. The system used for the desired dynamics block has a natural frequency w of 50rads/sec and a damping ratio ζ of 0.7 for both pitch and roll rate. It produces the desired pitch rate, the desired roll rate, the desired accelerations and its derivatives. These are further inputted to the next block which is the Dynamic Inversion block.

2.4 Dynamic Inversion Block

2.4.1 Simplified longitudinal controller for the Joker 3 helicopter

Longitudinal input to pitch rate behaves like a 2nd system given by the transfer function 2.4-1 [7]. In time domain it can be written as equation 2.4-2.

$$\frac{q}{\delta e} = \frac{w_q^{\,2}}{s^2 + 2\varsigma_q w_q s + w_q^{\,2}} \tag{2.4-1}$$

$$\ddot{q} + 2w_q\zeta_q\dot{q} + w_q^{\,2}q = w_q^{\,2}\delta_e \tag{2.4-2}$$

The $\ddot{q}$, $\dot{q}$ and q can be replaced by $\ddot{q}_{des}$, $\dot{q}_{des}$ obtained from section 2.3.2 and q_{meas} to give equation 2.4-3.

$$\ddot{q}_{des} + 2w_q\zeta_q\dot{q}_{des} + w_q^{\,2}q_{meas} = w_q^{\,2}\delta_e \tag{2.4-3}$$

Equation 2.4-3 can be rewritten in the DI control form:

$$\frac{1}{w_q^{\,2}}(\ddot{q}_{des} + 2w_q\zeta_q\dot{q}_{des} + w_q^{\,2}q_{meas}) = \delta_e \tag{2.4-4}$$

Response for the θ and the q using a DI controller are presented in Figure 4 and Figure 5. It can be observed from Figure 5 that the DI q follows the desired q perfectly. It is so good that the difference between both is not visible. The outer loop response for θ gives a settling time of 0.2 sec and a small overshoot of 5%.

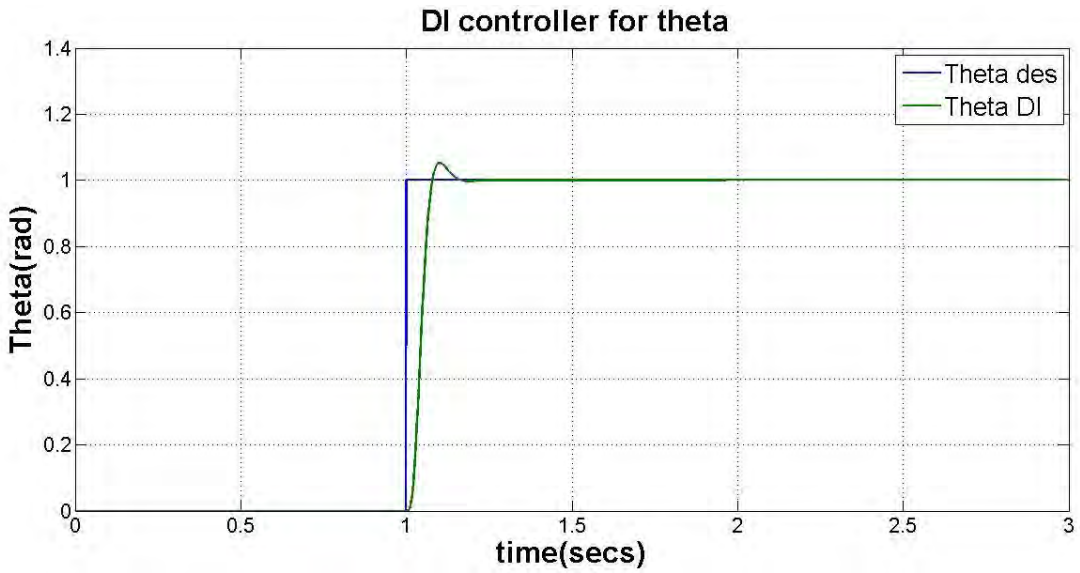

Figure 4: DI controller response for θ

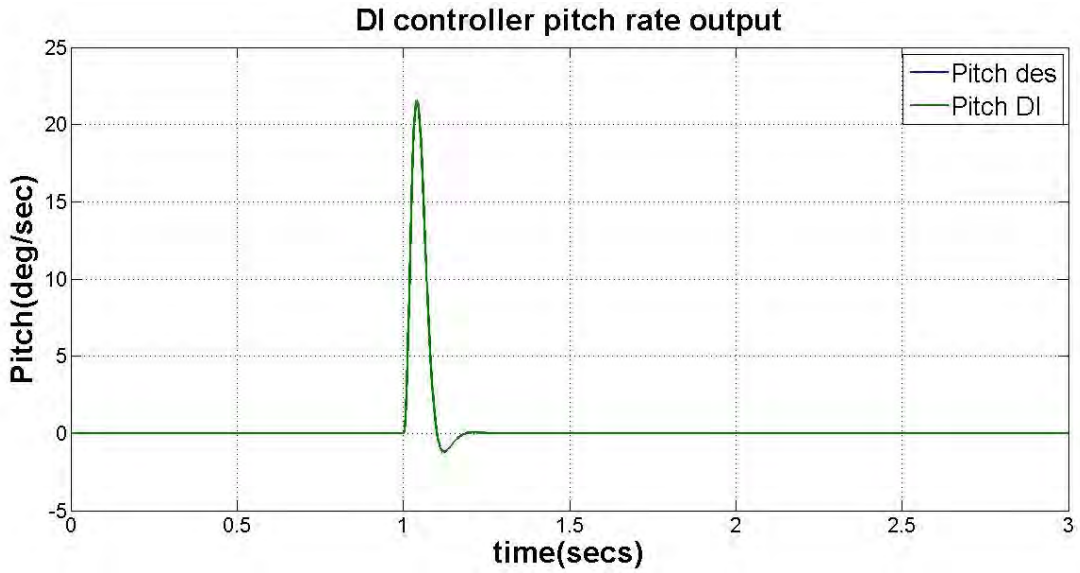

Figure 5: DI controller response for q

Similarly the DI controller needs to be developed for the roll rate of the Joker 3 helicopter. Section 2.4.2 describes the simplified lateral controller and plots the response for the DI controller developed for the roll rate in Figure 6 and Figure 7.

2.4.2 Simplified lateral controller for the Joker 3 Helicopter

Lateral input to roll rate behave like a 2nd order system given by the following transfer function 2.4-5 [7]. In time domain it can be written as equation 2.4-6.

$$\frac{p}{\delta a} = \frac{w_p{}^2}{s^2 + 2\varsigma_p w_p s + w_p{}^2} \tag{2.4-5}$$

$$\ddot{p} + 2w_p\zeta_p\dot{p} + w_p{}^2 p = w_p{}^2\delta_a \tag{2.4-6}$$

The $\ddot{p}, \dot{p}$ and p can be replaced by $\ddot{p}_{des}$, $\dot{p}_{des}$ obtained from the previous desired dynamics block and p_{meas} to give the equation 2.4-7.

$$\ddot{p}_{des} + 2w_p\zeta_p\dot{p}_{des} + w_p{}^2 p_{meas} = w_p{}^2\delta_e \tag{2.4-7}$$

Equation 2.4-7 can be rewritten in the DI control form:

$$\frac{1}{w_p{}^2}(\ddot{p}_{des} + 2w_p\zeta_p\dot{p}_{des} + w_q{}^2 p_{meas}) = \delta_a \tag{2.4-8}$$

The response for the φ and the p using a DI controller are presented in Figure 6 and Figure 7. Figure 6 is a plot of the outer loop response for φ which gives a settling time of 0.2 sec and a small overshoot of 5%. It can be observed from Figure 7 that the DI p follows the desired p perfectly; it shows a perfect match between both such that the difference is not visible.

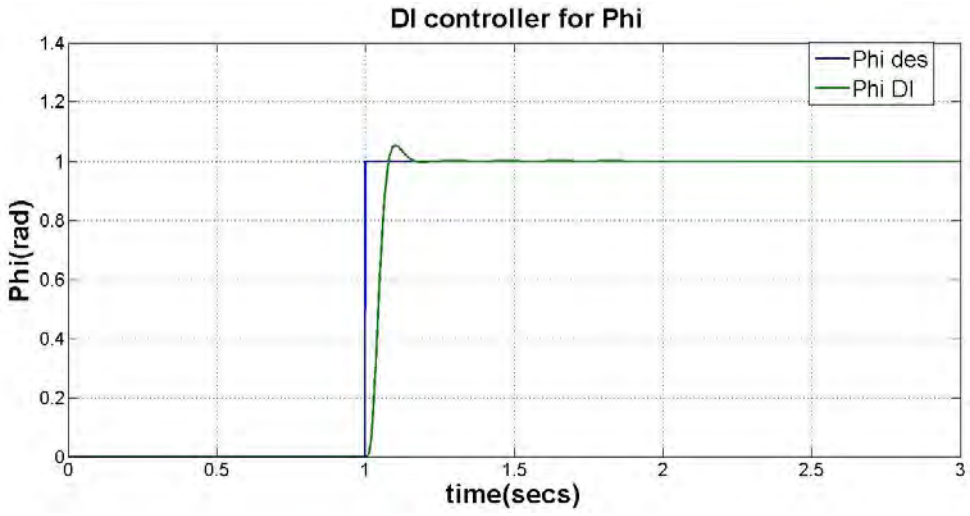

Figure 6: DI controller response for Φ

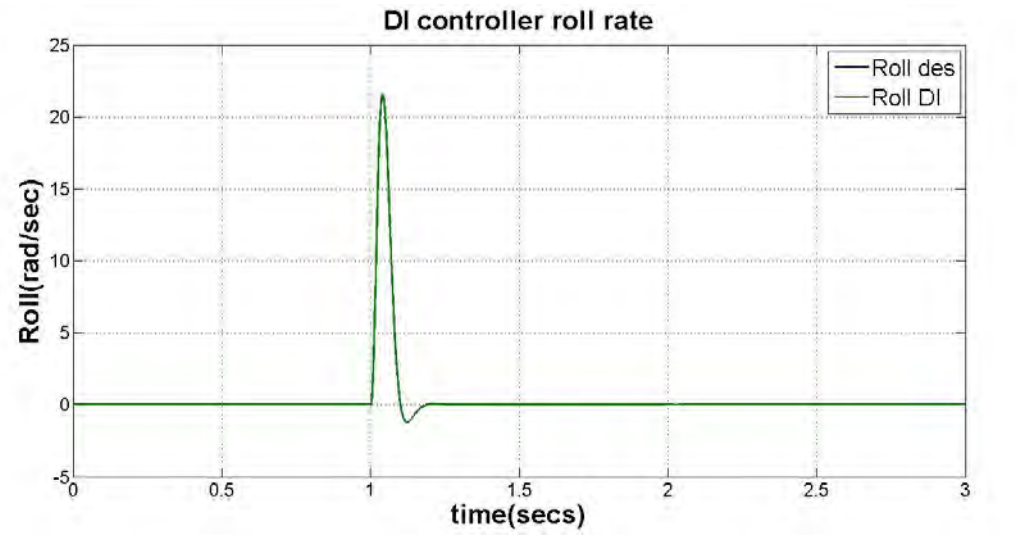

Figure 7: DI controller response for p

It can be seen from section 2.4 that DI results in perfect response but a few points need to be emphasized here, DI is essentially a special case of model following it requires the exact knowledge of the parameters to achieve good performance therefore any parametric uncertainty causes a degradation in the controllers performance. Figure 8 and Figure 9 show the response of φ and p respectively when uncertainties that amount to 10% in the natural frequency w_p and 5% in the damping ration ζ_p have been added resulting in φ and p degradation in performance.

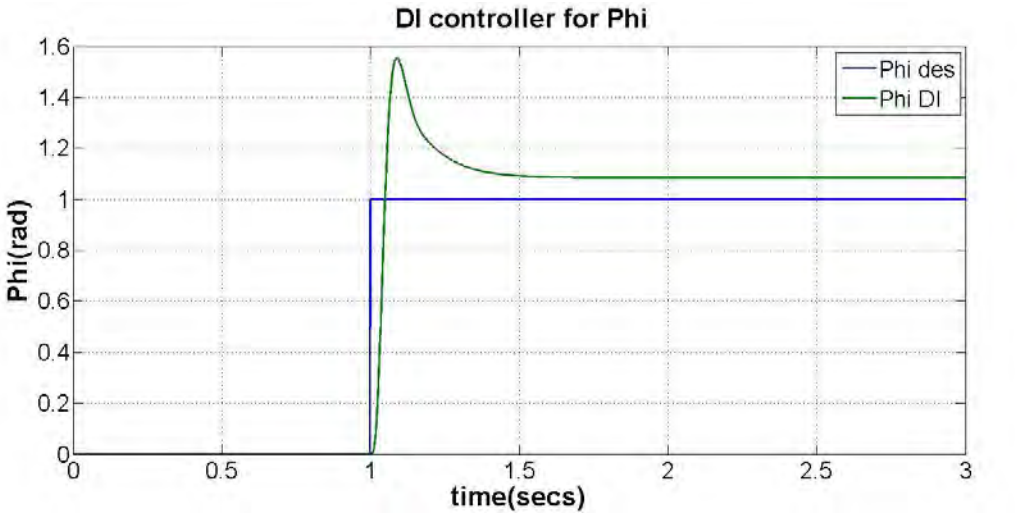

Figure 8: DI controller response for pitch rate when uncertainties are added

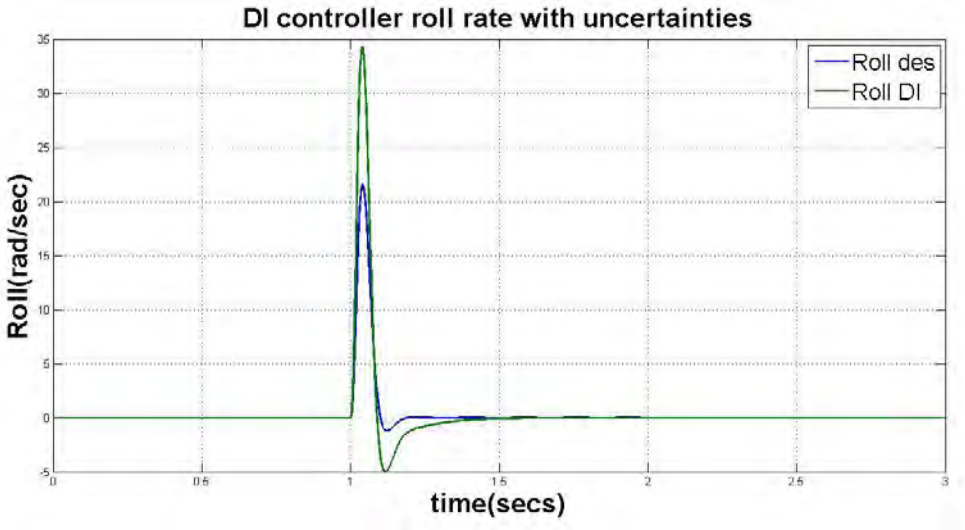

Figure 9: DI controller response for roll rate when uncertainties are added

Therefore robustness plays a significant process during the design process of the controller for Joker 3 helicopter. In the next 3 chapters three different robust controller have been designed to control the pitch rate and the roll rate of the Joker 3 helicopter.

Chapter 3

Design and Implementation of H∞ Controller

3.1 Introduction

Typically a control engineer is required to design a controller that will not only stabilize the plant but also satisfy certain performance criterion in the presence of noise, parametric variations and unmodelled plant dynamics [8, 18]. Multivariable design techniques were introduced in the 1960's, these techniques were mainly based on linear quadratic performance techniques, and the main focus of these techniques was good performance more than robustness. This led to a substantial research effort to develop a theory that would deal with the robustness issue on a feedback design basis thus introducing the H∞ technique. In the H∞ technique the designer beforehand specifies the uncertainties, such as additive perturbation and/or output disturbance that are most suited to the problem at hand [18, 19]. Only the structured (Parametric) uncertainties are considered in this case. By structured it means that the uncertainties can be described as a diagonal matrix with its diagonal elements equal to the uncertain terms [8, 18, 19, 20].

3.2 Steps followed to design H∞ controller

The following steps need to be followed to design and implement H∞ controller

1. System Modeling
2. Frequency Analysis of uncertain systems
3. Design requirements of a closed loop system
4. Selecting the weighing functions
5. Creating the open loop structure (system interconnection)
6. Optimal H∞ controller design
7. Robust control toolbox commands.
8. Analysis of Closed loop system with H∞ controller

3.3 System modeling

3.3.1 Dynamics of inputs to angular rate outputs

The dynamics of a longitudinal input to pitch rate output can be described by equation 2nd order differential equation [7, 41, 42]:

$$\frac{1}{w_q^2}\ddot{q} + \frac{2\zeta_q}{w_q}\dot{q} + q = \delta_e \tag{3.3-1}$$

The dynamics of a lateral input to roll rate can be described by the following 2nd order differential equation [11, 31]:

$$\frac{1}{w_p^2}\ddot{p} + \frac{2\zeta_p}{w_p}\dot{p} + p = \delta_a \tag{3.3-2}$$

The proceeding sections describe general framework of H∞ controller for pitch rate simultaneously roll rate controller would be developed. The second order system describing the longitudinal to pitch rate can be considered as a mass damper spring system where the following substitutions are considered $m = \frac{1}{w_q^2}, c = \frac{2\zeta_q}{w_q}, k = 1, u = \delta_e$ and $x = q$.

The differential equations can thus be written as:

$$m\ddot{x} + c\dot{x} + kx = u \tag{3.3-3}$$

$$\ddot{x} = \frac{1}{m}(-c\dot{x} - kx + u) \tag{3.3-4}$$

Figure 10 shows the block diagram representation of equation 3.3-4

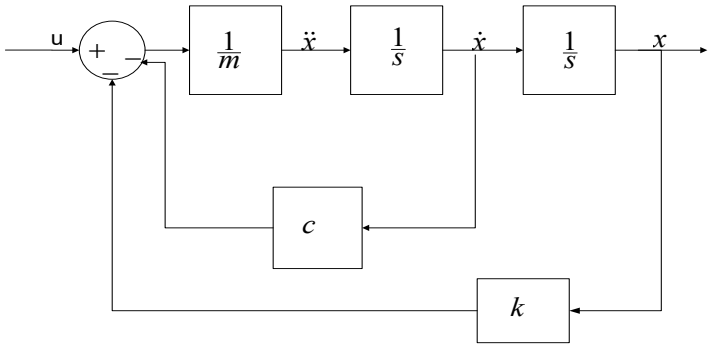

Figure 10: Block diagram representation of a 2nd order system [8]

3.3.2 Modeling the uncertainties

Basic idea in modeling an uncertain system is to isolate the known elements from the unknown elements in a feedback type connection called the linear fractional transformation (LFT) [21, 22, 23]. Practically the values of m, c and k are not known exactly but they are within certain limits of the nominal values of the parameters that are given as $\bar{m}$, $\bar{c}$ and $\bar{k}$. The values of m, c and k can be written as a function of their nominal value and uncertainty as given in equations 3.3-5, 3.3-6 and 3.3-7.

$$m = \bar{m}(1 + p_m \delta_m) \tag{3.3-5}$$

$$c = \bar{c}(1 + p_c \delta_c) \tag{3.3-6}$$

$$k = \bar{k}(1 + p_k \delta_k) \tag{3.3-7}$$

The three constants blocks in Figure 10 can be replaced by blocks in terms of $\bar{m}, \bar{c}, \bar{k}$, $p_m, p_c, p_k, \delta_m, \delta_c$ and δ_k. The 1st, 2nd and 3rd block formulation is given as:

The first block is given by equation 3.3-8 and can be rewritten as 3.3-9.

$$\frac{1}{m} = \frac{1}{\bar{m}(1 + p_m \delta_m)} \tag{3.3-8}$$

$$\frac{1}{m} = \frac{1}{\bar{m}(1 + p_m \delta_m)} = \frac{1}{\bar{m}} - \frac{p_m}{\bar{m}} \delta_m (1 + p_m \delta_m)^{-1} \tag{3.3-9}$$

Using LFT technique [1, 8] the following configuration is obtained:

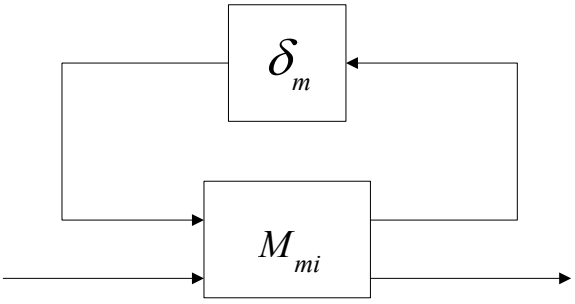

Figure 11: LFT representation of the 1st block [18, 27]

The upper LFT formulation is given as:

$$F_u(M_{mi}, \delta_m) = M_{22} + M_{21}\Delta(I - M_{11}\Delta)^{-1}M_{12} \tag{3.3-10}$$

Equation 3.3-8 can be compared with the upper LFT equation 3.3-10 to find the interconnected matrix M that doesn't have the uncertainty embedded in it. The matrix M_{mi} is given as:

$$M_{mi} = \begin{bmatrix} M_{11} & M_{12} \\ M_{21} & M_{22} \end{bmatrix} = \begin{bmatrix} -p_m & \frac{1}{\bar{m}} \\ -p_m & \frac{1}{\bar{m}} \end{bmatrix}$$

The second block can be written as equation 3.3-11

$$c = \bar{c} + \bar{c}p_c\delta_c \tag{3.3-11}$$

Using LFT technique the following configuration is obtained:

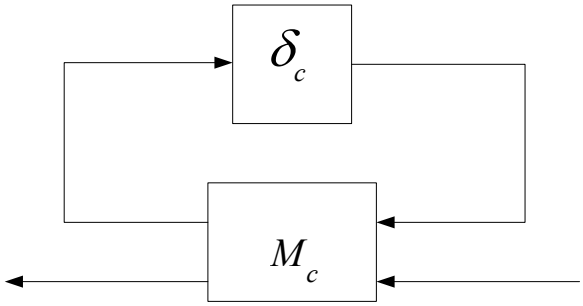

Figure 12: LFT representation of the 2nd block [18, 27]

3.3-11 is compared with the upper LFT formulation given in 3.3-10 to find the interconnected matrix M_c.

$$M_c = \begin{bmatrix} M_{11} & M_{12} \\ M_{21} & M_{22} \end{bmatrix} = \begin{bmatrix} 0 & \bar{c} \\ p_c & \bar{c} \end{bmatrix}$$

The third block can be written as equation 3.3-12

$$k = \bar{k}(1 + p_k\delta_k) = \bar{k} + \bar{k}p_k\delta_k \tag{3.3-12}$$

Figure 13 represent the configuration that is obtained using the LFT technique.

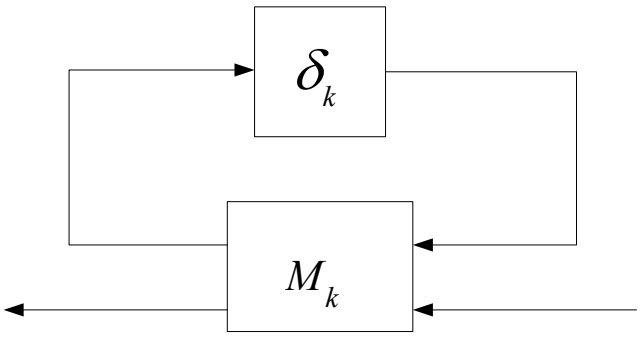

Figure 13: LFT representation of the 3rd block [18, 27]

3.3-12 is compared with the upper LFT formulation given in 3.3-10 to find the interconnected matrix M_k that has the following elements in it:

$$M_k = \begin{bmatrix} M_{11} & M_{12} \\ M_{21} & M_{22} \end{bmatrix} = \begin{bmatrix} 0 & \bar{k} \\ p_k & \bar{k} \end{bmatrix}$$

The system model as an LFT of the unknown real perturbations δ_m, δ_c and δ_k is represented in the Figures 11, 12 and 13 and denote the inputs and outputs of δm, δc and δk as y_m, y_c, y_k and u_m, u_c, u_k respectively.

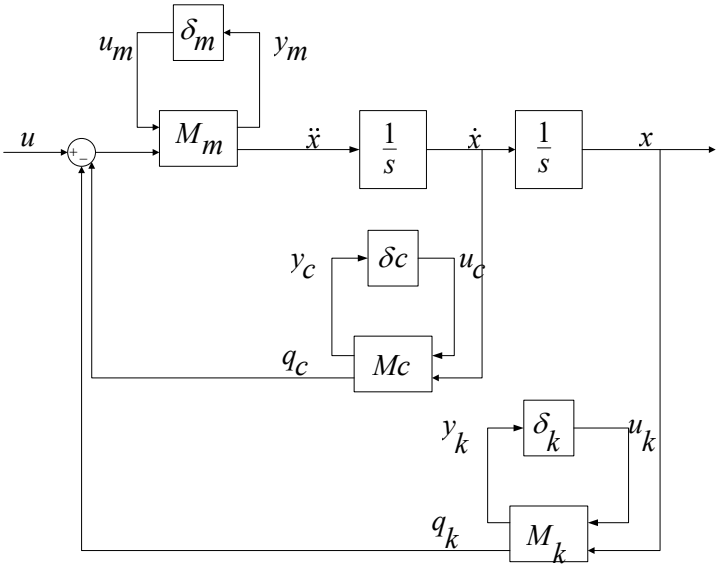

Figure 14 : Block diagram representation of 2nd order system with uncertainties [18]

The outputs from the first perturbation related to the inputs to the block M_{mi} can be written as:

$$\begin{bmatrix} y_m \\ \ddot{x} \end{bmatrix} = \begin{bmatrix} -p_m & \frac{1}{\bar{m}} \\ -p_m & \frac{1}{\bar{m}} \end{bmatrix} \begin{bmatrix} u_m \\ u - v_c - v_k \end{bmatrix}$$

The outputs from the second perturbation related to the inputs to the block M_c can be written as:

$$\begin{bmatrix} y_c \\ q_c \end{bmatrix} = \begin{bmatrix} 0 & \bar{c} \\ p_c & \bar{c} \end{bmatrix} \begin{bmatrix} u_c \\ \dot{x} \end{bmatrix}$$

The outputs from the third perturbation related to the inputs to the block M_k can be written as:

$$\begin{bmatrix} y_k \\ q_k \end{bmatrix} = \begin{bmatrix} 0 & \bar{k} \\ p_k & \bar{k} \end{bmatrix} \begin{bmatrix} u_k \\ x \end{bmatrix}$$

Figure 14 is used to obtain the following equations:

$$u_m = \delta_m y_m \tag{3.3-13}$$

$$u_c = \delta_c y_c \tag{3.3-14}$$

$$u_k = \delta_k y_k \tag{3.3-15}$$

By setting $x_1 = x$, $x_2 = \dot{x}$ and $y = x_1$ the following equations are obtained:

$$\dot{x}_1 = x_2 \tag{3.3-16}$$

$$\dot{x}_2 = \ddot{x} = -p_m u_m + \frac{1}{\bar{m}}(u - q_c - v_k) \tag{3.3-17}$$

$$y_m = -p_m u_m + \frac{1}{\bar{m}}(u - q_c - q_k) \tag{3.3-18}$$

$$y_c = \bar{c} x_2 \tag{3.3-19}$$

$$y_k = \bar{k} x_1 \tag{3.3-20}$$

$$q_c = p_c u_c + \bar{c} x_2 \tag{3.3-21}$$

$$q_k = p_k u_k + \bar{k} x_1 \tag{3.3-22}$$

Eliminating the intermediate variable q_c and q_k the equations 3.3-17, 3.3-18 can be rewritten as:

$$\dot{x}_2 = \frac{-\bar{k}}{\bar{m}} x_1 + \frac{-\bar{c}}{\bar{m}} x_2 - p_m u_m - \frac{p_c}{\bar{m}} u_c - \frac{p_k}{\bar{m}} u_k + \frac{u}{\bar{m}} \tag{3.3-23}$$

$$y_m = \frac{-\bar{k}}{\bar{m}} x_1 + \frac{-\bar{c}}{\bar{m}} x_2 - p_m u_m - \frac{p_c}{\bar{m}} u_c - \frac{p_k}{\bar{m}} u_k + \frac{u}{\bar{m}} \tag{3.3-24}$$

If we let G_{mds} denote the input/output dynamics of the system which also takes in account of the uncertainty of parameters. The inputs are given as u_m, u_c, u_k and u, the outputs are y_m, y_c, y_k, y and the states are given as x_1 and x_2.

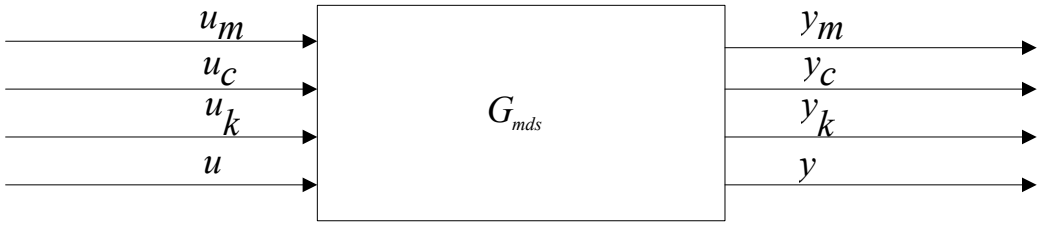

Figure 15: Input/Output block diagram of 2nd order system with uncertainties

The state space realization of G_{mds} is given as:

$$G_{mds} = \left[\begin{array}{c|cc} A & B_1 & B_2 \\ \hline C_1 & D_{11} & D_{12} \\ C_2 & D_{21} & D_{22} \end{array}\right]$$

The Equations governing the system dynamic behavior can be written as a system matrix:

$$\begin{bmatrix} \dot{x}_1 \\ \dot{x}_2 \\ y_m \\ y_c \\ y_k \\ y \end{bmatrix} = \left[\begin{array}{cc|ccc|c} 0 & 1 & 0 & 0 & 0 & 0 \\ \frac{-\bar{k}}{\bar{m}} & \frac{-\bar{c}}{\bar{m}} & -p_m & -\frac{p_c}{\bar{m}} & -\frac{p_k}{\bar{m}} & \frac{1}{\bar{m}} \\ \hline \frac{-\bar{k}}{\bar{m}} & \frac{-\bar{c}}{\bar{m}} & -p_m & -\frac{p_c}{\bar{m}} & -\frac{p_k}{\bar{m}} & \frac{1}{\bar{m}} \\ 0 & \bar{c} & 0 & 0 & 0 & 0 \\ \bar{k} & 0 & 0 & 0 & 0 & 0 \\ \hline 1 & 0 & 0 & 0 & 0 & 0 \end{array}\right] \begin{bmatrix} x_1 \\ x_2 \\ u_m \\ u_c \\ u_k \\ u \end{bmatrix}$$

$$\begin{bmatrix} u_m \\ u_c \\ u_k \end{bmatrix} = \begin{bmatrix} \delta_m & 0 & 0 \\ 0 & \delta_c & 0 \\ 0 & 0 & \delta_k \end{bmatrix} \begin{bmatrix} y_m \\ y_c \\ y_k \end{bmatrix}$$

Where A is a 2 by 2 matrix (*n* by *n* where *n* is the number of states)

$$A = \begin{bmatrix} 0 & 1 \\ \dfrac{-\bar{k}}{\bar{m}} & \dfrac{-\bar{c}}{\bar{m}} \end{bmatrix}$$

B_1 is a 2 by 3 matrix (*n* by *p* where *n* is the number of states and *p* is the number of inputs here the inputs are the 3 uncertain inputs)

$$B_1 = \begin{bmatrix} 0 & 0 & 0 \\ -p_m & -\dfrac{p_c}{\bar{m}} & -\dfrac{p_k}{\bar{m}} \end{bmatrix}$$

B_2 is a 2 by 1 matrix (*n* by *p* where *n* is the number of states and *p* is the number of input in this case it is the control input).

$$B_2 = \begin{bmatrix} 0 \\ \dfrac{1}{\bar{m}} \end{bmatrix}$$

C_1 is a 3 by 2 matrix (*q* by *n* where *q* represents the outputs from the uncertain block and *n* represents the states).

$$C_1 = \begin{bmatrix} \dfrac{-\bar{k}}{\bar{m}} & \dfrac{-\bar{c}}{\bar{m}} \\ 0 & \bar{c} \\ \bar{k} & 0 \end{bmatrix}$$

D_{11} is a 3 by 3 matrix which shows the relation between the input and output of the perturbations.

$$D_{11} = \begin{bmatrix} -p_m & -\dfrac{p_c}{\bar{m}} & -\dfrac{p_k}{\bar{m}} \\ 0 & 0 & 0 \\ 0 & 0 & 0 \end{bmatrix}$$

D_{12} is a 3 by 1 matrix which shows the relation between the uncertainty output and the control input *u*.

$$D_{12} = \begin{bmatrix} \frac{1}{\bar{m}} \\ 0 \\ 0 \\ \end{bmatrix}$$

D_{21} is a 1 by 3 matrix (it's all zero because it links the *y* with the inputs for uncertainty, since the output has no link to it therefore it's a null row vector).

$$D_{21} = \begin{bmatrix} 0 & 0 & 0 \end{bmatrix}$$

D_{22} 1 by 1 matrix (*q* by *q* here the main output is 1 also there is no connection between the measurement and the control input therefore its 0).

$$D_{22} = \begin{bmatrix} 0 \end{bmatrix}$$

The uncertain behavior of the original system can be described by the below diagram that shows upper LFT formulation for the system and the uncertainties block [8].

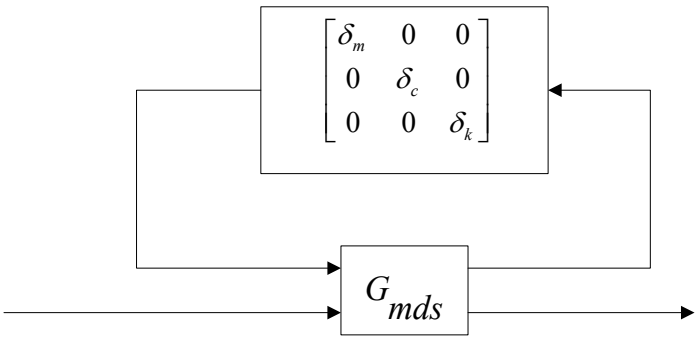

Figure 16: LFT representation of a 2nd order system with uncertainties [18]

3.4 Frequency analysis of uncertain systems

In order to compute the frequency response of the open perturbed system MATLAB was used for different values of perturbations, three values of each perturbation are chosen that lie within the range from -1 to 1, then the open loop transfer function matrix is found and the corresponding frequency response is plotted in Figure 17 for pitch rate and Figure18 for roll rate [8, 24].

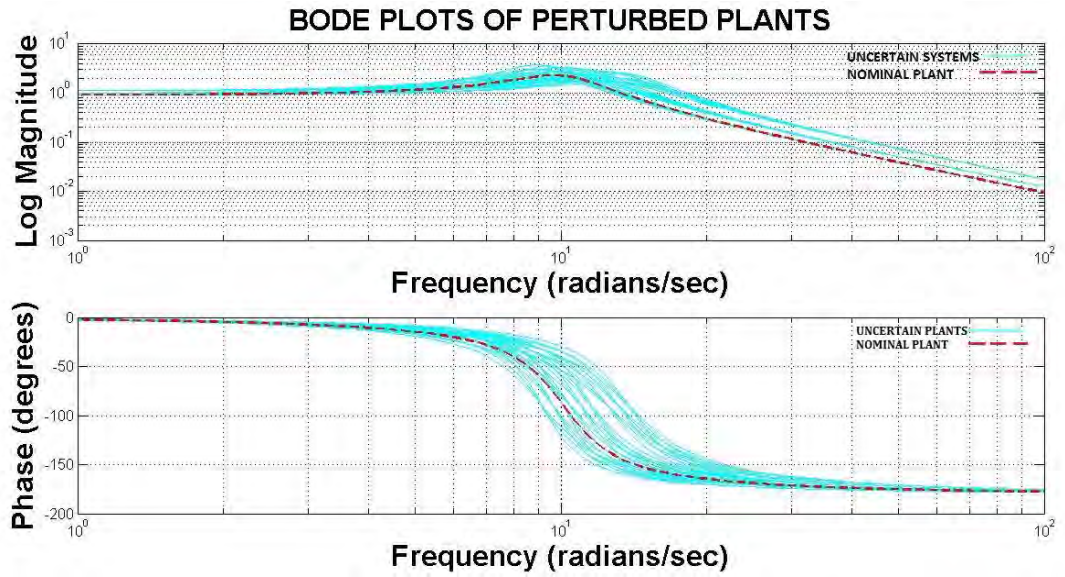

Figure 17: Frequency analysis of open loop perturbed pitch rate

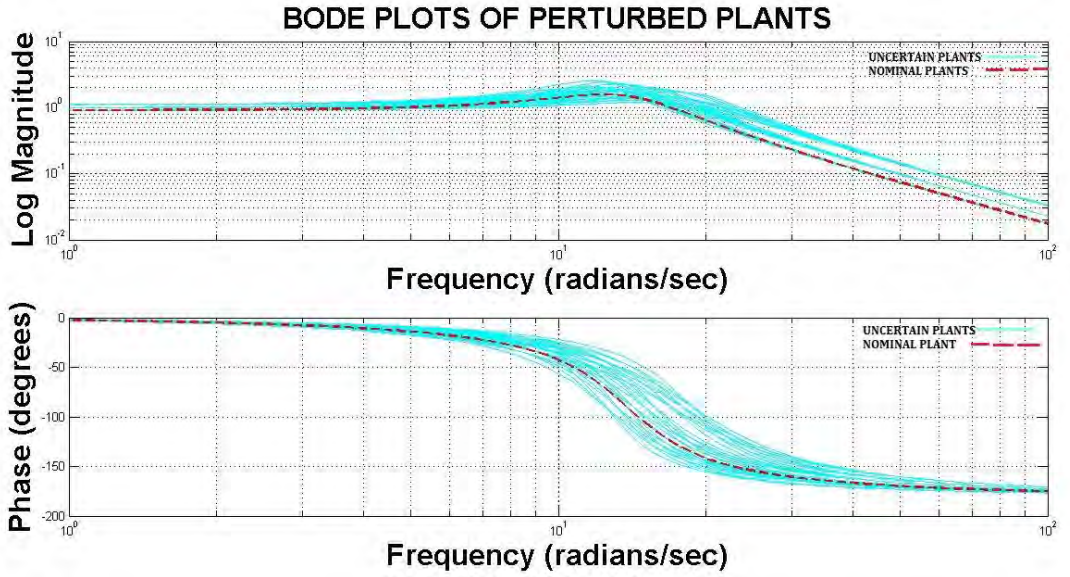

Figure 18: Frequency analysis of open loop perturbed roll rate

3.5 Design requirements of a closed loop system

The main design objective of this H∞ optimization is to find a linear output feedback control $u(s) = K(s)y(s)$ such that the following properties of the closed loop system are ensured.

Nominal Stability and Performance:

1. The controller designed should make the closed loop system internally stable and for the nominal plant Gmds the closed loop performance should be stable.

2. The performance criterion is mixed sensitivity i.e. S over KS design [8, 18, 19].

3.5.1 Mixed sensitivity function

It's not recommended for an engineer to develop a controller that minimizes just a single cost function. In this thesis a controller that minimizes the mixed sensitivity function (S over KS) [18, 20] i.e. providing a good tracking as well as restricting the control effort *u* is developed.

$$\min_{Kstabilizing} \left\| \begin{matrix} (I+GK)^{-1} \\ K(I+GK)^{-1} \end{matrix} \right\|$$

Consider the block diagram as shown in Figure 19, *G* represents the model of the helicopter and *K* is the controller that needs to be developed.

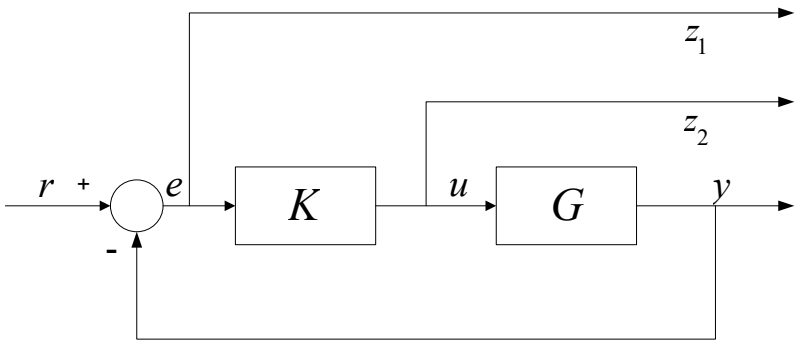

Figure 19: Closed loop system with unity feedback [19]

Good tracking performance/ Disturbance attenuation is one of the most important performance criterions. To achieve good tracking performance the transfer function that represents the tracking error with respect to the reference needs to be minimized. Finding the transfer function of the tracking error with respect to the reference input:

The error can be deduced from the block diagram as:

$$e = r - y \tag{3.5-1}$$

Where the output is given as:

$$y = Gu = GKe \tag{3.5-2}$$

Therefore the error can be written as:

$$e(1 + GK) = r \tag{3.5-3}$$

Thus the transfer function that represents the tracking error with respect to the reference input is given as:

$$Ter = (I + GK)^{-1} \tag{3.5-4}$$

This transfer function is also known as sensitivity function and it needs to be minimized to reduce the tracking error. The second performance criterion that needs to be achieved is reduced control effort so as to avoid the saturation of servomechanism. Finding the transfer function that represents the control input *u* with respect to the reference signal. The control input from the block diagram Figure 19 is given as:

$$u = Ke \tag{3.5-5}$$

The error given in equation 3.5-1 can be given by the equation 3.5-6

$$e = r - Gu \tag{3.5-6}$$

Therefore, the control input can be given by the equation 3.5-7

$$u(I + GK) = Kr \tag{3.5-7}$$

Thus, the transfer function that represents the control effort with respect to the reference input is given by 3.5-8 and is known as KS function and needs to be minimized to avoid saturation.

$$Tur = K(I + GK)^{-1} \tag{3.5-8}$$

3.6 Weighting functions

3.6.1 Selecting the weighting function

H∞ control is a design technique with a state space computational solution that utilizes frequency dependent weighting function to tune the controller's performance and robustness characteristics. The weights on the input and output variables are chosen to

reflect the frequency dependence of the respective signals and performance criterion [25, 26]. These input and output weighting functions are defined as rational, stable, minimum phase transfer functions. Also they are defined as such that the input and output energies are normalized to one. Figure 20 shows a closed loop system with weighing functions integrated to it.

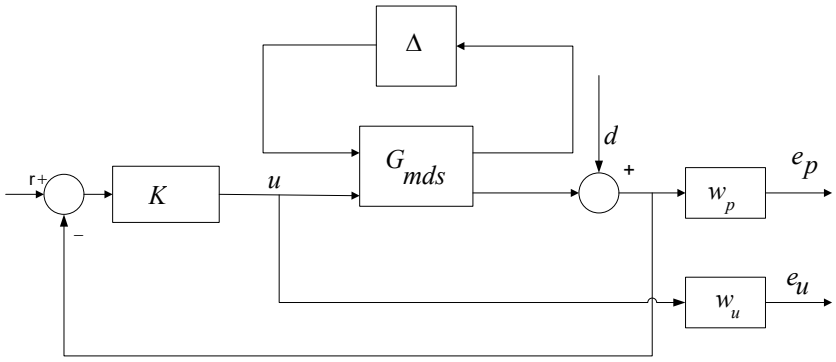

Figure 20: Closed loop system with weighting functions [18, 19]

The performance criteria of good tracking is now formulated with the weighting functions integrated to the closed loop system as shown in Figure 20. Finding the transfer function that represents the e_p with respect to the disturbance [8, 18]:
The error in performance e_p can be calculated from Figure 20.

$$e_p = w_p(Gu + d) \tag{3.6-1}$$

The control input is given by the equation 3.6-2

$$u = Ke \tag{3.6-2}$$

Considering the reference input to be zero the error in performance can be given by the equation 3.6-3

$$e_p = w_p(GK(-y) + d) \tag{3.6-3}$$

Thus, the transfer function that represents the error in performance with respect to the disturbance input is given by the equation 3.6-4

$$Te_p d = w_p(I + GK)^{-1} \tag{3.6-4}$$

The performance criteria of restricted control effort is again formulated with weighting functions integrated to the closed loop system as shown in Figure 20. Finding the transfer function that represents the control input u with the weighing function with respect to the

disturbance. The error in control effort e_u can be calculated from Figure 20. Since the reference input is zero the error in control input is given by 3.6-6.

$$e_u = w_u K e \tag{3.6-5}$$

$$e_u = -w_u.K(Gu + d) \tag{3.6-6}$$

The transfer function that represents the error in performance with respect to the disturbance input is given by 3.6-7.

$$Te_u d = -w_u K(I + GK)^{-1} \tag{3.6-7}$$

The mixed sensitivity function that needs to be minimized can be written as:

$$\left\| \begin{matrix} w_p(I + GK)^{-1} \\ w_u K(I + GK)^{-1} \end{matrix} \right\| < 1$$

The weighting functions w_p and w_u are chosen to represent the frequency characteristics of external (output) disturbance d and performance requirement (including consideration of control-effort constraint) respectively they are used to reflect the relative significance of the performance requirement over different frequency ranges. Satisfaction of the norm proves that the closed loop system that consists of the controller successfully rejects the disturbance and achieves the desired performance mainly limiting the control effort.

3.6.2 Weighting functions for pitch and roll rate

For pitch rate and roll rate the weighting functions for performance and disturbance attenuation have been selected such that apart from disturbance rejection, good transient response for the nominal system is also ensured. The settling time is less than 10sec and the overshoot is less than 20%. The weighting transfer functions for pitch rate are given as:

$$w_p(s) = 0.95\frac{s^2 + 6.5s + 30}{s^2 + 2.55s + 0.01}$$

$$w_u = 0.01$$

The weighting transfer functions for roll rate is given as:

$$w_p(s) = 0.95\frac{s^2 + 7s + 27}{s^2 + 3s + 0.01}$$

$$w_u = 0.01$$

The inverse of the weighing functions are calculated and shown in Figure 21 for pitch rate and in Figure 22 for roll rate. As specified in the mixed sensitivity function norm in order to achieve the desired disturbance rejection or to reduce the tracking error it is necessary that the following inequality is satisfied.

$$\left\| w_p (I + GK)^{-1} \right\| < 1$$

This occurs if and only if for all frequencies the maximum value of the sensitivity function for all frequencies is less than the inverse of the weighting function which is given as $\sigma[(I + GK)^{-1}(jw)] < \left|\frac{1}{w_p}\right|$

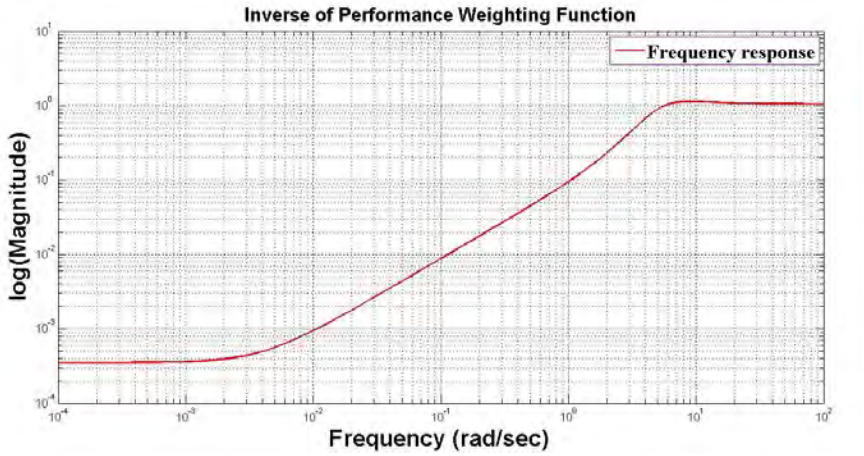

Figure 21: Singular values of 1/Wp for pitch rate

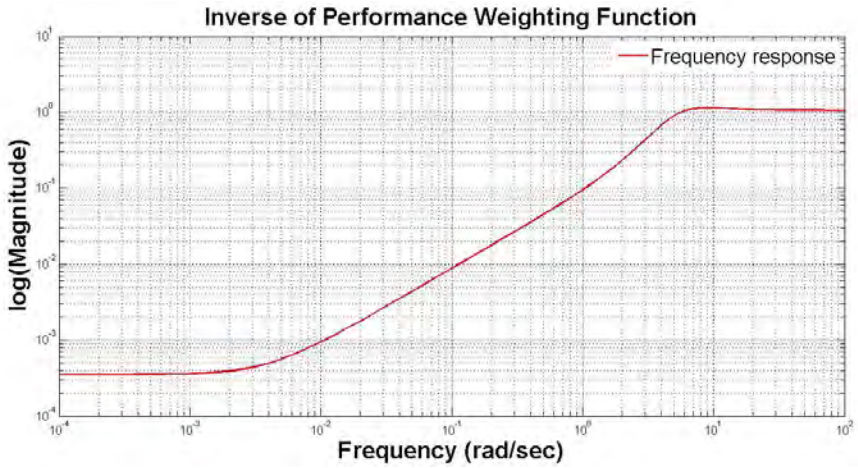

Figure 22: Singular values of 1/Wp for roll rate

3.7 System interconnection

The state space representation of the generalized (interconnected) system *P* [8, 18, 19, 25] is given in the following equations.

$$\dot{x} = Ax(t) + B_1 w(t) + B_2 u(t) \tag{3.7-1}$$

$$\dot{z} = C_1 x(t) + D_{11} w(t) + D_{12} u(t) \tag{3.7-2}$$

$$y = C_2 x(t) + D_{21} w(t) + D_{22} u(t) \tag{3.7-3}$$

Here $x(t) \in R^n$ is the state vector, $w(t) \in R^{m1}$ is the exogenous input vector whereas $u(t) \in R^{m2}$ is the control input vector, $z(t) \in R^{p1}$ is the error output vector and $y(t) \in R^{p2}$ is the measurement vector. The state space realization of P(s) is given as:

$$P(s) = \left[\begin{array}{c|cc} A & B_1 & B_2 \\ \hline C_1 & D_{11} & D_{12} \\ C_2 & D_{21} & D_{22} \end{array}\right]$$

In this section the open-loop structure *P* is developed using the sysic command from MATLAB Robust Control Tool box [8, 24]. Figure 23 shows the structure of the open-loop system.

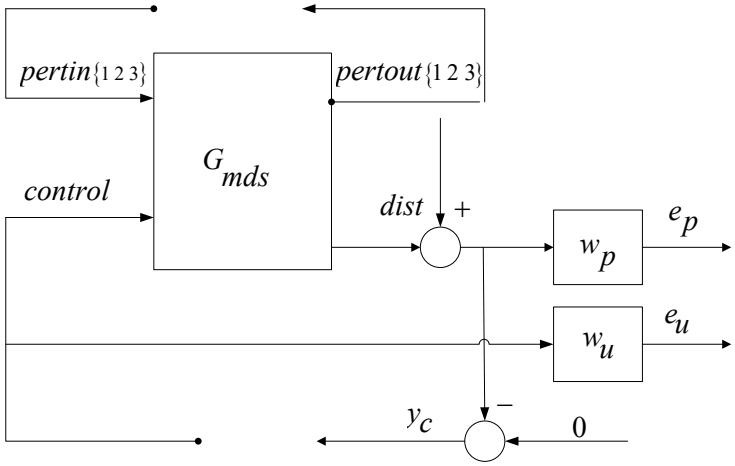

Figure 23: Open loop structure [18]

As shown in Figure 23 open loop structure has three main inputs: perturbation entering *pertin*, *control* and *disturbance* whereas the perturbation input itself has three elements therefore a total of five inputs are present whereas the outputs are: perturations going out *pertout*, e_p, e_u and y_c. Where *pertout* is the output due to the perturbation input therefore, it has three elements, e_p is the effect of the disturbance and e_u is the control effort. The main performance criterion is to reduce infinity norm of the transfer function from d to e_p and e_u. It needs to be noted that y_c is taken negative because the robust control toolbox creates positive feedback. The open loop system has five inputs, six outputs as described above and four states.

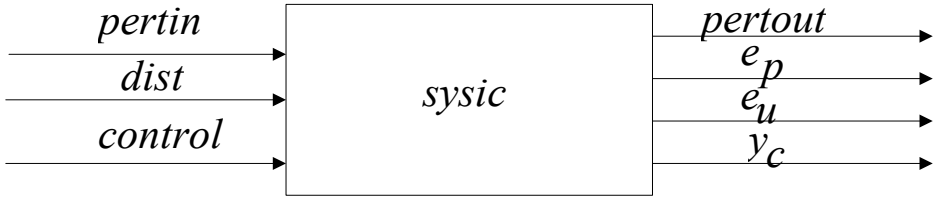

Figure 24: Generalized block diagram of open loop structure

The open loop structure gives the following matrix which is a system matrix:

$$\begin{bmatrix} \dot{x}_1 \\ \dot{x}_2 \\ \dot{s}_1 \\ \dot{s}_2 \\ y_m \\ y_c \\ y_k \\ e\_p \\ e\_u \\ y \end{bmatrix} = \left[\begin{array}{cccc|cccc|c} 0 & 1 & 0 & 0 & 0 & 0 & 0 & 0 & 0 \\ -\frac{\bar{k}}{\bar{m}} & -\frac{\bar{c}}{\bar{m}} & 0 & 0 & -p_m & -\frac{p_c}{\bar{m}} & -\frac{p_k}{\bar{m}} & 0 & \frac{1}{\bar{m}} \\ B_1 & 0 & A_{11} & A_{12} & 0 & 0 & 0 & B_1 & 0 \\ B_2 & 0 & A_{21} & A_{22} & 0 & 0 & 0 & B_2 & 0 \\ \hline -\frac{\bar{k}}{\bar{m}} & -\frac{\bar{c}}{\bar{m}} & 0 & 0 & -p_m & -\frac{p_c}{\bar{m}} & -\frac{p_k}{\bar{m}} & 0 & \frac{1}{\bar{m}} \\ 0 & c & 0 & 0 & 0 & 0 & 0 & 0 & 0 \\ k & 0 & 0 & 0 & 0 & 0 & 0 & 0 & 0 \\ D & 0 & C_1 & C_2 & 0 & 0 & 0 & D & 0 \\ 0 & 0 & 0 & 0 & 0 & 0 & 0 & -w_u & 0 \\ \hline -1 & 0 & 0 & 0 & 0 & 0 & 0 & -1 & 0 \end{array}\right] \begin{bmatrix} x_1 \\ x_2 \\ s_1 \\ s_2 \\ u_m \\ u_c \\ u_k \\ d \\ u \end{bmatrix}$$

Here s_1 and s_2 are the states that are introduced because of the weighting function w_p, the system matrix equations of w_p are given as:

$$\begin{bmatrix} \dot{s}_1 \\ \dot{s}_2 \end{bmatrix} = \begin{bmatrix} A_{11} & A_{12} \\ A_{21} & A_{22} \end{bmatrix} \begin{bmatrix} s_1 \\ s_2 \end{bmatrix} + \begin{bmatrix} B1 \\ B2 \end{bmatrix} (x_1 + d)$$

$$e\_p = \begin{bmatrix} C_1 & C_2 \end{bmatrix} \begin{bmatrix} s_1 \\ s_2 \end{bmatrix} + [D](x_1 + d)$$

3.7.1 Open loop interconnected matrix for pitch rate

The open loop interconnected matrix for pitch rate is calculated for the Joker 3 helicopter and gives the following result:

$$Ppitch = \begin{bmatrix} 0 & 1 & 0 & 0 & 0 & 0 & 0 & 0 & 0 \\ -121.00 & -4.40 & 0 & 0 & -0.30 & -24.20 & -12.10 & 0 & 121.00 \\ -3.3731 & 0 & -0.0040 & -0.0065 & 0 & 0 & 0 & -3.3731 & 0 \\ 2.7528 & 0 & 0.0065 & -2.4960 & 0 & 0 & 0 & 2.7528 & 0 \\ -121.00 & -4.40 & 0 & 0 & -0.30 & -24.20 & -12.10 & 0 & 121.00 \\ 0 & 0.03 & 0 & 0 & 0 & 0 & 0 & 0 & 0 \\ 1.00 & 0 & 0 & 0 & 0 & 0 & 0 & 0 & 0 \\ 0.95 & 0 & -3.37 & -2.75 & 0 & 0 & 0 & 0.95 & 0 \\ 0 & 0 & 0 & 0 & 0 & 0 & 0 & 0 & -0.01 \\ -1.00 & 0 & 0 & 0 & 0 & 0 & 0 & -1.00 & 0 \end{bmatrix}$$

3.7.2 Open loop interconnected matrix for roll rate

The open loop interconnected matrix for pitch rate is calculated for the Joker 3 helicopter and gives the following result:

$$Proll = \begin{bmatrix} 0 & 1.00 & 0 & 0 & 0 & 0 & 0 & 0 & 0 \\ -225.00 & -9.00 & 0 & 0 & -0.300 & -45.00 & -22.50 & 0 & 225.00 \\ -3.34 & 0 & -0.0039 & -0.0063 & 0 & 0 & 0 & -3.34 & 0 \\ 2.6682 & 0 & 0.0063 & -2.546 & 0 & 0 & 0 & 2.66 & 0 \\ -225.00 & -9.00 & 0 & 0 & -0.30 & -45.00 & -22.50 & 0 & 225.00 \\ 0 & 0.04 & 0 & 0 & 0 & 0 & 0 & 0 & 0 \\ 1.00 & 0 & 0 & 0 & 0 & 0 & 0 & 0 & 0 \\ 0.95 & 0 & -3.34 & -2.66 & 0 & 0 & 0 & 0.95 & 0 \\ 0 & 0 & 0 & 0 & 0 & 0 & 0 & 0 & -0.01 \\ -1.00 & 0 & 0 & 0 & 0 & 0 & 0 & 0 & -1.00 \end{bmatrix}$$

3.8 Optimal H∞ controller design:

A control system is robust if it remains stable and achieves certain performance criteria in the presence of possible uncertainties. The robust design is to find a controller such that the closed loop system is robust.

3.8.1 H∞ Controller design theory

The H∞ solution formulae uses solutions of two ARE (Algebraic Ricatti Equations). The Algebraic Ricatti Equation are introduced first; basically ARE is a matrix quadratic equation non-linear in nature with a quadratic term, two linear terms and a constant term. It usually arises in optimal control problems for continuous or discrete systems. In such a problem, one cares about the value of some variable of interest arbitrarily far into the future, and one must optimally choose a value of a controlled variable right now, knowing that one will also behave optimally at all times in the future. The optimal current values of the problem's control variables at any time can be found using the solution of the Riccati equation and the current observations on evolving state variables. The Algebraic Riccati equation is given in equation [8, 19].

$$E^T X + XE - XWX + Q = 0 \tag{3.8-1}$$

Here E, W, Q are real n by n matrix and W and Q are symmetric matrices. To each Riccati Equation belongs the following Hamiltonian matrix:

$$H = \begin{bmatrix} E & -W \\ -Q & -E^T \end{bmatrix}$$

The special property of H is that if Λ is an eigenvalue of H then so is – Λ. Specifically, if H has no eigenvalues on the imaginary axis, then n of the eigenvalues of H are in the open left half plane and the remaining are in the open right half plane. Let U be the matrix of eigenvectors of H ordered in such a way that the first n columns starting from the left correspond to eigenvalues in Re s<0 and the remaining n columns correspond to eigenvalues in Re s>0. Partitioning the matrix into four n by n block matrix:

$$U = \begin{bmatrix} U_{11} & U_{12} \\ U_{21} & U_{22} \end{bmatrix}$$

If U_{11} is non-singular, solution of the Riccati equation X is given as $X = U_{11}U_{21}^{-1}$.
Therefore, a special class of Hamiltonian matrices that exhibit the following twin properties are required.

- H has no eigenvalues on the imaginary axis.
- U_{11} is non- singular.

The following points need to be kept in consideration if $H \in Dom(Ric)$ that is if H possesses the above twin properties and $X = Ric(H)$ that is X is a solution of Riccati Equation then the following are also true [8, 18, 19].

- X is symmetric.
- X is the solution to the Riccati Equation 3.8-1.
- X shows signs definite properties.
- $A - WX$ is stable.

Also let B and C be full rank matrices with $W = BB^T$ where the rank of W is equivalent to the rank of B and $Q = CC^T$ where the rank of Q is equivalent to the rank of C. Therefore H can be redefined as:

$$H = \begin{bmatrix} E & -BB^T \\ CC^T & -E^T \end{bmatrix}$$

The sufficiency conditions in reference to the Riccati equation (3.8-1) are given as:

- If (A, B) is controllable, then there exists a solution $X \geq 0$ (X would be positive semi definite).
- If (A, B) is controllable and (C, A) is observable then there exist a unique solution $X > 0$ and further it is a stabilizing solution in the sense that $A - BB^T X$ is asymptotically stable.

Therefore if X is defined as the stabilizing solution of the Riccati equation then it can be denoted as:

$$X = Ric\begin{bmatrix} E & -W \\ -Q & -E^T \end{bmatrix}$$

Also [10, 27] defines:

$$R_n = D_x^T D_x - \begin{bmatrix} \gamma^2 I_{m_1} & 0 \\ 0 & 0 \end{bmatrix} \tag{3.8-2}$$

$$\tilde{R}_n = D_y^T D_y - \begin{bmatrix} \gamma^2 I_{p_1} & 0 \\ 0 & 0 \end{bmatrix} \tag{3.8-3}$$

$$where\ D_x = \begin{bmatrix} D_{11} & D_{12} \end{bmatrix} \text{ and } D_y = \begin{bmatrix} D_{11} \\ D_{21} \end{bmatrix}$$

Assuming that R_n and $\tilde{R}_n$ are non- singular, two Hamiltonian matrices H and J are defined as [10, 27]:

$$H = \begin{bmatrix} A & 0 \\ -C_1 C_1^T & -A^T \end{bmatrix} - \begin{bmatrix} B \\ -C_1^T D_x \end{bmatrix} R_n^{-1} \begin{bmatrix} D_x^T C_1 & B^T \end{bmatrix} \tag{3.8-4}$$

$$J = \begin{bmatrix} A^T & 0 \\ -B_1 B_1^T & -A \end{bmatrix} - \begin{bmatrix} C^T \\ -B_1 D_y^T \end{bmatrix} \tilde{R}_n^{-1} \begin{bmatrix} D_y B_1^T & C \end{bmatrix} \tag{3.8-5}$$

Also the solution of the above Hamiltonian matrices that represent the Riccati Equations can be given as $X = Ric\ (H)$ and $Y = Ric\ (J)$. Based on X and Y, a state feedback matrix F and an observer gain matrix L can be constructed, which is used in the solution formulae.

$$F = -R_n^{-1}(D_x^T C_1 + B^T X) = \begin{bmatrix} F_1 \\ F_2 \end{bmatrix} = \begin{bmatrix} F_{11} \\ F_{12} \\ F_2 \end{bmatrix} \tag{3.8-6}$$

$$L = -(B_1 D_y^T + Y C^T)\tilde{R}_n^{-1} = \begin{bmatrix} L_1 & L_2 \end{bmatrix} = \begin{bmatrix} L_{11} & L_{12} & L_2 \end{bmatrix} \tag{3.8-7}$$

[18] derived necessary and sufficient conditions for the existence of an H∞ suboptimal solution and further parameterized all such controllers. The results are obtained under the following assumptions for P.

1. (A, B_2) is stabilizable and (C_2, A) is detectable.
2. D_{12} is full column rank and D_{21} is full row rank.
3. $\begin{bmatrix} A - jwI & B_2 \\ C_1 & D_{12} \end{bmatrix}$ Has a full rank for all values of w.
4. $\begin{bmatrix} A - jwI & B_1 \\ C_2 & D_{21} \end{bmatrix}$ Has a full rank for all values of w.

Assumption 1 is necessary and sufficient for the existence of admissible controllers. Assumption 2 is merely required for normalization purpose and does not have any other significance. Assumptions 3 and 4 are required to ensure that the Ricatti Equations have stabilizing solutions. Suppose P(s) satisfies the above given assumptions [8] then:

1. There exists an internally stabilizing controller K(s) such that $\|F_L(P,K)\|_\infty < \gamma$ if and only if $\gamma > \max(\bar{\sigma}[D_{1111}, D_{1112}], \bar{\sigma}[D_{1111}{}^T, D_{1121}{}^T])$.

2. There exist stabilizing solutions $X \geq 0$ and $Y \geq 0$ satisfying the two AREs corresponding to the Hamiltonian matrices H and J, respectively, and such that $\rho(XY) < \gamma^2$ where ρ (▪) denotes the spectral radius.

3. Given that the conditions of part (a) and (b) are satisfied, then all rational, internally stabilizing controllers, K(s), satisfying $\|F_L(P,K)\|_\infty < \gamma$ are given by $K(s) = F_l(M, \phi)$ For any rational $\phi(s) \in H_\infty$ such that $\|\Phi(s)\|_\infty < \gamma$ where M(s) has the realization:

$$M(s) = \left[\begin{array}{c|cc} \hat{A} & \hat{B}_1 & \hat{B}_2 \\ \hline \hat{C}_1 & \hat{D}_{11} & \hat{D}_{12} \\ \hat{C}_2 & \hat{D}_{21} & \hat{D}_{22} \end{array}\right]$$

The elements of M can be found out in the following way:

$$\hat{D}_{11} = -D_{1121} D_{1111}{}^T (\gamma^2 I - D_{1111} D_{1111}{}^T)^{-1} D_{1112} - D_{1122} \tag{3.8-8}$$

Where $\hat{D}_{12} \in R^{m_2 \times m_2}$ and $\hat{D}_{21} \in R^{p_2 \times p_2}$ are any matrices satisfying the two equations 3.8-9 and 3.8-10.

$$\hat{D}_{12} \hat{D}_{12}^T = I - D_{1121} (\gamma^2 I - D_{1111} D_{1111}{}^T)^{-1} D_{1121}{}^T \tag{3.8-9}$$

$$\hat{D}_{21}^{T}\hat{D}_{21} = I - D_{1112}{}^{T}(\gamma^2 I - D_{1111}D_{1111}{}^{T})^{-1}D_{1112} \tag{3.8-10}$$

The matrix elements can therefore, be calculated as [10, 27]:

$$\hat{A} = A + BF - \hat{B}_1(C_2 + F_{12}) \tag{3.8-11}$$

$$\hat{B}_1 = -ZL_2 + Z(B_2 + L_{12})\hat{D}_{11} \tag{3.8-12}$$

$$\hat{B}_2 = Z(B_2 + L_{12})\hat{D}_{12} \tag{3.8-13}$$

$$\hat{C}_1 = F_2 - \hat{D}_{11}(C_2 + F_{12}) \tag{3.8-14}$$

$$\hat{C}_2 = -\hat{D}_{21}(C_2 + F_{12}) \tag{3.8-15}$$

$$Z = (I - \gamma^{-2}YX)^{-1} \tag{3.8-16}$$

When $\varphi(s) = 0$ is chosen, the corresponding suboptimal controller is called the central controller that is widely used in the H∞ optimal design and has the state-space form:

$$K_o(s) = \begin{bmatrix} \hat{A} & \hat{B}_1 \\ \hat{C}_1 & \hat{D}_{11} \end{bmatrix}$$

3.9 Robust control toolbox commands (MATLAB)

An H_∞ suboptimal controller is the first controller to be designed for the connection of type system. The standard state-space technique to calculate H∞ output feedback controllers is to select a value of γ (positive constant) and determine if there exists a controller *K* such that $||F_L(P,K)||_\infty < \gamma$. This value of γ is updated based on a modified bisection algorithm, called γ iteration. This iteration procedure continues until the magnitude of the difference between the smallest γ value that has passed and the largest γ value that has failed is smaller than the tolerance specified. Also the transfer function matrix of the nominal closed loop system $F_L(P,K)$ is that from *disturbance* to the errors *e*.

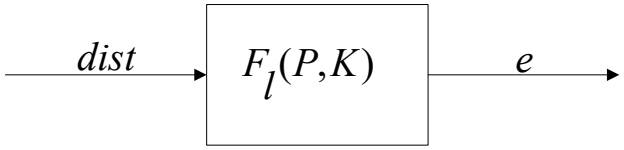

Figure 25: Closed loop LFT in H∞ design [8]

Therefore, we need to extract from the open loop transfer function matrix P from the system matrix that relates the specific inputs and outputs.

3.9.1 Using *sel* command from MATLAB

Sel command from MATLAB selects desired outputs and inputs from a system matrix [24]. The outputs and inputs are row vectors with the desired inputs/outputs specified. For pitch rate the command is given as follows:

$$hin\_ic = sel(long\_main\_sys, 4{:}6, 4{:}5)$$

where long_main_sys is given as:

$$\begin{bmatrix} \dot{x}_1 \\ \dot{x}_2 \\ \dot{s}_1 \\ \dot{s}_2 \\ y_m \\ y_c \\ y_k \\ e\_p \\ e\_u \\ y \end{bmatrix} = \begin{bmatrix} 0 & 1 & 0 & 0 & 0 & 0 & 0 & 0 & 0 \\ -121.0000 & -4.4000 & 0 & 0 & -0.3000 & -24.2000 & -12.1000 & 0 & 121.0000 \\ -3.3731 & 0 & -0.0040 & -0.0065 & 0 & 0 & 0 & -3.3731 & 0 \\ 2.7528 & 0 & 0.0065 & -2.4960 & 0 & 0 & 0 & 2.7528 & 0 \\ -121.0000 & -4.4000 & 0 & 0 & -0.3000 & -24.2000 & -12.1000 & 0 & 121.0000 \\ 0 & 0.0300 & 0 & 0 & 0 & 0 & 0 & 0 & 0 \\ 1.0000 & 0 & 0 & 0 & 0 & 0 & 0 & 0 & 0 \\ 0.9500 & 0 & -3.3700 & -2.7500 & 0 & 0 & 0 & 0.9500 & 0 \\ 0 & 0 & 0 & 0 & 0 & 0 & 0 & 0 & -0.0100 \\ -1.0000 & 0 & 0 & 0 & 0 & 0 & 0 & -1.0000 & 0 \end{bmatrix} \begin{bmatrix} x_1 \\ x_2 \\ s_1 \\ s_2 \\ u_m \\ u_c \\ u_k \\ d \\ u \end{bmatrix}$$

Therefore, the following matrix is saved in hin_ic:

$$\begin{bmatrix} \dot{x}_1 \\ \dot{x}_2 \\ \dot{s}_1 \\ \dot{s}_2 \\ e\_p \\ e\_u \\ y \end{bmatrix} = \begin{bmatrix} 0 & 1.0000 & 0 & 0 & 0 & 0 \\ -121.0000 & -4.4000 & 0 & 0 & 0 & 121.0000 \\ -3.37 & 0 & -0.0040 & -0.0065 & -3.3730 & 0 \\ 2.7528 & 0 & 0.0065 & -2.4900 & 2.7500 & 0 \\ 0.9500 & 0 & -3.3731 & -2.7528 & 0.9500 & 0 \\ 0 & 0 & 0 & 0 & 0 & -0.0100 \\ -1.0000 & 0 & 0 & 0 & -1.0000 & 0 \end{bmatrix} \begin{bmatrix} x_1 \\ x_2 \\ s_1 \\ s_2 \\ d \\ u \end{bmatrix}$$

Similarly for roll rate using the command sel from MATLAB the specific inputs and outputs are selected from the lat_main_sys given below:

$$\begin{bmatrix} \dot{x}_1 \\ \dot{x}_2 \\ \dot{s}_1 \\ \dot{s}_2 \\ y_m \\ y_c \\ y_k \\ e\_p \\ e\_u \\ y \end{bmatrix} = \begin{bmatrix} 0 & 1.00 & 0 & 0 & 0 & 0 & 0 & 0 & 0 \\ -225.00 & -9.00 & 0 & 0 & -0.300 & -45.00 & -22.50 & 0 & 225.00 \\ -3.34 & 0 & -0.0039 & -0.0063 & 0 & 0 & 0 & -3.34 & 0 \\ 2.6682 & 0 & 0.0063 & -2.546 & 0 & 0 & 0 & 2.66 & 0 \\ -225.00 & -9.00 & 0 & 0 & -0.30 & -45.00 & -22.50 & 0 & 225.00 \\ 0 & 0.04 & 0 & 0 & 0 & 0 & 0 & 0 & 0 \\ 1.00 & 0 & 0 & 0 & 0 & 0 & 0 & 0 & 0 \\ 0.95 & 0 & -3.34 & -2.66 & 0 & 0 & 0 & 0.95 & 0 \\ 0 & 0 & 0 & 0 & 0 & 0 & 0 & 0 & -0.01 \\ -1.00 & 0 & 0 & 0 & 0 & 0 & 0 & 0 & -1.00 \end{bmatrix} \begin{bmatrix} x_1 \\ x_2 \\ s_1 \\ s_2 \\ u_m \\ u_c \\ u_k \\ d \\ u \end{bmatrix}$$

Therefore, the following matrix is saved in hin_ic for roll rate:

$$\begin{bmatrix} \dot{x}_1 \\ \dot{x}_2 \\ \dot{s}_1 \\ \dot{s}_2 \\ e\_p \\ e\_u \\ y \end{bmatrix} = \begin{bmatrix} 0 & 1.0000 & 0 & 0 & 0 & 0 \\ -225.0000 & -9.0000 & 0 & 0 & 0 & 225.0000 \\ -3.3402 & 0 & -0.0039 & -0.0063 & -3.3402 & 0 \\ 2.6682 & 0 & 0.0063 & -2.5461 & 2.6682 & 0 \\ 0.9500 & 0 & -3.3402 & -2.6682 & 0.9500 & 0 \\ 0 & 0 & 0 & 0 & 0 & -0.0100 \\ -1.0000 & 0 & 0 & 0 & -1.0000 & 0 \end{bmatrix} \begin{bmatrix} x_1 \\ x_2 \\ s_1 \\ s_2 \\ d \\ u \end{bmatrix}$$

3.9.2 Using the H∞ command from MATLAB

The design uses *hinfsyn* command from MATLAB to compute a centralized H∞ controller based on the open loop structure *P* [8, 24]. The *hinfsyn* command assumes the following about the open loop matrix *P*:

1. (A, B_2) is stabilizable and (C_2, A) is detectable.
2. D_{12} is full column rank and D_{21} is full row rank.
3. $\begin{bmatrix} A - jwI & B_2 \\ C_1 & D_{12} \end{bmatrix}$ Has a full rank for all values of w.
4. $\begin{bmatrix} A - jwI & B_1 \\ C_2 & D_{21} \end{bmatrix}$ Has a full rank for all values of w.

The *hinfsyn* command returns the H∞ controller, the closed loop system and the value of γ achieved. The bisection algorithm stops when the difference between the smallest value of γ that has passed and the largest value of γ that has failed is less than tolerance

limit. The syntax, input and output arguments of *hinfsyn* command are provided in Table1 and Table 2.

$$[k, clp] = hinfsyn(p, mea, ncon, \gamma\ low, \gamma\ high, tol)$$

Table 1: Input Arguments of the H∞ MATLAB command

INPUT ARGUMENTS	
Open-loop interconnection (matrix of type SYSTEM	P
Number of measurements	nmeas
Number of controls	ncons
Lower bound of bisection	γ low
Upper bound of bisection	γ high
Absolute tolerance for the bisection method	tol

Table 2: Output arguments of the H∞ MATLAB command

OUTPUT ARGUMENTS:	
H∞ optimal controller	K
Closed loop system with controller implemented	clp= (starp(P,K))

Table 3: Extract of code

GAMA	HAMX_EIG	XINF_EIG	HAMY_EIG	YINF_EIG	NRHO_XY	P/F
10.000	3.4E+00	1.9E-04	3.9E-03	-5.5E-17	0.0000	P
5.500	3.4E+00	1.9E-04	3.9E-03	0.0E+00	0.0000	P
3.250	3.4E+00	1.9E-04	3.9E-03	-5.5E-17	0.0000	P
2.125	3.4E+00	1.9E-04	3.9E-03	0.0E+00	0.0000	P
1.563	3.4E+00	1.9E-04	3.9E-03	0.0E+00	0.0000	P
1.281	3.4E+00	1.9E-04	3.9E-03	0.0E+00	0.0000	P
1.141	3.4E+00	1.9E-04	3.9E-03	0.0E+00	0.0000	P
1.070	3.4E+00	2.0E-04	3.9E-03	0.0E+00	0.0000	P
1.035	3.4E+00	2.0E-04	3.9E-03	0.0E+00	0.0000	P
1.018	3.4E+00	2.0E-04	3.9E-03	0.0E+00	0.0000	P

From Table 3 it can be concluded that the following conditions need to be true for the γ to pass:

- H and J Hamiltonian matrices (which are formed from the state-space data of P) must have no eigenvalues at the imaginary axis.
- The stabilizing Ricatti solutions X∞ and Y∞ associated with the Hamiltonian matrices H and J must exist and be positive, semi-definite.
- Spectral radius of (X, Y) must be less than or equal to γ^2.

The results for the H∞ controller for pitch rate and for roll rate are given as:

$$Kpitch = \frac{1731s^3 + 2020s^2 + 2.648e05s + 1.522e06}{s^4 + 329.5s^3 + 5.289e04s^2 + 1.302e05s + 520.7}$$

$$Kroll = \frac{1675s^3 + 26640s^2 + 4.81\text{e}05s + 2.603\text{e}06}{s^4 + 426.4s^3 + 8.967\text{e}04s^2 + 2.259\text{e}05s + 885.9}$$

3.10 Analysis of closed loop system with H∞ controller:

3.10.1 Nominal performance

Nominal performance can be achieved by the optimization of the mixed sensitivity S/KS cost problem where S is the sensitivity function and K is the H∞ controller developed in section 3.9. Nominal performance of the closed loop system can be analyzed by computing the sensitivity function for both pitch rate and roll rate and comparing them with their respective inverse of weighing function. In both cases the following in equality should be true

$$\left\| w_p (I + GK)^{-1} \right\|_\infty < 1$$

This occurs if and only if for all frequencies the maximum of the sensitivity function is less than the inverse of the weighing function.

Plots of sensitivity function and inverse of weighing function for both pitch rate and roll rate are shown in Figure 26 and Figure 27. For both cases it can be observed that the closed loop system achieves nominal performance.

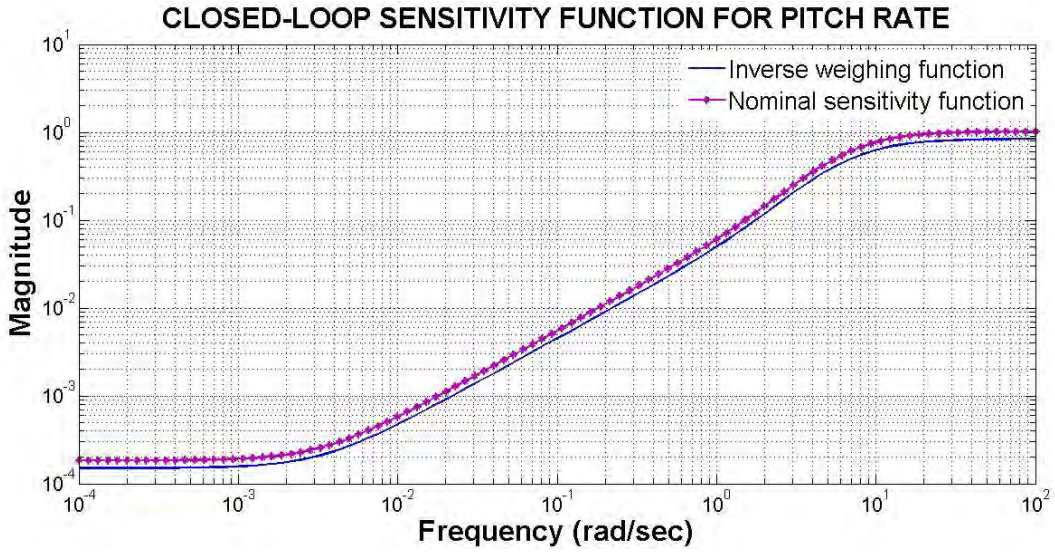

Figure 26: Closed loop sensitivity function for pitch rate

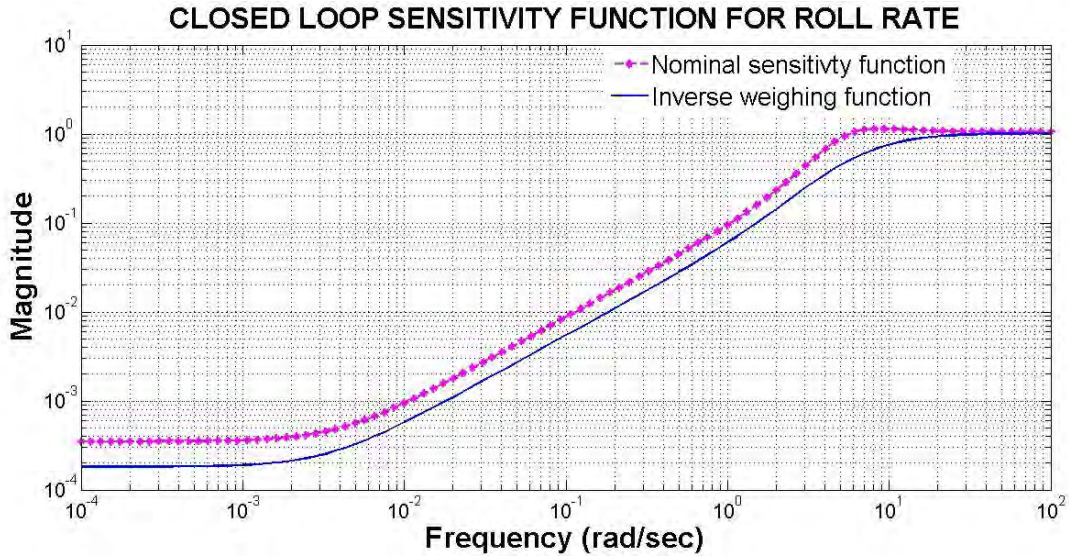

Figure 27: Closed loop sensitivity function for roll rate

3.10.2 Robustness analysis of the closed loop system

Robustness analysis for a closed loop system means whether stability is preserved as the system varies within a specified set of uncertainties (for both pitch rate and roll rate analyzed the uncertainty is a Δ block which is structured and bounded). Therefore ideally a feedback control system should be robust with respect to the uncertainties or perturbations in the plant characteristics [8, 20]. In performing robustness analysis there are two principal concerns, namely robust stability and robust performance. Robust stability addresses the qualitative question as to whether or not the system remains stable for all plant perturbations within a specified class of uncertainties. A related problem involves determining the largest class of plant perturbations under which stability is preserved. The test for robust stability is conducted on the leading 3 by 3 diagonal block of the of the closed loop transfer matrix function that represents the uncertainties. The upper bound of μ (singular structured value) [27] should be less than one then robust stability is achieved.

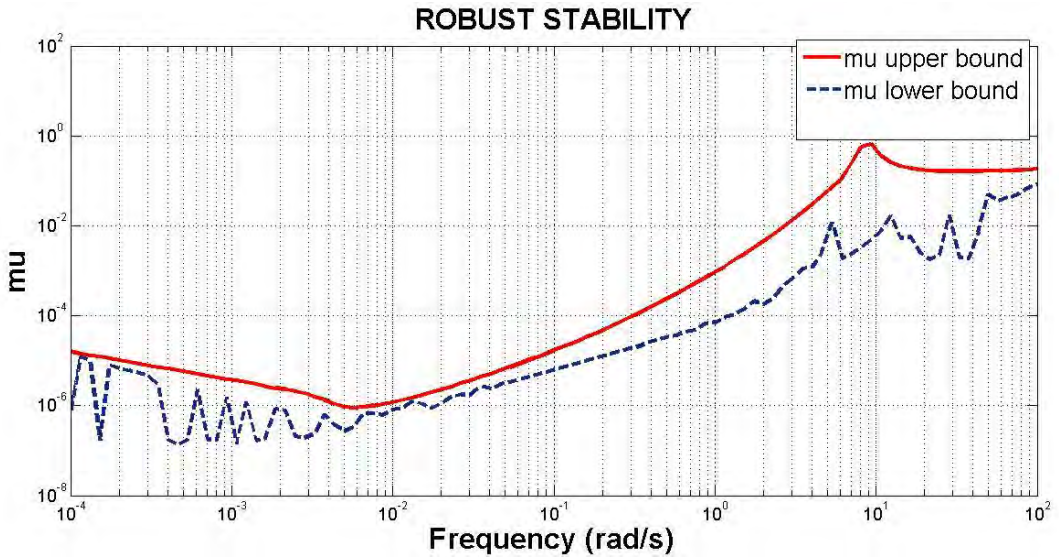

Figure 28: Robust stability for pitch rate

It can be observed from Figure 28 and Figure 29 that the upper and lower bound of μ value is less than one for all frequencies under consideration for pitch rate of the helicopter. The maximum value of μ for pitch rate is 0.6586 that shows that structured perturbations with norm less than $1/.6585$ are allowable, i.e. the stability maintains for

$\|\Delta\| < \frac{1}{0.6586}$. The maximum value of μ for roll rate from Figure 29 is 0.4525 that shows that structured perturbations with norm less than $1/.4525$ are allowable, i.e. the stability maintains for $\|\Delta\| < \frac{1}{0.4525}$

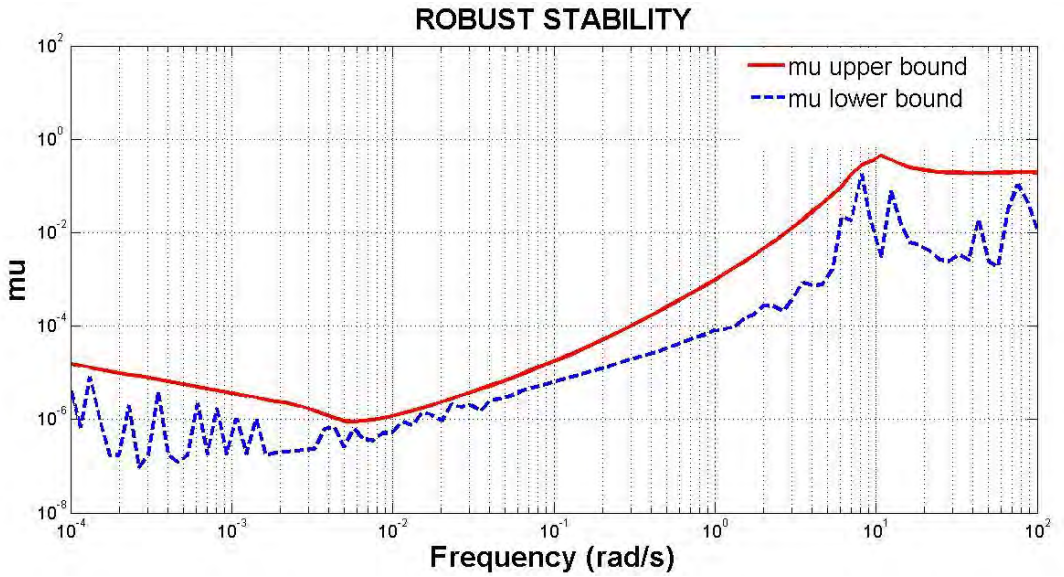

Figure 29: Robust stability for roll rate

To find out quantitatively the performance degradation of a feedback closed loop system within the given robust stability range is called robust performance [20]. The robust performance of a closed loop system with H∞ controller can be tested by means of μ analysis. The closed loop transfer function for both pitch rate and roll rate plant has for inputs and five outputs where the initial three inputs and outputs represents the relation between the uncertainties whereas the 4th input to 4th output and the 4th input to the 5th output represents the mixed sensitivity case. Therefore the μ analysis for robust performance should have a block structure that contains a 3 by 3 uncertainty block and a 1 by 2 block for performance. The robust performance is thus achieved if the value of μ is less to 1 for all frequencies considered. Figure 30 and Figure 31 are plots for robust performance and nominal performance for the pitch rate and the roll rate respectively.

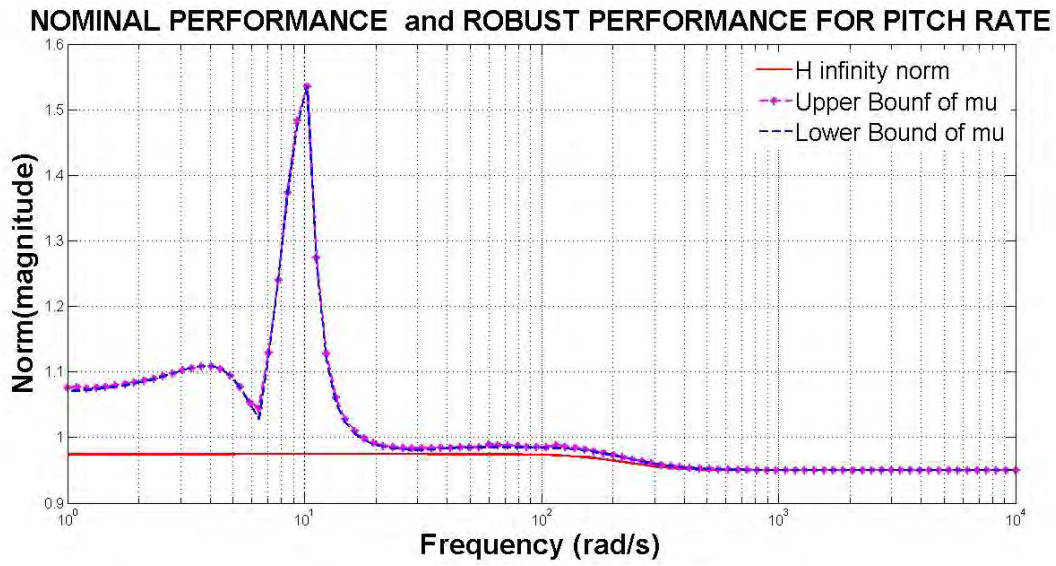

Figure 30: Nominal and robust performance measure for pitch rate

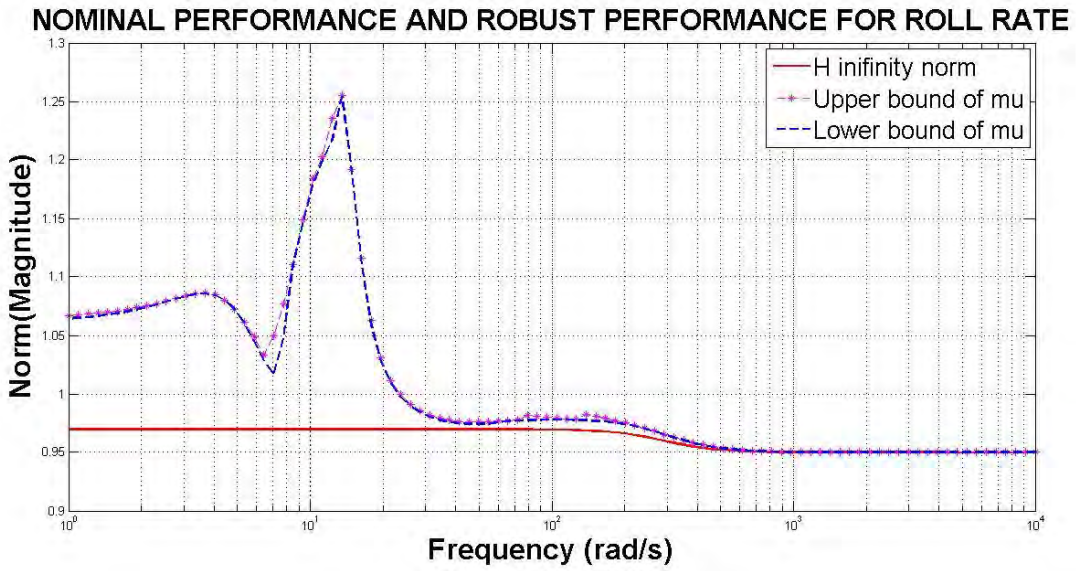

Figure 31: Nominal and robust performance for roll rate

It can be seen from Figure 30 and Figure 31 that both the angular rates with H∞ controllers achieve nominal performance but fail to satisfy the robust performance specification. This conclusion comes from the fact that the frequency response of the nominal performance for pitch rate as shown in Figure 30 has a maximum of 0.9745, while the μ curve for the robust performance for pitch rate has a maximum of 1.535 and the frequency response of the nominal performance for roll rate as shown in Figure 31

has a maximum of 0.9697, while the μ curve for the robust performance for pitch rate has a maximum of 1.255. For both pitch and roll rate the maximum value of μ is above one thus, failing to satisy the robust performance specification.

3.10.3 Transient analysis of the closed loop system

The transient responses to a reference input are shown for both pitch rate and roll rate. The transient responses have a maximum overshoot of 20% and settling time of 2 sec. Different uncertainties are added to natural frequency (w_p and w_q) and to the damping ration (ζp and ζq). The range of uncertainty in the natural frequency is given from -30% to 30% and that in the damping ratio is given from -25% to 25%, the transient responses for the uncertain plants as well as the nominal plant are plotted. Figure 32 and Figure 33 show that the response for systems with parametric variations is also stable and close to the nominal plant representing nominal performance and robust stability as already shown in section 3.10.2.

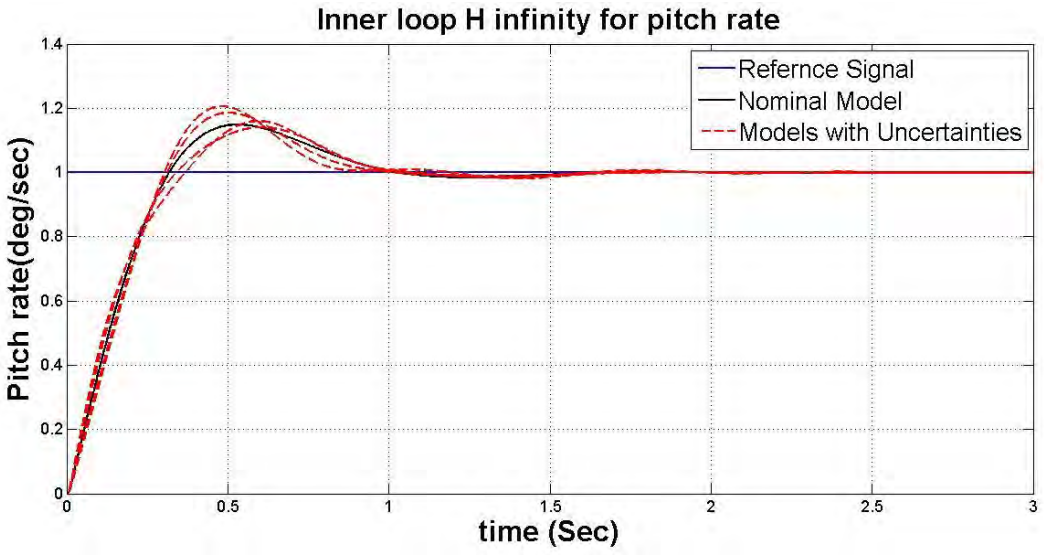

Figure 32: Transient response to a reference input for pitch rate

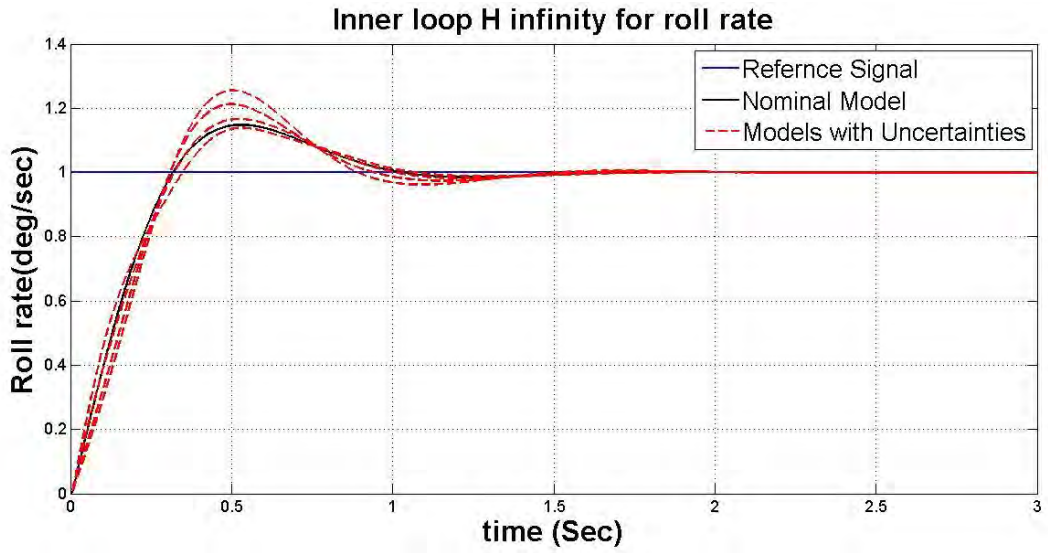

Figure 33: Transient response to a reference input for roll rate

Figure 34 and Figure 35 show the transient response of the pitch rate and roll rate plant respectively when a step disturbance of $0.1\,deg/sec$ is added to it. Disturbance rejection/attenuation can be seen for both the figures as the response goes back to zero within the range of $1sec$ of the added disturbance.

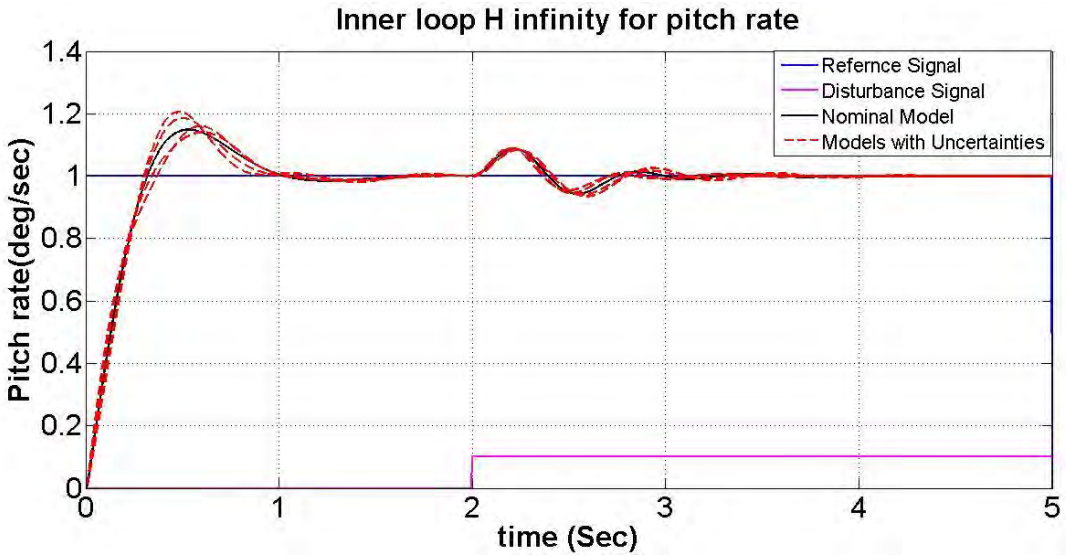

Figure 34: Pitch rate response for a disturbance of 0.1 magnitude

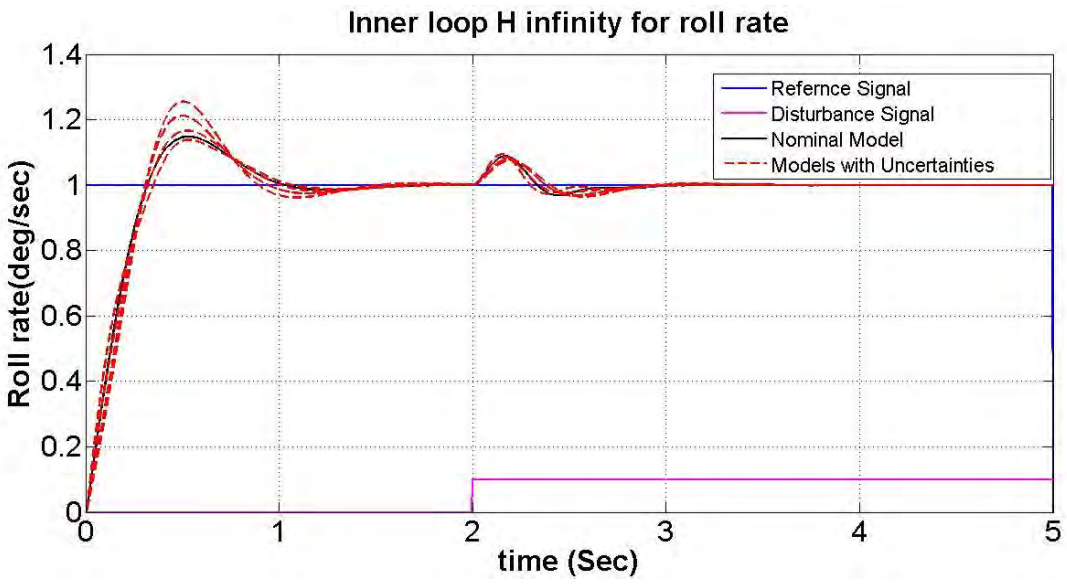

Figure 35: Roll rate response for a disturbance of 0.1 magnitude

Chapter 4

Loop Shaping Design Procedure

4.1 Introduction

A well-known method for the design of robust feedback controller for single input single output (SISO) as well as multi input and multi output (MIMO) systems is the so-called Loop Shaping Design Procedure (LSDP). It is a robust design method based on the H∞ control theory. This method has been proposed by Mc Farlane and Glover [9] and has been successfully used in various applications. For this thesis LSDP is used to create controllers for the Joker 3 rotary wing helicopter longitudinal input to pitch rate and lateral input to roll rate system. LSDP is different from H∞ optimal controller design introduced in the Chapter 3 as it provides an alternate way of representing uncertainty. The uncertainty is described by the perturbations directly on the co-prime factors of the plant [9, 28] unlike the linear fractional transformation method that was used in chapter 3. This design method is called H∞ loop shape designing method procedure (LSDP) [29, 30].

4.2 Advantages of Loop Shaping Designing Procedure (LSDP)

When the perturbed system doesn't have the same number of poles in the closed right half plane as the nominal model this method need to be implemented since the iterative or bisection method of finding the optimal solution cannot be implemented in this case [8, 31]. Advantages of this method are:

- It relaxes the restrictions on the number of right half plane poles.
- Doesn't produce any pole-zero cancellation between the nominal model and the controller designed.
- The computer efficiency is increased by application of this process as it doesn't adopt an iterative procedure or method to obtain the optimal solution.
- It is easier to understand as it applies the classical loop-shaping design techniques.

4.3 Theoretical background

4.3.1 Co-Prime factorization:

In order to understand co-prime factorization we will consider a linear time invariant system that is governed by differential equations and can be represented by the following state space model [8, 18].

$$\dot{x}(t) = Ax(t) + Bu(t) \tag{4.3-1}$$

$$y(t) = Cx(t) + Du(t) \tag{4.3-2}$$

Where x(t) is a state vector, u(t) is a control vector and y(t) is a measurement vector. The transfer function matrix for the above model is given as:

$$G(s) = C(sI - A)^{-1}B \tag{4.3-3}$$

The state space realization of the above transfer function is given as:

$$G(s) = \left[\begin{array}{c|c} A & B \\ \hline C & D \end{array}\right]$$

Let's assume 4 matrices $M, N, \tilde{M}, \tilde{N} \in H\infty$ here $H\infty$ denotes the space of functions where no poles exist in the closed right-half complex plane, constitute of right and left co-prime factors if and only if the following conditions are true [8, 19]:

1. M or $\tilde{M}$ need to be a square matrix and det(M) or det($\tilde{M}$) shouldn't be equal to zero that is it cannot be singular at any value.
2. The plant model should be given by: $G = \tilde{M}^{-1}\tilde{N}$ or $G = NM^{-1}$ depending whether the left or the right co-prime factorization is being calculated.
3. Bezout right and left identity need to be true. The Bezout identities are given as (4.3-4) and (4.3-5).

Two matrices M and N($\tilde{M}$ and $\tilde{N}$) are right co-primes (left co-primes) if and only if there exist two unimodular matrices U and V ($\tilde{U}$ and $\tilde{V}$) that give the following relation:

$$UN + VM = I(Bezout\ Right\ Identity) \tag{4.3-4}$$

$$\tilde{N}\tilde{U} + \tilde{M}\tilde{V} = I(Bezout\ Left\ Identity) \tag{4.3-5}$$

4.3.2 State space for left and right co–prime factorization

The state space realization for the normalized left co-prime factorization can be obtained in terms of the solution of the generalized filter algebraic Ricatti equation that is given in equation 4.3-6 [27]. Where $R = I + DD^T$ and $Z \geq 0$ is the unique stabilizing solution. If $H = (ZC^T + BD^T)R^{-1}$ then the state space realization of the co-prime factors is given as the matrix after equation 4.3-6.

$$(A - BD^T R^{-1}C)Z + Z(A - BD^T R^{-1}C)^T - ZC^T R^{-1}CZ + B(I - D^T R^{-1}D)B^T = 0 \qquad (4.3\text{-}6)$$

$$[\tilde{N}, \tilde{M}] = \begin{bmatrix} A + HC & B + HD & H \\ R^{-1/2}C & R^{-1/2}D & R^{-1/2} \end{bmatrix}$$

Similarly the state space construction and realization for the normalized right co-prime factorization can be obtained in terms of the solution to the generalized control Algebraic Riccati Equation shown in equation 4.3-7. Where $S = I + D^T D$ and $X \geq 0$ is the unique stabilizing solution.

$$(A - BS^{-1}D^T C^T)X + X(A - BS^{-1}D^T C) - XBS^{-1}B^T X + C^T(I - DS^{-1}D^T)C = 0 \qquad (4.3\text{-}7)$$

The perturbed /disturbed plant transfer function is described in equation 4.3-8 [8].

$$G = (\tilde{M} + \Delta_{\tilde{M}})^{-1}(\tilde{N} + \Delta_{\tilde{N}}) \qquad (4.3\text{-}8)$$

The uncertainties $(\Delta_{\tilde{M}}, \Delta_{\tilde{N}})$ are unknown but are stable transfer functions therefore; this is an alternative way of representing the perturbations on a plant by directly adding them on the co-prime factors of the plant. The design objective is not only to stabilize the main nominal plant but a family of perturbed plants that can be represented in 4.3-9.

$$G_\eta = \{(\tilde{M} + \Delta_{\tilde{M}})^{-1}(\tilde{N} + \Delta_{\tilde{N}}) : \left\| \Delta_{\tilde{M}}, \Delta_{\tilde{N}} \right\|_\infty < \eta\} \qquad (4.3\text{-}9)$$

Where $\eta > 0$ is the stability margin. The LSDP method augments the plant with appropriately chosen weights so that the frequency response of the open loop system (the weighted plant) is reshaped in order to meet the closed loop system performance requirements. Then a robust controller is created to meet the stability.

4.4 Loop Shape Designing Procedure

In classical control systems using the single input and single output (SISO) systems a very well-known technique to acquire stability, good performance and certain robustness from unity feedback system is to alter the frequency response (Bode Plot) of the open loop transfer function [30, 46, 47]. As we wish to have the unity feedback system to be stable, robust and have a minimum tracking error therefore we alter the frequency response of the open loop system by adding pre-compensator or/and post compensator to it [25, 26, 32]. Loop Shape design procedure can be divided into the following three steps:

1. Using a pre compensator W_1 and/or a post compensator W_2 the singular values of the nominal system are altered to give a desired loop shape. The nominal plant G and shaping functions W_1, W_2 are combined to form the shaped plant as given equation 4.4-1.

$$G_s = W_1 G W_2 \tag{4.4-1}$$

2. It is assumed that the weighting functions W_1 and W_2 when combined with the nominal system G give G_s with no hidden unstable modes.

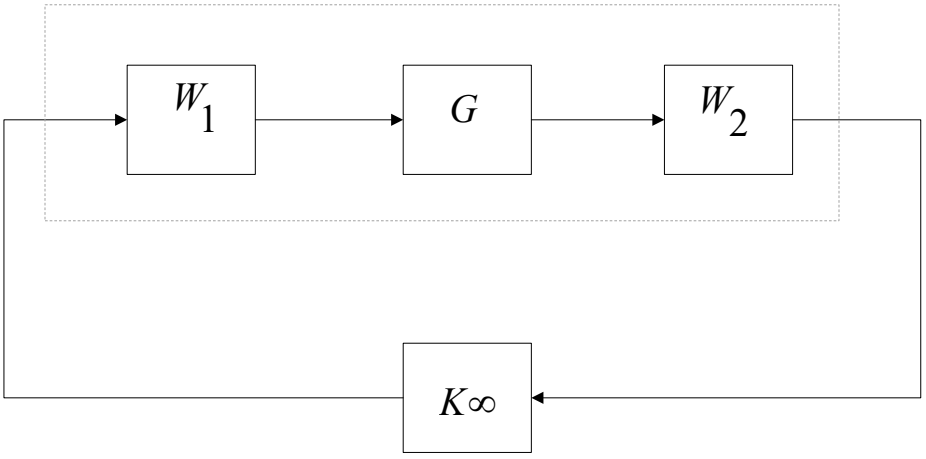

Figure 36: Closed loop system with pre and post compensators

3. Next a feedback controller K_∞ is synthesized that robustly stabilizes the normalized left co-prime factorization of G_s with a stability margin η, it can be shown that if the

stability margin is not less than 0.2, the frequency response $K_S W_2 G W_1$ would be almost equivalent to $W_2 G W_1$.

4. The final controller is then created by obtaining the product of the weighting functions with the feedback controller $K\infty$ given as:

$$K_{final} = W_1 K_\infty W_2$$

4.5 Selecting the pre-compensator and post-compensator functions.

The pre-compensator and post-compensator functions are selected such that after modification of the plant the modified singular values should achieve the following [8, 33, 44, 46]:

- For good performance in tracking the least singular value of the weighted system should be large over the low-frequency range.
- To handle the unmodelled dynamics the largest singular value should be small over the high frequency range.
- Also the bandwidth affects the speed of the system's response still the slope of the singular value near the bandwidth frequency shouldn't be too steep.

4.5.1 Pitch rate

The pre-compensator and the post compensator for the pitch rate have been chosen so as to introduce an integrating effect in the low frequency range which leads to good rejection of disturbance inputs.

$$w_1(s) = 9\frac{0.8s + 7}{s + 0.03}$$

$$w_2(s) = 1$$

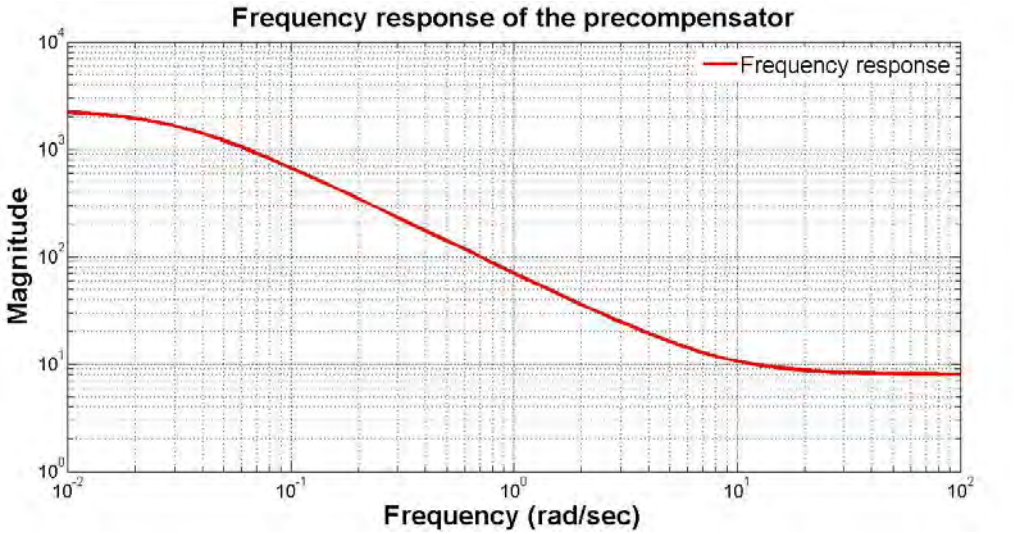

Figure 37: Frequency response of the pre-compensator selected

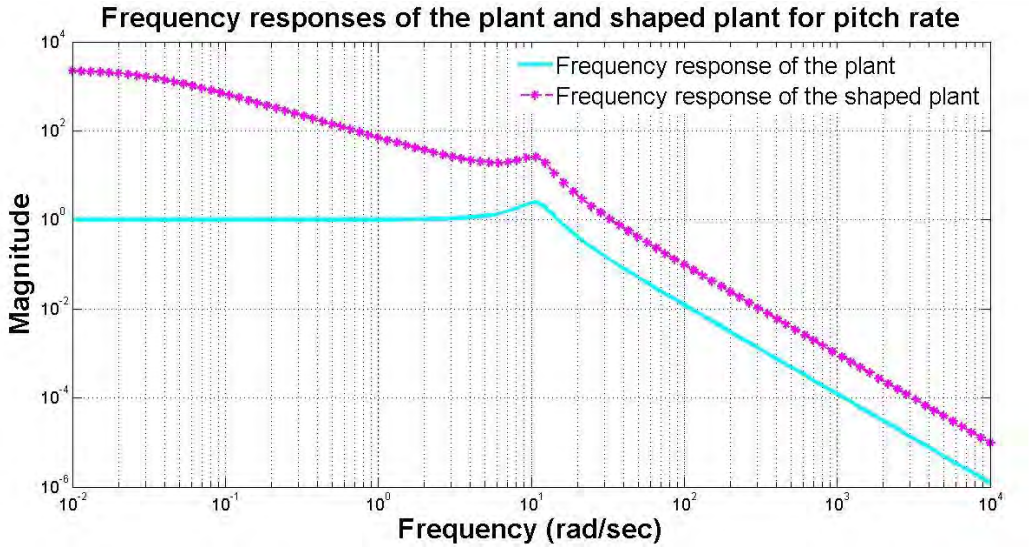

Figure 38: Frequency response of the original and the shaped plant

4.5.2 Roll rate:

The pre-compensator for the roll rate has been chosen such that gain is sufficiently high at frequencies where good disturbance rejection is required and is sufficiently low at frequencies where robust stability is required. The pre and post compensator are given as:

$$w_1(s) = 10\frac{s+6.5}{s+0.02}$$

$$w_2(s) = 1$$

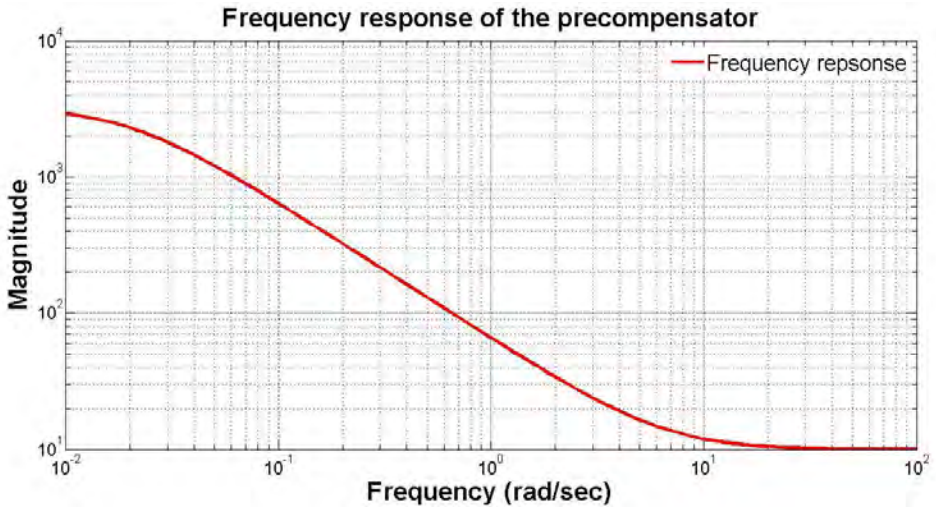

Figure 39: Frequency response of the pre-compensator selected

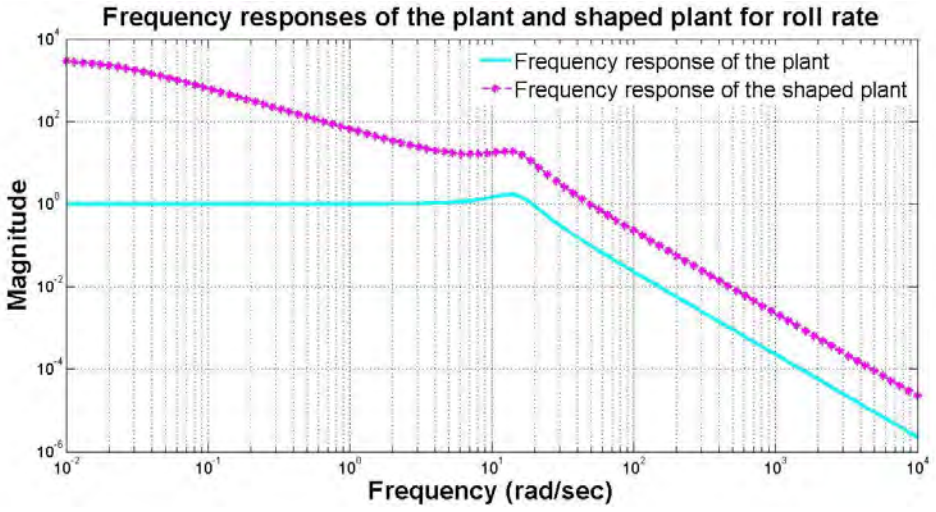

Figure 40: Frequency response of the original and shaped plant

4.6 Robust control toolbox commands (MATLAB):

4.6.1 Using *ncfsyn* command from MATLAB

The H∞ LSDP controller is developed using the *ncfsyn* function from MATLAB. The ncfsyn synthesizes an H∞ LSDP controller to robustly stabilize a family of systems that contain uncertainty in the normalized co-prime factors of the system. The syntax, input and output arguments of ncfsyn are given in Table 4 and Table 5 [24, 27]:

$$[sysk, emax, sysobs] = ncfsyn(sysgw, factor, opt)$$

Table 4: Input arguments of the μ analysis MATLAB command [27]

Input Arguments	
sysgw	The weighted system to be controlled
factor	=1 implies that an optimal controller is required. >1 implies that a suboptimal controller is required achieving a performance FACTOR less than optimal.
opt	'ref' the controller includes an extra set of reference input

Table 5: Output arguments of the μ analysis MATLAB command [27]

Output arguments	
sysk	H∞ loopshaping controller
emax	Stability margin as an indication robustness to unstructured perturbations. emax is always less than 1 and values of emax greater than 0.3 generally indicate good robustness margins.
sysobs	H∞ loopshaping observer controller. This variable is created only if factor>1 and opt = 'ref'

By using the *ncfsyn* command to build the H∞ we get a stability margin $emax = 0.38435$ for the pitch rate and a stability margin of $emax = 0.41718$ which are less than 1 and value of stability margin greater than 0.3 indicates good robustness margin. For the pitch rate and roll rate controllers we get the following results:

$$Kpitch\_lsdp = \frac{-516.6s^2 - 8325s - 5.634e04}{s^3 + 275.1s^2 + 1.939e04s + 1.496e05}$$

$$Kroll\_lsdp = \frac{-645s^2 - 1543s - 9.517e04}{s^3 + 380.8s^2 + 3.773e04s + 2.296e05}$$

4.6.2 Using mmult command

In order to find the final LSDP controller the command mmult from the robust control toolbox is used, *mmult* performs the arithmetic operation of multiplication of two system type matrices. The syntax used for performing mmult is given as [24]:

$$mmult(mat1, mat2)$$

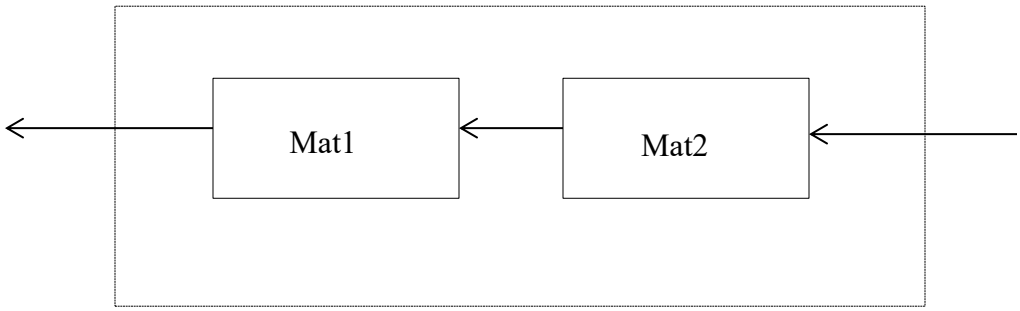

Figure 41: Block diagram representation of the mmult

The *mmult* command is used to find the product of the controller created with the pre-compensator and post-compensator function. The final negative feedback controller for pitch rate and roll rate are given as:

$$Kfinal\_pitch = \frac{4133\ s^3 + 1.028e05\ s^2 + 1.033e06\ s + 3.944e06}{s^4 + 275.1\ s^3 + 1.94e04\ s^2 + 1.501e05s + 4487}$$

$$Kfinal\_roll = \frac{6450\ s^3 + 1.962e05\ s^2 + 1.954e06\ s + 6.186e06}{s^4 + 380.8\ s^3 + 3.774e04\ s^2 + 2.304e05s + 4593}$$

4.7 Analysis of closed loop with controller obtained using LSDP:

4.7.1 Nominal performance

Nominal performance can be achieved by the optimization of the mixed sensitivity *S/KS* cost problem where *S* is the sensitivity function and *K* is Loop Shape design procedure that is developed in section 4.6. Nominal performance of the closed loop system can be analyzed by computing the sensitivity function for both pitch rate and roll rate and comparing them with their respective inverse of pre-compensator or/and post compensator transfer function.

In both cases the following in equality should be true

$$\left\| w_1 (I + GK)^{-1} \right\|_\infty < 1$$

This occurs if and only if for all frequencies the maximum of the sensitivity function is less than the inverse of the pre-compensator transfer function since for both pitch rate and roll rate the post compensator has been defined as one. Figure 42 and Figure 43 show plots of sensitivity function and inverse of pre-compensator function for both pitch rate and roll rate. For both cases it can be observed that the closed loop system achieves nominal performance.

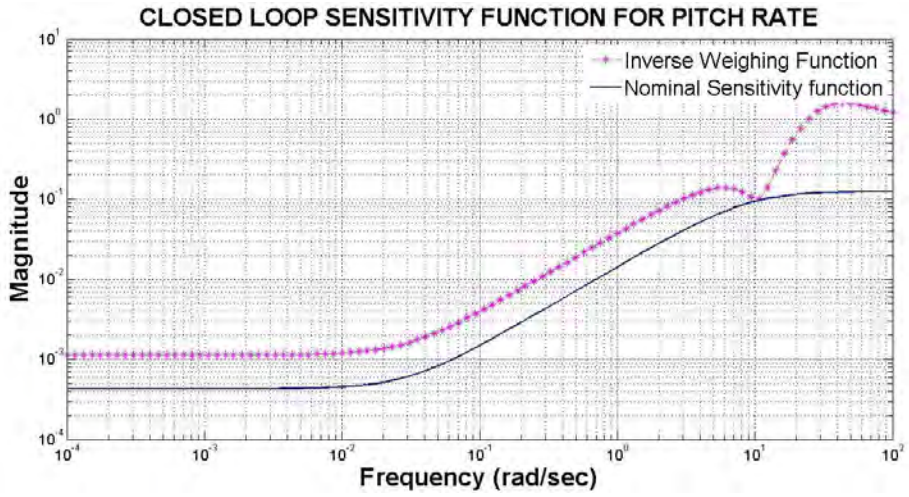

Figure 42: Sensitivity function for pitch rate on implementation of LSDP controller

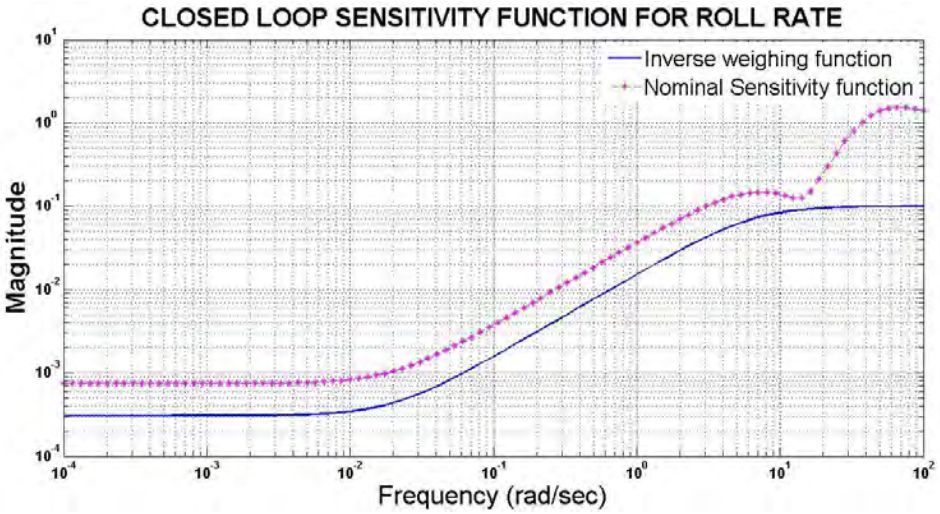

Figure 43: Sensitivity function for roll rate on implementation of LSDP controller

4.7.2 Robust stability

The test for robust stability is conducted on the leading uncertainty diagonal block of the closed loop transfer matrix function *M* that is created by using the *starp* command in MATLAB for the open loop interconnected matrix *Ppitch* and the final controller developed in the section 4.6.2 for pitch rate given by *Kfinal_pitch*.

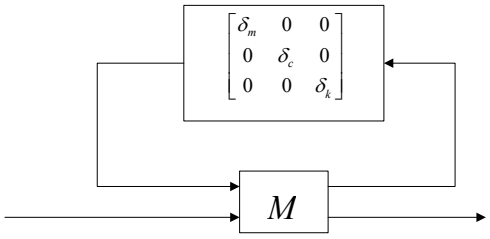

Figure 44: Block diagram representation for robust stability [8]

It can be recalled that *starp* command in MATLAB gives the star product realization (LFT) of the two matrices. The upper bound of μ (singular structured value) should be less than one then robust stability is achieved.

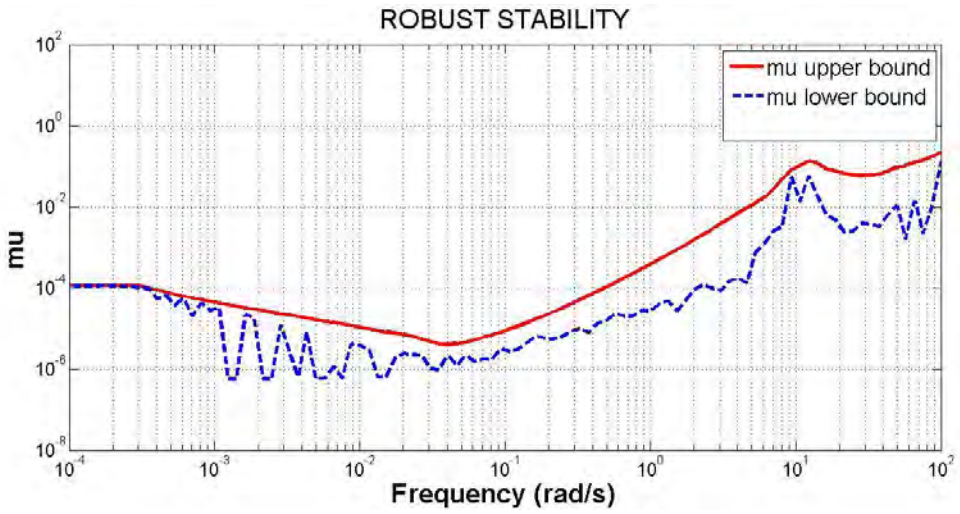

Figure 45: Robust stability for pitch rate

Figure 45 shows that the upper bound of μ have a value of less than 1 for all the frequencies under consideration therefore robust stability is achieved. The maximum value of is 0.2201 that shows that structured perturbations with norm less than $1/0.2201$ are allowable, i.e., the stability maintains for $\|\Delta\| < \frac{1}{0.2201}$

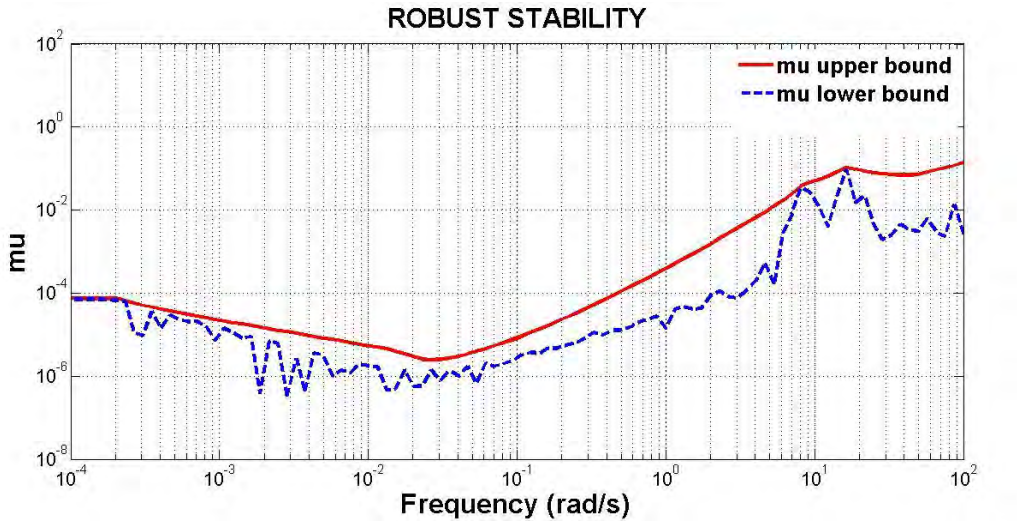

Figure 46: Robust stability for roll rate

It can be observed from Figure 46 that the upper bound of μ have a value of less than 1 for all the frequencies under consideration therefore robust stability is achieved. The maximum value of is 0.1509 that shows that structured perturbations with norm less than $1/0.01509$ are allowable, i.e. the stability maintains for $\|\Delta\| < \frac{1}{0.1509}$

4.7.3 Robust performance

To find out quantitatively the performance degradation of a feedback closed loop system within the given robust stability range is called robust performance. The robust performance of a closed loop system with controller (LSDP) can be tested by means of μ analysis. The μ-analysis for robust performance should have a block structure that contains a 3 by 3 uncertainty block and a 1 by 2 block for performance. The difference between robust stability and robust performance is the uncertainty block; robust stability is checked on the leading diagonal of the closed loop transfer function matrix whereas for

robust performance the uncertainty block structure has a 3 by 3 uncertainty block and 1 by 2 performance block which is given as:

$$\Delta_p = \left\{ \begin{bmatrix} \Delta & 0 \\ 0 & \Delta_f \end{bmatrix} \Delta \in \mathrm{R}^{3\times 3}, \Delta_f \in C^{1\times 2} \right\}$$

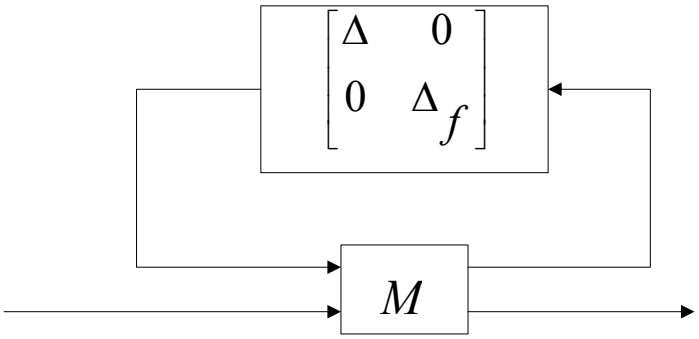

Figure 47: Block diagram representation of robust performance

The robust performance is thus achieved if the value of μ is less than one for all frequencies considered. Figure 48 and Figure 49 represent plots for robust performance and nominal performance for the pitch rate and the roll rate.

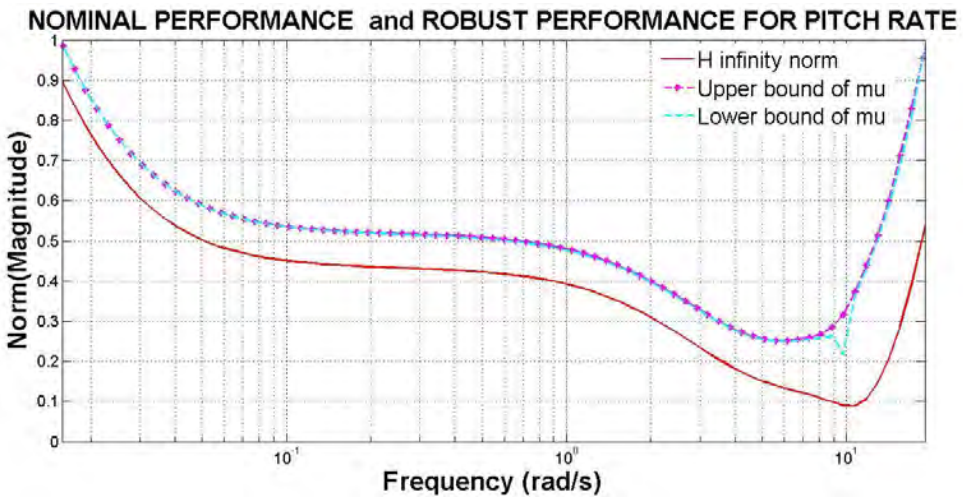

Figure 48: Nominal and robust performance for pitch rate

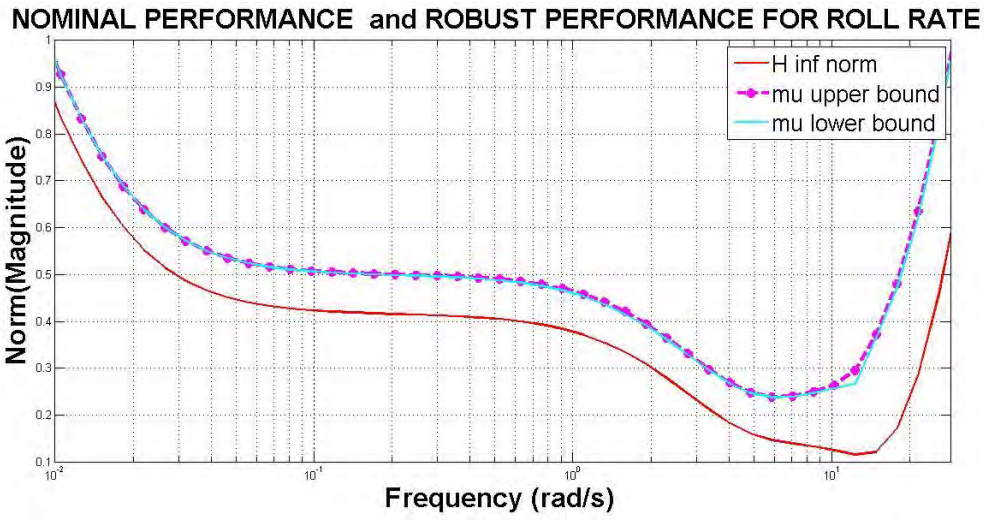

Figure 49: Nominal and robust performance for roll rate

It can be observed that both nominal performance and robust performance have been achieved for pitch and roll rate while using the LSDP controller whereas for the H∞ controller which was developed in the chapter 3 robust performance was not achieved.

4.7.4 Transient analysis of the closed loop system:

The transient responses to a reference input are shown for both pitch rate and roll rate. The transient responses have a settling time of $0.7sec$ which is way better than the H∞ controller developed in chapter 3 but the overshoots reach a maximum of 30%.The uncertainties allowed are $-1 < \|\Delta\| < 1$, the different uncertainties injected range in natural frequency from $-30\% < w < 30\%$ and that in the damping ratio is given from -$-25\% < \zeta < 25\%$. The transient responses for the uncertain plants as well as the nominal plant are shown in Figure 50 and Figure 51. These figures show that the response for systems with parametric variations is also stable and close to the nominal plant representing nominal performance and robust stability as proved in section.

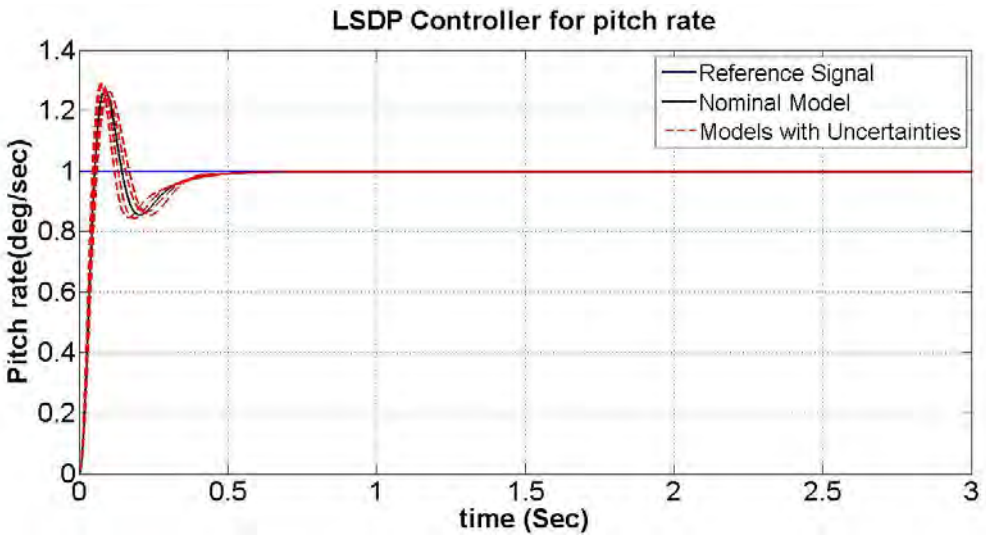

Figure 50: Transient response to reference input for pitch rate

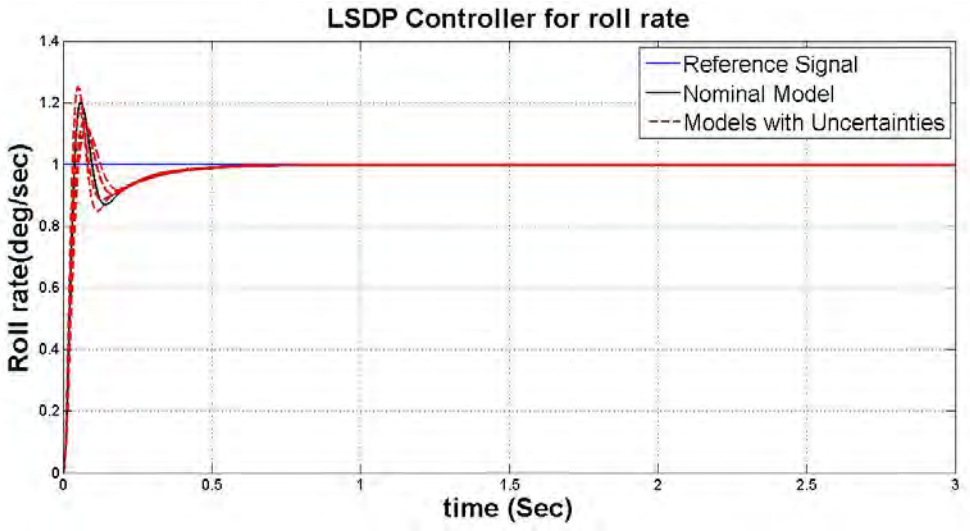

Figure 51: Transient response to a reference input for roll rate

Figure 52 and Figure 53 show the transient response of the pitch rate and roll rate plant respectively when a step disturbance of $0.1deg/sec$ magnitude is added to it. Disturbance rejection/attenuation shows that the closed loop system has achieved nominal performance.

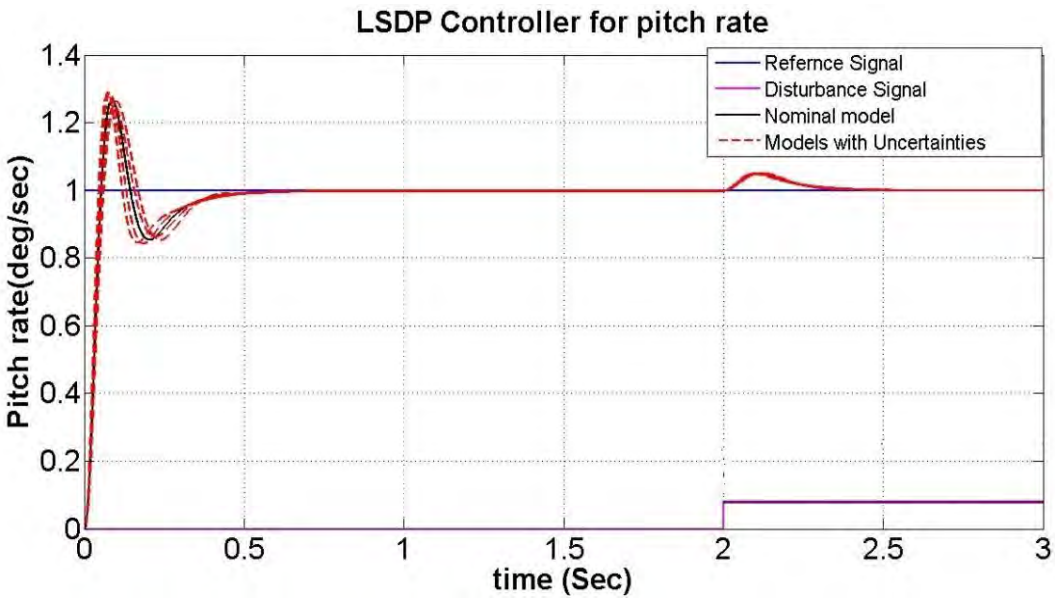

Figure 52: Pitch rate response for a disturbance of 0.1 magnitude

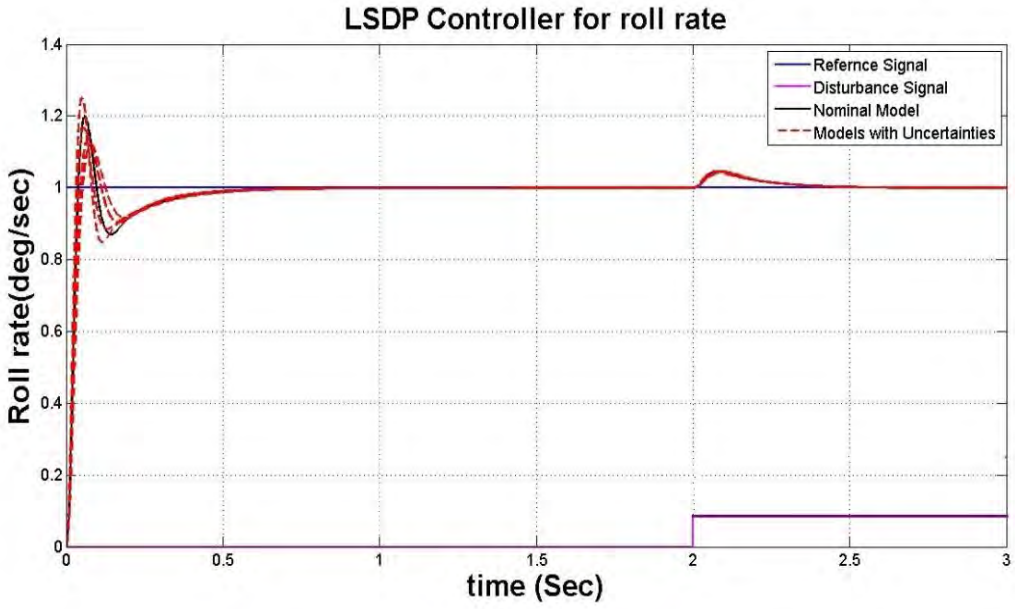

Figure 53: Roll rate response for a disturbance of 0.1 magnitude

Chapter 5

μ-Synthesis

5.1 Introduction

For building a robust controller another technique has been developed in the past few years called the μ-synthesis for the plant. Where the H_∞ design achieves robust stability and nominal performance it lacks robust performance therefore design methods that use the structured value μ are implemented [9, 10, 14]. Also for uncertainties that are structured the frequency response in terms of μ values needs to be found out. Conversion of robust design problems with structured or unstructured perturbations are converted to robust stabilization problem with structured uncertainty using μ synthesis. In order to understand the background of the singular structured value μ the small gain theorem need to be understood.

5.2 Small gain theorem

5.2.1 Background

The small gain theorem has central importance in the derivation of many stability tests [8]. Let's consider a closed system of the plant G and controller K as shown in Figure 52, the system is robustly stable if it remains stable for all possible (under certain definition), perturbations on the plant, this also includes the nominal plant because the case in which the perturbations are all to zero is also considered.

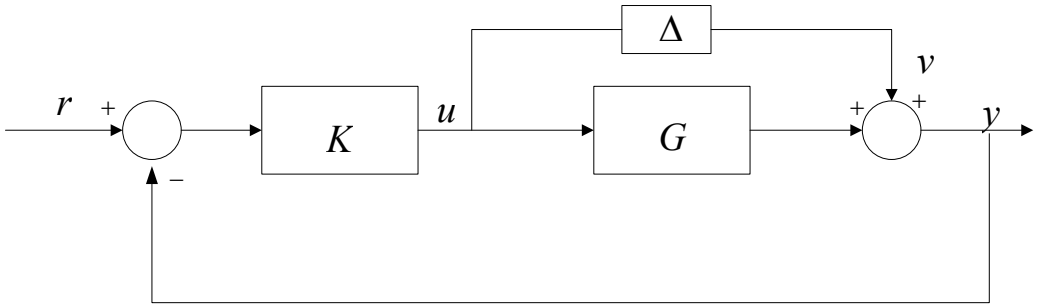

Figure 54: Closed loop feedback system with uncertainty [18]

The transfer function from u to v can be easily calculated as:

$$T_{uv} = -K(I + GK)^{-1} \tag{5.2-1}$$

The small gain theorem states that for stable Δ the closed loop system is robustly stable if K stabilizes the nominal plant and either of the following inequalities is true:

$$\left\| K(I + GK)^{-1}\Delta \right\|_\infty < 1$$

$$\left\| \Delta K(I + GK)^{-1} \right\|_\infty < 1$$

The above inequalities can be re-written as:

$$\left\| K(I + GK)^{-1} \right\|_\infty < \frac{1}{\|\Delta\|_\infty}$$

5.2.2 General framework for uncertainty

The general framework for uncertainty together with the open loop interconnection and the controller is shown in Figure 55 [19]. The uncertainty block outputs the perturbations w_p that are inputted to the P block. The measurement variable y is inputted to the controller K which gives the control effort u as output.

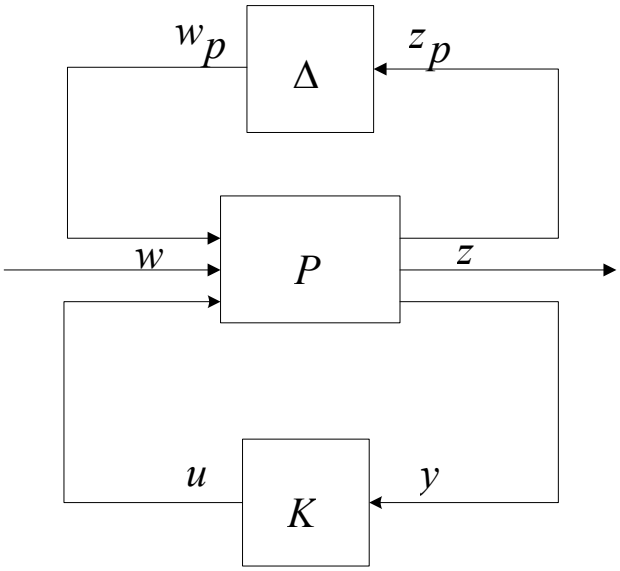

Figure 55: Lower and upper LFT representation of uncertainty and controller [18]

The interconnection matrix between P and K can be found out by applying lower linear fractional transformation. Therefore, the interconnected matrix can be given by equation 5.2-2 and has the following realization:

$$M(s) = \begin{bmatrix} M_{11} & M_{12} \\ M_{21} & M_{22} \end{bmatrix}$$

$$M(s) = F_l(P(s), K(s)) \tag{5.2-2}$$

The uncertainty framework is reduced from Figure 55 to Figure 56 and has two elements the interconnected matrix M and the uncertainty block Δ as shown in Figure 56.

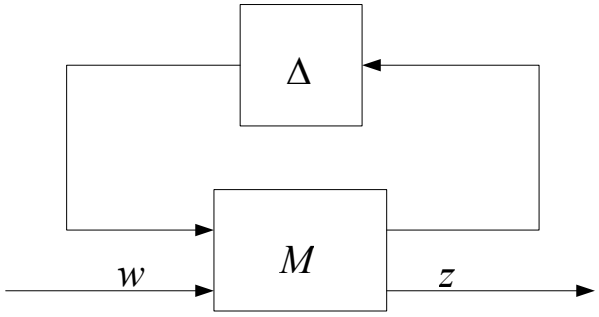

Figure 56: LFT representation of M (closed loop transfer function) [18, 19]

For the feedback system shown in Figure 56, to be internally stable the transfer function from the reference w to the error output z should be stable and for it to fulfill the performance criterion it needs to be less than the stability margin γ.The transfer function from w to z is given by the upper linear fractional transformation formulation.

$$Fu(M,\Delta) = [M_{22} + M_{21}\Delta(I - M_{11}\Delta)^{-1}M_{12}] \tag{5.2-3}$$

Transfer function 5.2-3 can only be stable if and only if $(I - M_{11}\Delta)$ is non- singular for all frequencies in consideration and for performance requirement the norm of transfer function given in the above equation should be less than the stability margin given as:

$$Fu(M,\Delta) < \gamma$$

Therefore the internal stability of the perturbed system depends on M_{11}. The small gain theorem leads to the fact:

$$\det[I - M_{11}(jw)\Delta(jw)] \neq 0 \tag{5.2-4}$$

Here M is the nominal closed loop plant (closed loop transfer function matrix that includes the feedback controller K in it) equation 5.2-4 represents that for a closed loop system to be stable the uncertainties should be small enough not to violate the above condition that is not to make $(I - M_{11}(jw)\Delta(jw))$ singular at any frequency.

5.3 Structured singular value μ

Structure Singular value is the measurement such that for a given M with a fixed K (closed loop system) and given known structure of uncertainty, the smallest value of Δ that makes $(I - M_{11}(jw)\Delta(jw))$ singular at any frequency describes how robustly stable the controller K is in dealing with such structured uncertainty [27]. For any structured uncertainty we need the frequency response in terms of the structured singular value μ where $\mu_\Delta(M)$ can be defined as the number such that $\mu_\Delta^{-1}(M)$ is equal to the smallest $\sigma(\Delta)$ that makes $(I - M_{11}(jw)\Delta(jw))$ singular. If the nominal feedback system M is stable and $\beta > 0$ (the uncertainty bound) i.e. $\|\Delta\| < \beta$ then the system is stable if and only if $\mu < \frac{1}{\beta}$ where β is the smallest value at which Δ gets unstable therefore $\mu < \frac{1}{\beta}$.

5.4 Upper and lower bounds of μ

It is extremely difficult to find the singular structured value instead the bounds of μ are calculated, but the upper and lower bound of μ are not useful for the computation of μ itself because there is a large gap between them. Therefore certain transformations need to be done on M so as to close the gap between them without altering the value of μ [9, 27]. The bounds of μ are given as:

$$\rho(M) < \mu(M) < \bar{\sigma}(M)$$

Where M is a constant square matrix and $\rho(M)$ is the spectral radius of M and $\sigma(M)$ is the maximum value of M. For the purpose of reducing the gap between the bounds two new matrices U and D are introduced which are given as:

$$\boldsymbol{U} = \left\{U \in \Delta : UU^{-1} = I_n\right\}$$

$$\boldsymbol{D} = \left\{ D = diag[D_1, ..., D_s, d_1 \, \mathrm{I}_{\mathrm{m}1}, ...df \, \mathrm{I}_{\mathrm{m}f}] \right\}$$

The matrices $\boldsymbol{U}$ and $\boldsymbol{D}$ match the structure of Δ where $\boldsymbol{U}$ is a block-diagonal structure of unitary matrices and for any $D \in \boldsymbol{D}$, DD^{-1} commutes with Δ. Therefore, the most important relation to keep in mind is given as:

$$\rho(MU) \leq \mu(MU) = \mu(M) = \mu(DMD^{-1}) < \bar{\sigma}(DMD^{-1})$$

The relations lead to the following theorem:

$$\max_{U \in \boldsymbol{U}} \rho(MU) \leq \mu(M) \leq \inf_{D \in \boldsymbol{D}} \bar{\sigma}(DMD^{-1})$$

5.5 D-K Iteration method

For the robust stability robust performance criteria it is required to find a controller K and a diagonal constant scaling matrix that minimizes the optimization problem given by the following norm.

$$\min_{\substack{K \\ stabilizing}} \min_{\substack{D \\ stable}} \left\| DF_l(P,K)D^{-1} \right\|$$

By minimizing the above optimization problem the upper bound of μ is minimized which means that the peak value of μ is reduced thus increasing the size of uncertainty allowed. The D-K iteration method used follows the given steps [9, 18, 27]:

1. Starts with an initial guess for D, usually sets $D=I$.
2. Fix D and solve the optimization problem for K.

$$K = \arg \inf_K \left\| F_l(P,K) \right\|$$

3. Fix K and solve the optimization problem for D at each frequency over a selected range of frequencies.
4. Curve fit D to get a stable minimum phase D matrix step 2 is then repeated until a pre specified tolerance is achieved or the maximum iteration number is reached.

5.6 Robust control toolbox commands (MATLAB)

5.6.1 Using DKit command

The μ synthesis is executed by the M file dkit in the robust control toolbox, which automates the procedure by using *D-K* iterations [18]. To implement the dkit function it is important for certain variables to be in the workspace.

Table 6: Variables used for DK iterations [27]

NOMINAL DK	A variable containing the nominal open-loop system
NMEAS DK	Number of measurements (number of inputs of K)
NCONT DK	Number of control inputs (number of outputs of K)
BLK DK	Block structure for computation of μ (involves the uncertainty blocks as well as the performance block)
OMEGA DK	Frequency response range
AUTINFO DK	Variable, which is used for full automation of the D-K-iteration. It has the following components:
AUTOINFO DK(1)	Initial iteration
AUTOINFO DK(2)	Final iteration
AUTOINFO DK(3)	Visualization flag (1 - the results appear on the display, 2 - the results are not displayed) The rest elements in AUTOINFO DK (their number is equal to the number of blocks in BLK DK) set the maximum dynamic order of the transfer functions
NAME DK	Suffix to the names of the saved variables

Table 7 and Table 8 show the iteration summary for pitch rate and roll rate obtained after the dk iterations script is run.

Table 7: Iteration summary for pitch rate

Iteration #	1	2	3	4
Controller Order	4	6	22	22
Total D-Scale Order	0	2	18	18
Gamma Achieved	61.819	1.845	1.144	0.987
Peak mu-Value	12.638	1.647	1.143	0.975

Table 8: Iteration summary for roll rate

Iteration #	1	2	3	4
Controller Order	4	6	22	22
Total D-Scale Order	0	2	18	18
Gamma Achieved	64.57	1.798`	1.1388	0.925
Peak mu-Value	13.34	1.567	1.079	0.966

5.7 Analysis of closed loop with μ-synthesis controller

5.7.1 Nominal performance:

Figure 57 and Figure 58 show the sensitivity function of the closed loop system with the μ-controller. It is obvious for both pitch rate and roll rate that the sensitivity function lies below the inverse of the weighing function specified in chapter 3 section 3.6.3. Thus the nominal performance is observed for both the closed loop systems.

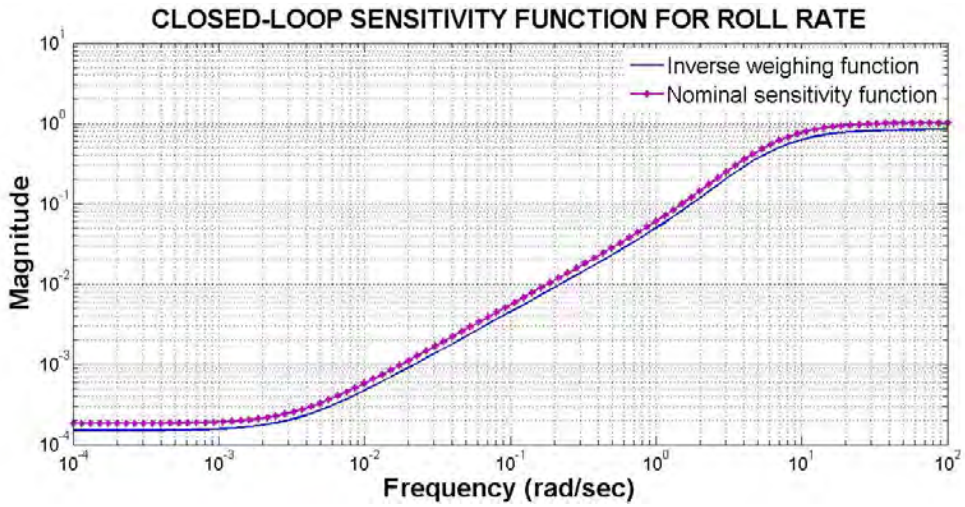

Figure 57: Closed loop sensitivity function for roll rate

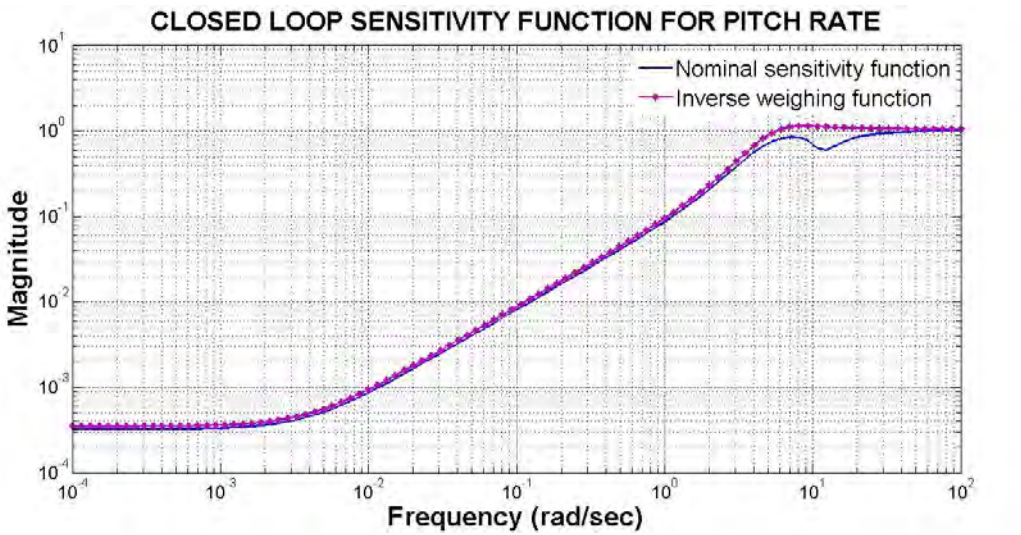

Figure 58: Closed loop sensitivity function for pitch rate

5.7.2 Robust stability:

The test for robust stability is conducted on the leading 3 by 3 diagonal block of the closed loop transfer matrix function that is created by using the *starp* command from MATLAB for the open loop interconnected matrix P and the μ controllers developed. The upper bound of μ (singular structured value) should be less than one for robust stability. Figure 59 shows that the maximum value of μ is equal to 0.3901 therefore the system stability is preserved for $\|\Delta\| < \frac{1}{0.3901}$. Figure 60 shows that the maximum value of μ is equal to 0.2503 therefore the system stability is preserved for $\|\Delta\| < \frac{1}{0.2503}$.

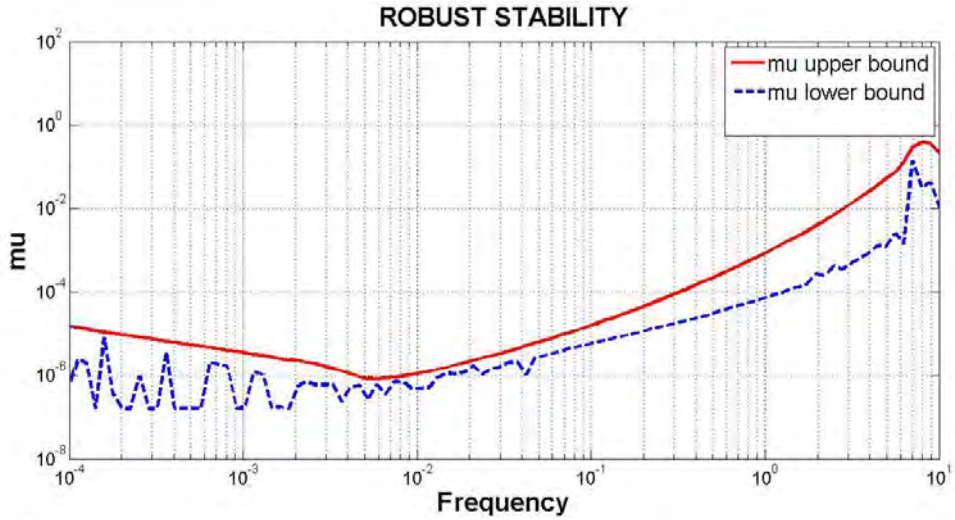

Figure 59: Robust stability for pitch rate

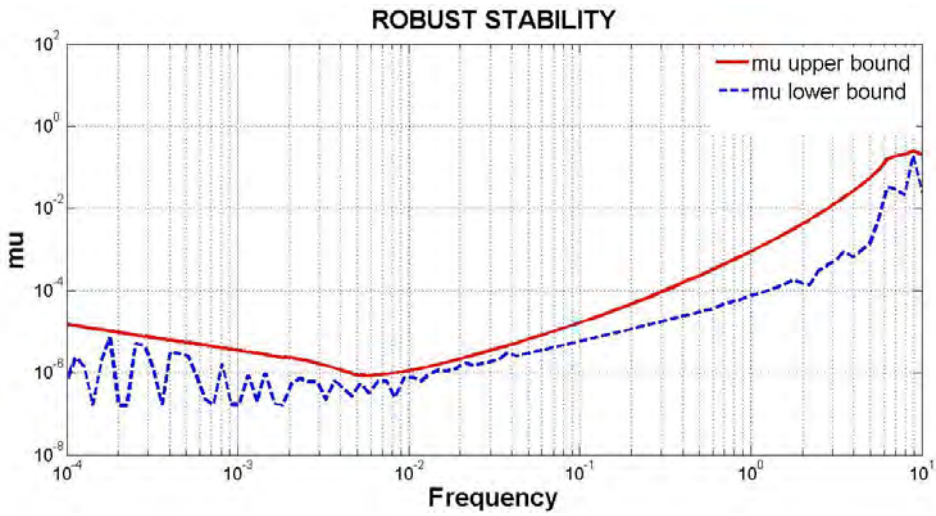

Figure 60: Robust stability for roll rate

5.7.3 Robust performance:

The frequency responses of the nominal and robust performance criteria are obtained in the Figure 61 and Figure 62 for pitch rate and roll rate. The maximum value of μ in the robust performance analysis for the pitch rate is equal to 1. This means that the closed loop system with the μ -controller achieves robust performance since:

$$\left\| \begin{bmatrix} w_p(I + F_U(G_{mds}, \Delta)K)^{-1} \\ w_u K(I + FU(Gmds, \Delta)K)^{-1} \end{bmatrix} \right\| < 0.98$$

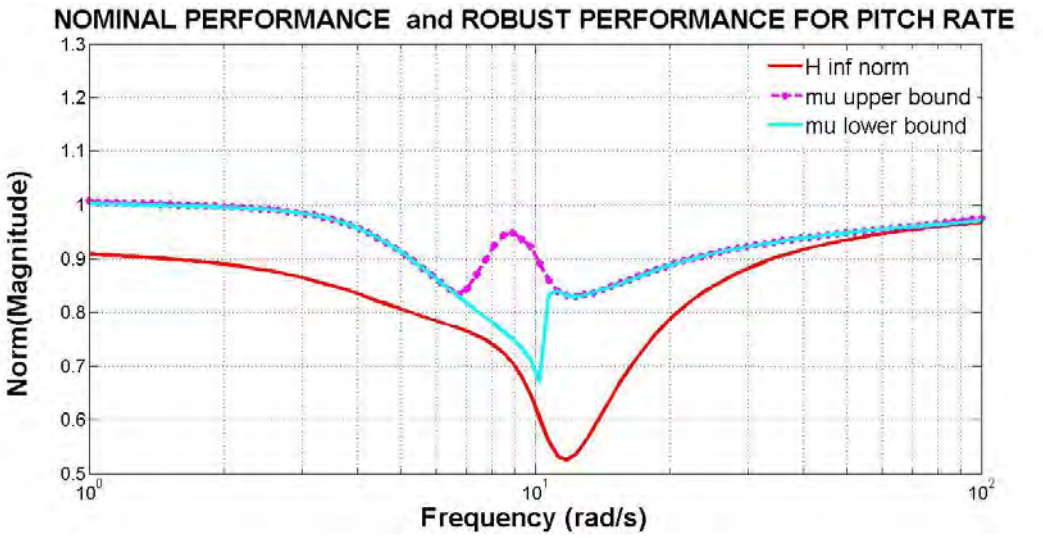

Figure 61: Nominal and robust performance for pitch rate with μ -controller

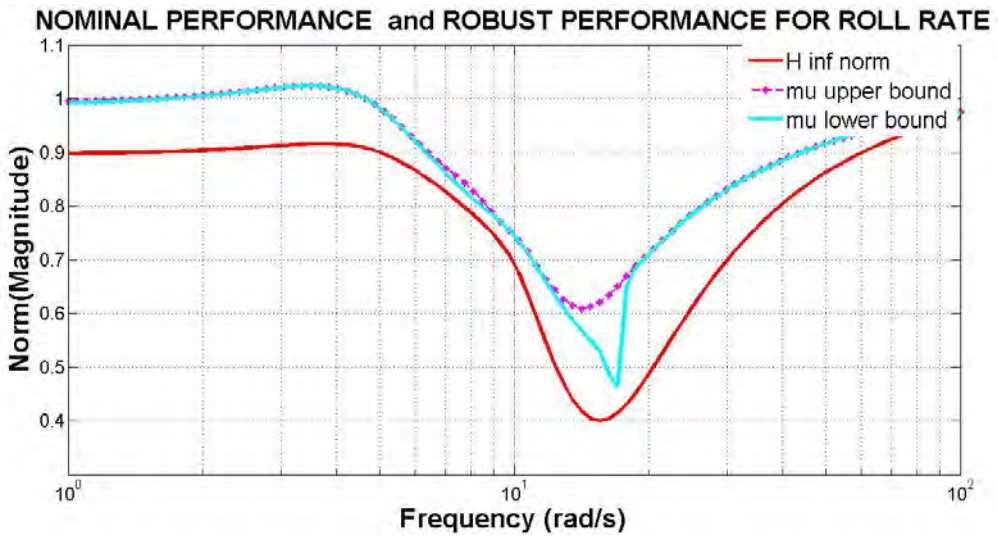

Figure 62: Nominal and robust performance for roll rate with μ -controller

5.7.4 Robustness analysis with perturbed systems

To illustrate the robust properties of the system with the μ -controller the frequency response of the sensitivity function of the perturbed closed loop systems is shown in Figure 63 and Figure 64 for pitch and roll rate respectively. It can be observed from both the Figures that the frequency responses of the perturbed sensitivity functions remain below the frequency response of the inverse of the weighing function.

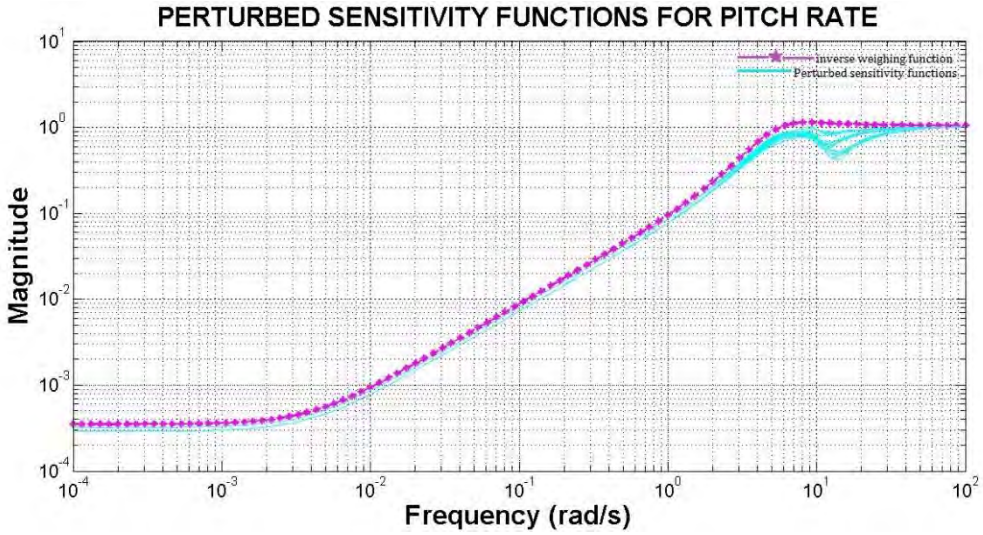

Figure 63: Sensitivity functions of perturbed systems for pitch rate

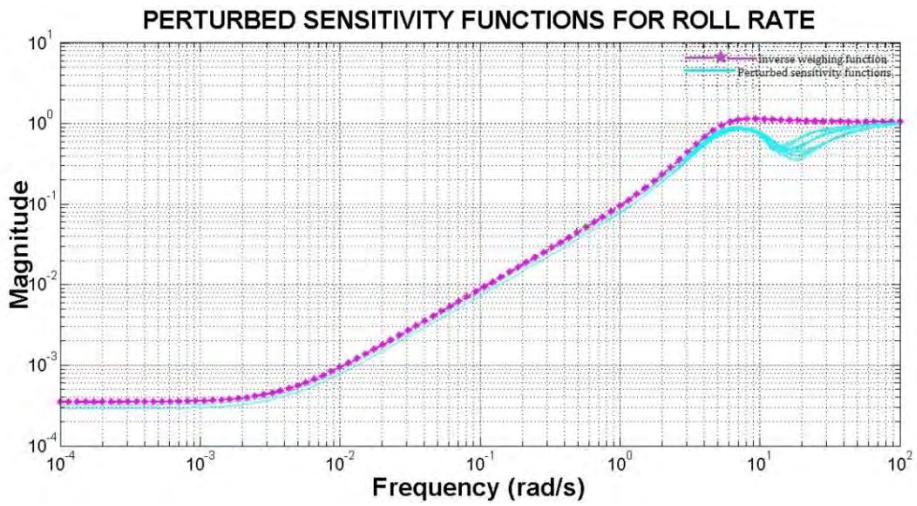

Figure 64: Sensitivity function of perturbed systems for roll rate

The Performance of Perturbed Systems with μ controller is checked to find the performance of the controller. The magnitude responses of the weighted mixed sensitivity function given as:

$$\left\| \begin{bmatrix} w_p(I + F_U(G_{mds}, \Delta)K)^{-1} \\ w_u K(I + FU(Gmds, \Delta)K)^{-1} \end{bmatrix} \right\|$$

Figure 65 and Figure 66 show are plotted for all the perturbed systems using μ controller for pitch rate and roll rate. It can be seen that for all the perturbed systems, the magnitudes over the frequency range are below the criterion for the closed loop robust performance for both cases.

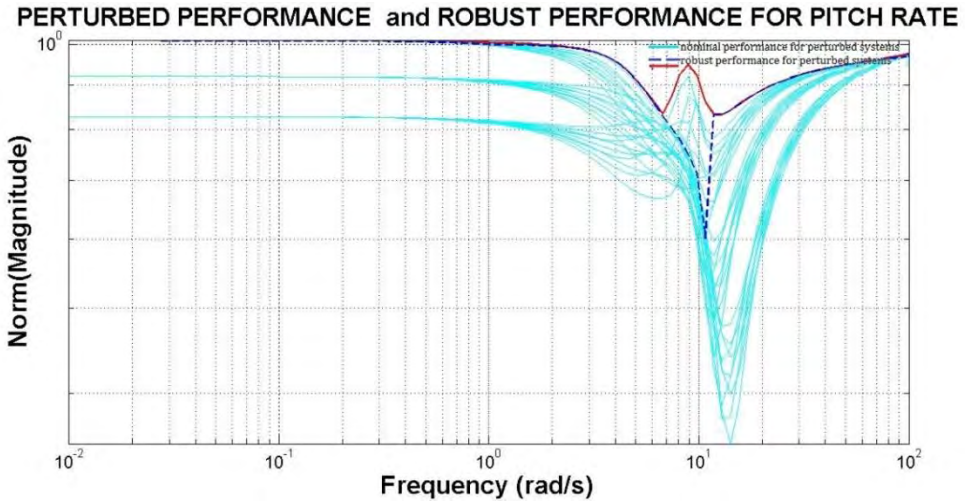

Figure 65: Nominal and robust performance for perturbed pitch rate

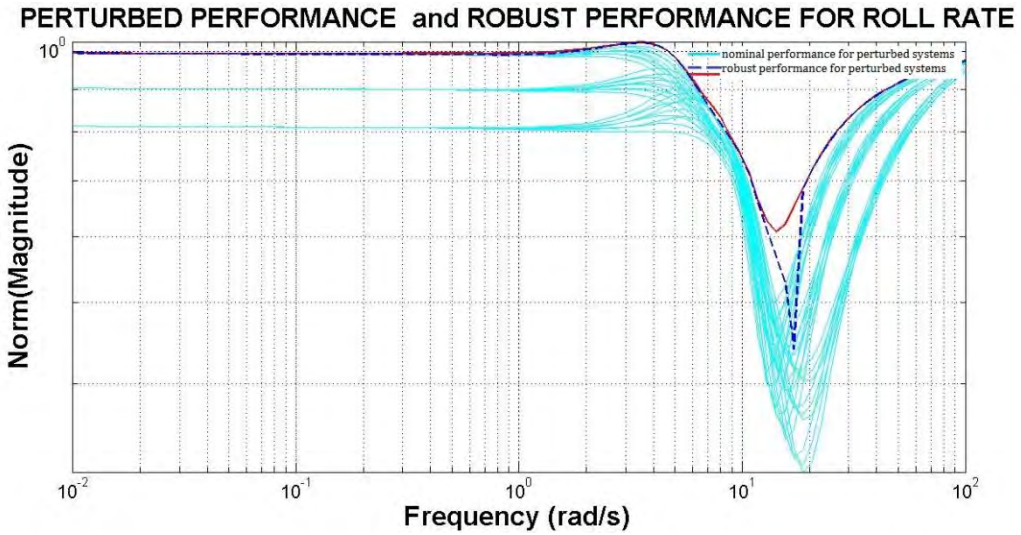

Figure 66: Nominal and robust performance for perturbed roll rate systems

5.7.5 Transient analysis of the closed loop system

The transient response (to a reference input) for a nominal plant as well as a family of perturbed closed loop systems for both pitch rate with K-μ controllers are shown below. Comparing with the responses in the case of LSDP controllers μ -controller ensures smaller overshoot (10%) while the settling time is almost 1.8secs. For the perturbed closed loop systems it can be observed that the overshoot does not exceed 20% that demonstrates satisfactory performance in the presence of parametric perturbations.

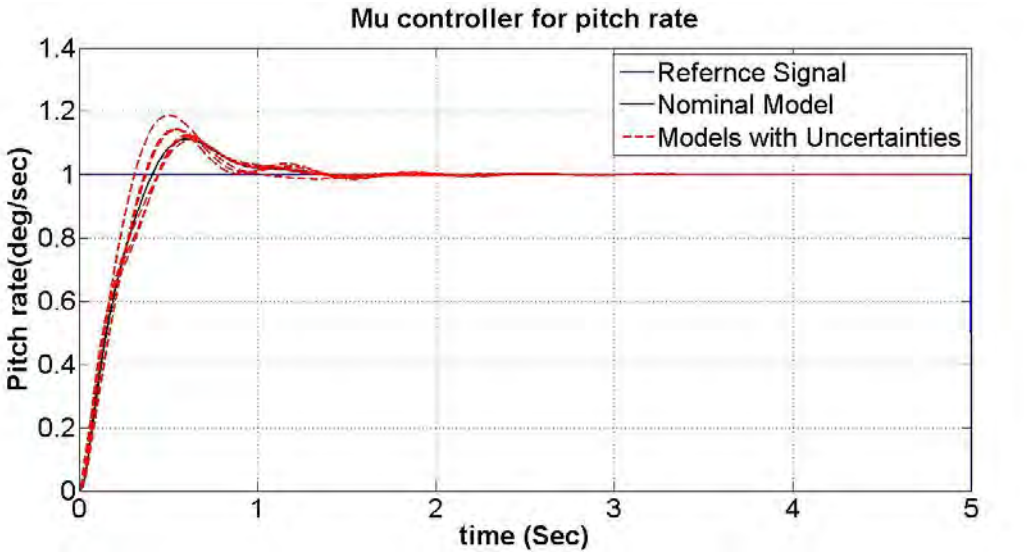

Figure 67: Transient response to a reference input for pitch rate

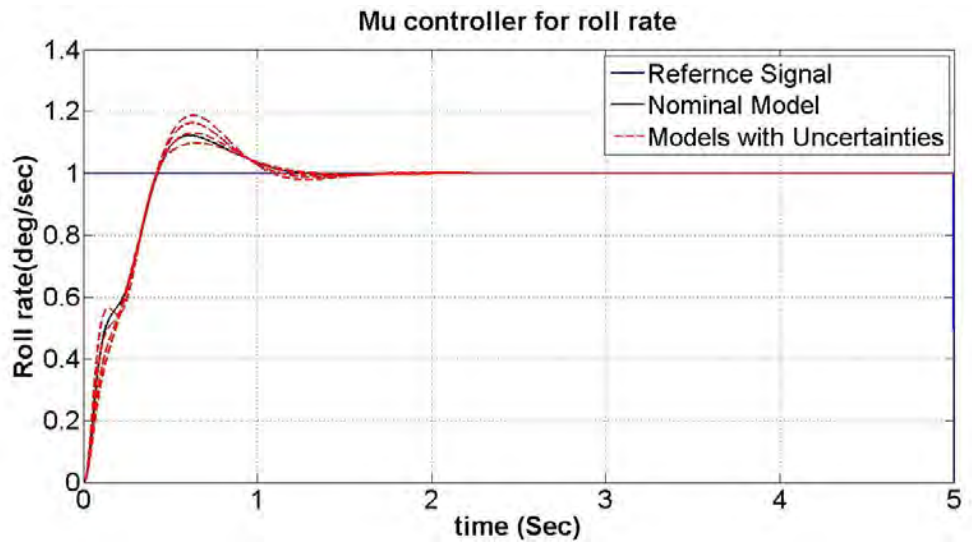

Figure 68: Transient response to reference input for roll rate

Figure 69 and Figure 70 show the transient response of the pitch rate and roll rate plant respectively when a step disturbance of 0.1 magnitude is added to it. Disturbance rejection/attenuation shows that the closed loop system has achieved nominal performance.

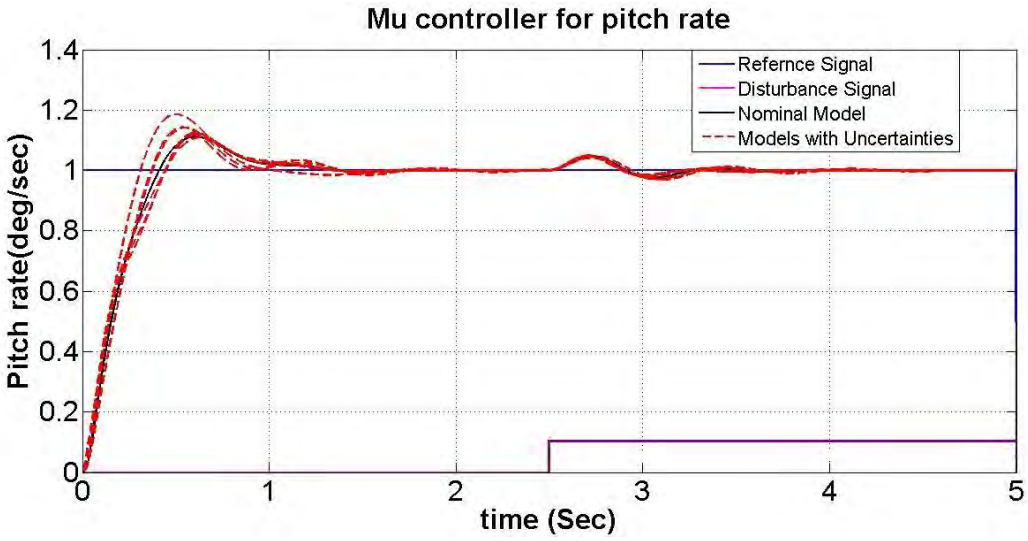

Figure 69: Pitch rate response for disturbance of 0.1 magnitude

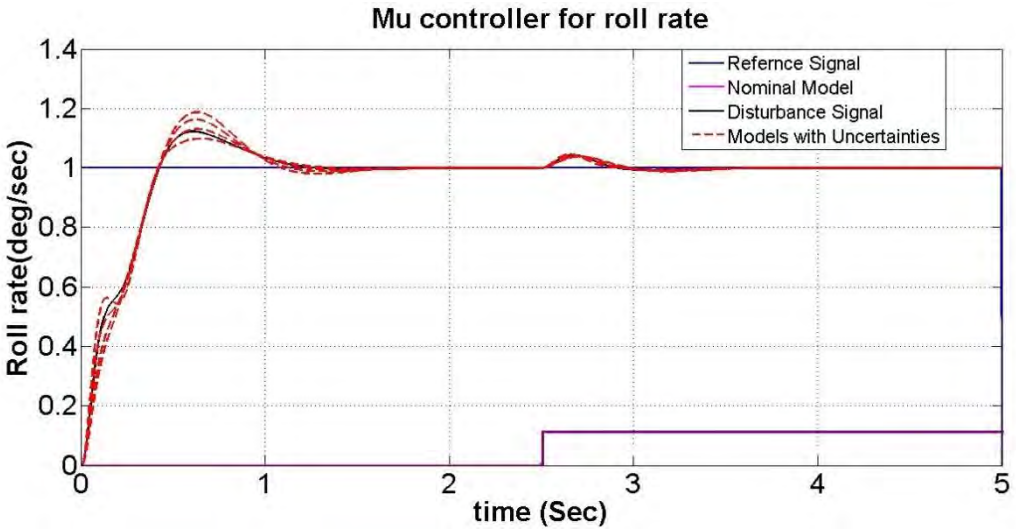

Figure 70: Roll rate response for disturbance of 0.1 magnitude

Chapter 6

Comparison between the controllers

6.1 Criteria of comparison:

The criteria of comparison for robust controllers are nominal performance, robust stability and robust performance. To check the nominal performance means to check if the controllers have achieved optimization of the mixed sensitivity function as described in Chapter 3 in section 3.5.1. Where robust analysis includes robust stability and robust performance and is done to check whether the stability of a system is preserved for a system as it varies for a bounded set of uncertainties. The controllers discussed in the chapter 3: H∞, chapter4: LSDP controller and chapter 5: μ-synthesis controller has been compared in this chapter according to the different criteria of comparison.

6.2 Nominal performance:

Figure 71 represents the nominal performance for all three controllers for pitch rate. In order to calculate the nominal performance of all the controllers the frequency response of the weighted sensitivity functions is calculated. It can be observed that the entire three controllers perform well, as for the considered range the magnitude of the norm is less than one, which represents the internal stability of the system.

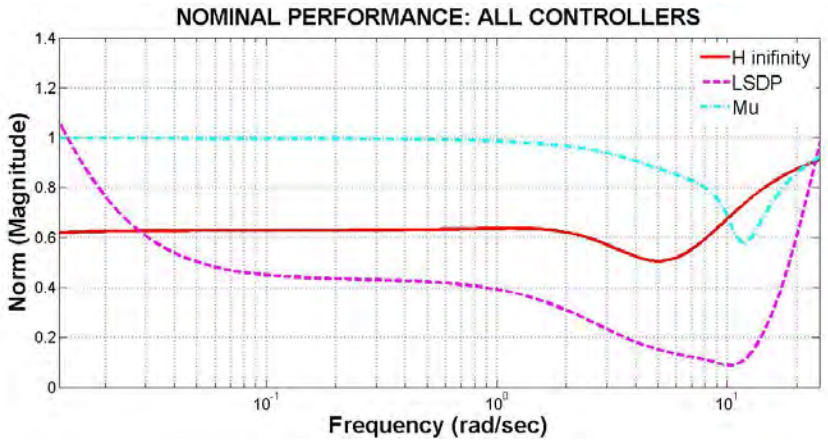

Figure 71: Comparison of nominal performance for all controllers

6.3 Robust stability:

The system which uses LSDP is considered to have achieved the best robust stability as can be seen in the Figure 72 since for LSDP response the perturbations would have the largest value because the value of μ is smallest for it. The point to remember here is that the norm of the uncertainty is inversely proportional to the maximum value of μ achieved.

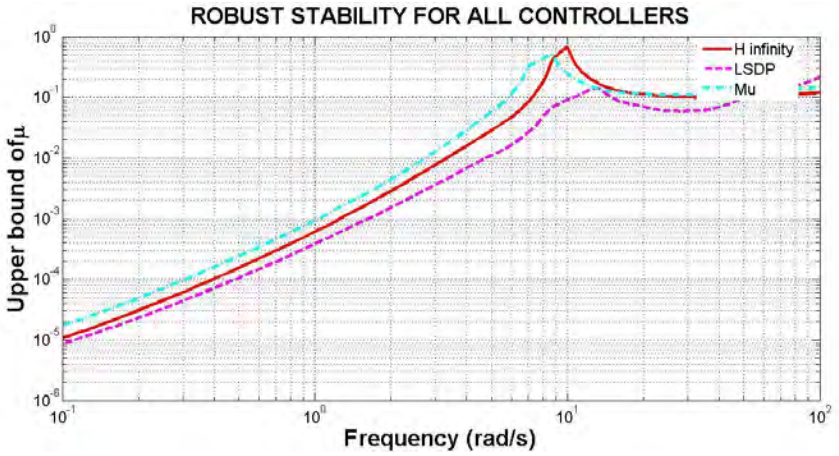

Figure 72: Comparison of robust stability for all controllers

6.4 Robust performance:

The μ values over a frequency range are plotted for all 3 controllers it can be observed here again as it was derived in chapter 3 that the H∞ controller doesn't achieve robust performance criteria whereas the remaining two show robust performance since the value of μ is equal or less than 1 for both.

Figure 73: Comparison of robust performance for all controllers

Chapter 7

Summary

In conclusion it can be said that this thesis has explored different robust control laws for a small scaled Joker 3 helicopter, the controllers developed have high potential of being implemented in real time flight tests. Chapter 2 of the thesis discusses a model following control law Dynamic Inversion and it shows that the rate responses obtained from this controller is almost perfect but with the disadvantage of it not being robust. In chapter 3 the first robust controller has been developed for the Joker 3 helicopter pitch and roll rate, the uncertainties injected in the system are structured and follow linear fractional transformation formulation, the controller is seen to achieve nominal performance and robust stability but fails to achieve robust performance. Chapter 4 describes another way of designing a robust controller which is loop shape designing procedure that utilizes the H∞ technique but the uncertainties injected here are directly on the co-prime factors of the plant. Again the robust controller is tested for the difference performance criterion and the controller succeeds in achieving all. Chapter 5 describes the μ synthesis which uses μ analysis for the development of the controller, here the perturbed performance of the system are checked to prove that robust performance is achieved. Chapter 6 describes a comparison between all the controller's performance criteria.

References

[1] Gareth Padfield. *Helicopter Flight Dynamics: The Theory and Application of Flying Qualities and Simulation Modeling*. Washington: AIAA, 1996.

[2] Brian L. Stevens, Frank L. Lewis. *Aircraft Control and Simulation*. John Wiley & Sons Inc., 1992.

[3] Salah I. AlSwailem. "Application of Robust Control in Unmanned Vehicle Flight Control System Design". PhD thesis, Cranfield University, College of Aeronautics, 2003-2004.

[4] Guowei Cai, Lin Feng, Ben M. Chen, Tong H. Lee. "Systematic design methodology and construction of UAV helicopter". *Mechatronics18(2008).* 545-558 .2008.

[5] B. Kada, Y. Ghazzawi. "Robust PID Controller Design for an UAV Flight Control System". *Proceedings of the World Congress on Engineering and Computer Science.* Vol II. 2011.

[6] Kamran Turkoglu, Ugur Ozdemir, Melike Nikbay, and Elbrous M. Jafarov. "PID Parameter Optimization of an UAV Longitudinal Flight Control System". World Academy of Science, Engineering and Technology 21. *2008.*

[7] Amer A. Al-Radaideh, Ali A. Jhemi And Mohammad-Amin Al-Jarrah. "System Identification Of The Joker-3 Unmanned Helicopter". ISMA, The American University Of Sharjah, Sharjah, UAE, 2008.

[8] Da-Wei Gu, Petko Hristov Petkov and Mihail Mihaylov Konstantinov. *Robust Control Design With MATLAB.* London: Springer-Verlag London Limited. 2005.

[9] K. Glover, D. Mc Farlane. “Robust stabilization of normalized co-prime factors: An explicit *H*∞ solution”. IEEE American Control Conference, Atlanta, GA, 1988.

[10] D.J. Walker and I. Postlethwaite. “Advanced helicopter flight control using two degree-of-freedom H∞ optimization”. *Journal of Guidance, Control, and Dynamics*, vol. 19, pp. 461-468, 1996.

[11] A. Smerlas, I. Postlethwaite, D. J. Walker, M. E. Strange, J. Howitt, R. I. Horton, A.W.Gubbels, and S.W.Baillie. “Design and flight testing of an *H*∞ controller for the NRC Bell 205 experimental fly-by-wire helicopter”. *In: AIAA Guidance, Navigation, and Control Conference and Exhibit, Boston, MA, Aug*, vol.2, pp.1023-1033, 1998.

[12] R. A. Hyde. *H∞ Aerospace Control Design : A VSTOL Flight Application*. Berlin; New York: Springer, 1995.

[13] J. Markerink, S. Bennani, and B. Mulder. “Design of a Robust, Scheduled Controller for the HIRM using μ-synthesis" GARTEUR FM(AG08) TP-088-29,1997.

[14] K. Y. Tu, A.Sideris, K. D. Mease, J. Nathan, and J. Carter. “Robust lateral directional control design for the F/A-18”. *In: AIAA Guidance, Navigation, and Control Conference and Exhibit, Portland, OR, Aug*, vol. 2, pp. 1213-1219, 1999.

[15] Daigoro Ito, Jennifer Georgie, John Valasek and Donald T. Ward. “Reentry Vehicle Flight Controls Design Gudidelines: Dynamic Inversion”. Flight Simulation Laboratory, NASA, March 2002.

[16] Jennifer Georgie and John Valasek, "Evaluation of Longitudinal Desired Dynamics for Dynamic-Inversion Controlled Generic Reentry Vehicles", *Journal of guidance, control, and dynamics,* Vol. 26, No. 5, September–October 2003.

[17] Pedro Valerio Menino Simlicio. "Helicopter Nonlinear Flight Control using Nonlinear Dynamic Inversion." Masters of Science Thesis, Instituto Superior T´ecnico , 2011.

[18] P.C Chandrasekharan. *Robust control of Linear Dynamical Systems*. Academic Press Limited. 1996.

[19] Uwe Mackenroth**.** *Robust control systems: Theory and case studies*. Springer 2004.

[20] K. Zhou and J.C. Doyle. *Essentials of Robust Control*. New Jersey: Prentice Hall, 1998.

[21] M.Vidyasagar. *Control system Synthesis- A factorization approach*. Cambridge: MIT Press, M A, 1985.

[22] Gábor Rödönyi, Péter Gáspár, Zoltán Szabó, József Bokor. "Uncertainty remodeling for robust control of linear time-invariant plant". Mediterranean Control Conference, Ajaccio, Corsica, 2008.

[23] Ryosuke Ito, Goro Obinata, Chikara Nagai and Youngwoo Kim. "A Method for Identifying Physical Parameters with Linear Fractional Transformation". World Academy of Science, Engineering and Technology 62, 2012.

[24] Gary J.Balas, John C.Doyle, Keith Glover, Andy Packard and Roy Smith, μ-*Analysis and Synthesis toolbox For Use with MATLAB ,* MUSYN Inc. and The MathWorks. Inc, 1993 – 2001.

[25] P. Lundstrom, S. Skogstad, Z.C. Wang, "Weight selection for *H*∞ and mu-control methods: insights and examples from process control". *Workshop on H∞ Control*, *Brighton, U.K.,* pp.139–1991, 1991.

[26] John E.bibel and Stephen Malyevac, "Guidelines For the Selection of Weighting Functions for H-Infinity control", January 1992.

[27] Gary J. Balas, *Mu-Synthesis,* Aerospace Engineering and Mechanics, University of Minnesota, Minneapolis, 1995.

[28] K. Glover, D. Mc Farlane, "Robust Stabilization of normalized co-prime factor plant descriptions with *H*∞ bounded uncertainly". *IEEE Transactions on Automatic Control*, vol. 34, pp. 821–830, 1989.

[29] McFarlane. D, Glover. K, *"*A loop shaping design procedure using H∞ synthesis". *IEEE Transactions on Automatic Control, 37(6),* pp. 759-769, 1992.

[30] G. Vinnicombe. *Uncertainty and Feedback - H∞ loop-shaping and the v-gap metric*. Imperial College Press, 2000.

[31] M. L. Civita, G. Papageorgiou, W. C. Messner, and T. Kanade. "Design and Flight Testing of a High-Bandwidth H∞ Loop Shaping Controller for a Robotic Helicopter", AIAA Guidance, Navigation, and Control, Monterey, California USA, 2002.

[32] M. Osinuga , S. Patra , A. Lanzon. "State-space solution to weight optimization problem in H∞ loop-shaping control", *Automatica Volume 48(3) Elsevier* 2012.

[33] Isharaka Gunasinghe and Alexander Lanzon. “A Systematic Weight Synthesis Procedure for Performance Optimisation In H∞ Loop Shaping.” *Proceedings of the European Control Conference,* Kos, Greece, July 2-5, 2007.

[34] A. El-Saadany, A.Medhat and Y.Z Elhalwagy. “Flight Simulation Model for Small scaled Rotor Craft-Based UAV”*,* 13th International Conference onAerospace Sciences & Aviation Technology. ASAT-13, 2009.

[35] Naohiro Ban, Hiromitsu Ogawa, Manato Ono and Yoshihisa Ishida, “A Servo Control System Using the Loop Shaping Design Procedure*”.* World Academy of Science, Engineering and Technology 36, 2009 .

[36] C. Huang, Q. Shao, P. Jin, Z. Zhu, P. Luoyang, “Pitch Attitude Controller Design and Simulation for a Small Unmanned Aerial Vehicle”. *International Conference on Intelligent Human-MachineSystems and Cybernetics, IHMSC '09,* Hangzhou, Zhejiang, 26-27 Aug, 2009, pp. 58-61.

[37] M. Steinbuch, J.C terlouw, O.H Bosgra and S.G Smit, “Uncertainty modelling and structured singular value computation applied to an electromechanical system”. *IEEE Proceedings,* vol 139, no.3, May 1992.

[38] B. S. Chen and Y. M. Cheng. “A structure-specified optimal control design for practical applications: a genetic approach”, *IEEE Trans. on Control System Technology,* vol. 6, pp. 707-718, 1998.

[39] D. Moormann, A. Varga, G. Looye, and G. Gruebel. “Robustness analysis applied to autopilot design. III - Physical modeling of aircraft for automated LFT generation applied to the Research Civil Aircraft Model”. *ICAS, Congress, 21st, Melbourne,* Australia, Sept, 1998.

[40] Bernard Mettler, Takeo Kanade, Mark B. Tischler , "System Identification of Small-Size Unmanned Helicopter Dynamics", *American Helicopter Society 55th Forum. Montreal, Quebec, Canada, May 25-27, 1999.*

[41] Bernard Mettler, Takeo Kanade, Mark B. Tischler System "Identification Modeling of a Model-Scale Helicopter", CMU-RI-TR-00-03,2000.

[42] B. Mettler, M. B. Tischler and T. Kanade, "System Identification Modeling of a Small-Scale Unmanned Helicopter," Journal of the American Helicopter Society, 47(1), Jan. 2002.

[43] Caglar Karasu, "Small-Size Unmannaed Model Helicopter Guidance and Control." Masters of Science thesis, The graduate school of Natural and Applied sciences of Middle East Technical University, 2004.

[44] S. Kaitwanidvilai, M. Parnichkun. "Genetic Algorithm based Fixed-Structure Robust H infinity Loop Shaping Control of a Pneumatic Servo System". *International Journal of Robotics and Mechatronics,* Vol.16 No.4, 2004.

[45] A. Budiyono, T. Sudiyanto and H. Lesmana, "First Principle Approach to Modeling of Small Scale Helicopter", ICIUS, Bali, Indonesia, Oct 24-25, 2007.

[46] Sohail. Iqbal, Aamer Iqbal Bhatti, Muhammad Akhtar, Saif Ullah "Design and Robustness Evaluation of an H∞ Loop Shaping Controller for a 2DOF Stabilized Platform", *In proceeding of: European Control Conference (ECC'07),* Kos, Greece 2 – 5, Volume: pp. 2098 – 2104, July 2007.

[47] S. Kaitwanidvilai and Manukid Parnichkun, "Design of Structured Controller Satisfying H∞ Loop Shaping using Evolutionary Optimization: Application to a Pneumatic Robot Arm", Engineering Letters, Vol. 16 No.2, 2008.

Vita

Rabiya Ahmed was born on 28th December, 1986, in Al-Ain, UAE. She did her primary and secondary schooling from Al-Ain Juniors School, her high school (Pre-Engineering) from Agha Kha Higher Secondary School. From there she went on to the NED university of Science and Technology Karachi where she obtained her B.E. in Electronics in January 2011. She is currently enrolled in her final semester for Masters of Science in Mechatronics from American University of Sharjah and will hopefully graduate in June 2013.